

MOTC-IOT-91-HA13

仔波分析與時頻或時尺分析在波浪 研究之應用 (1/2)



交通部運輸研究所

中華民國九十二年六月

MOTC-IOT-91-HA13

仔波分析與時頻或時尺分析在波浪 研究之應用 (1/2)

著者：李勇榮

交通部運輸研究所

中華民國九十二年六月

仔波分析與時頻或時尺分析在波浪研究之應用 (1/2)

著 者：李勇榮

出版機關：交通部運輸研究所

地 址：台北市敦化北路 240 號

網 址：www.iot.gov.tw

電 話：(02)23496789

出版年月：中華民國九十二年六月

印 刷 者：

版(刷)次冊數：初版一刷 110 冊

本書同時登載於交通部運輸研究所網站

定 價：

展 售 處：

交通部運輸研究所運輸資訊組•電話：(02)23496880

三民書局重南店：台北市重慶南路一段 61 號 4 樓•電話：(02)23617511

三民書局復北店：台北市復興北路 386 號 4 樓•電話：(02)25006600

國家書坊台視總店：台北市八德路三段 10 號 B1•電話：(02)25787542

五南文化廣場：台中市中山路 2 號 B1•電話：(04)22260330

新進圖書廣場：彰化市光復路 177 號•電話：(04)7252792

青年書局：高雄市青年一路 141 號 3 樓•電話：(07)3324910

GPN：

**PUBLICATION ABSTRACTS OF RESEARCH PROJECTS
INSTITUTE OF TRANSPORTATION
MINISTRY OF TRANSPORTATION AND COMMUNICATIONS**

TITLE: Wavelet Time-Frequency Analysis and Its Applications to Water Waves – Wavelet Characterizations and the Optimum Basis			
ISBN(OR ISSN)	GOVERNMENT PUBLICATIONS NUMBER 1009202115	IOT SERIAL NUMBER 92-84-763	PROJECT NUMBER 91-HA13
DIVISION: CENTER OF HARBOR & MARINE TECHNOLOGY DIVISION CHIEF: Yung-Fang Chiu PRINCIPAL INVESTIGATOR: Yueon-Ron Lee PROJECT STAFF: Yueon-Ron Lee PHONE: 886-4-26587183 FAX: 886-4-26587183, 886-4-26571329			PROJECT PERIOD FROM Jan. 2002 TO Dec. 2002
KEY WORDS: discrete wavelet categories, comprehensive programming, characteristic phase, entropy statistics, optimal basis			
ABSTRACT: <p>Comprehensive categories of discrete wavelet are examined in this study. The relevant characterizations and various intrinsic properties are extensively illustrated. Physical counterparts of analytical aspects are provided when possible. The entropy criteria are applied to the whole set of wavelets for signals obtained from wave-tank experiments, and the optimal wavelet basis is identified to be the semi-orthogonal dual wavelet. Besides, each individual wavelet's pertinency to the applications of water-wave-related signals is linked to the phase distribution of a wavelet characteristic function.</p>			
DATE OF PUBLICATION June 2003	NUMBER OF PAGES 97	PRICE 100	CLASSIFICATION SECRET CONFIDENTIAL UNCLASSIFIED
The views expressed in this publication are not necessarily those of the Ministry of Transportation and Communications.			

Wavelet Time-Frequency Analysis and
Its Applications to Water Waves
– Wavelet Characterizations and
the Optimum Basis

Yueon-Ron Lee
Institute of Harbor and Marine Technology

Email: ronlee@ms4.hinet.net

Revision: 1.0, December 24, 2002, 02:18:11
Printed: September 24, 2003

LIST OF CONTENTS

LIST OF FIGURES	iii
LIST OF TABLES	vi
中文摘要	vii
ABSTRACT	viii
1 Introduction	1
1.1 Background	1
1.2 Non-stationary effects	2
1.3 Windowed transforms	4
1.4 The objectives	10
2 The Wavelet Bases Tested and Their Characterizations	12
2.1 Introduction	12
2.2 The numerical programming	13
2.3 Wavelet bases tested and the relevant notations	14
2.4 Orthonormal wavelets	15
2.4.1 Daubechies most compactly supported wavelets (ON _{xx} A)	22
2.4.2 Daubechies least asymmetric wavelets (ON _{xx} S)	22
2.4.3 Coiflets (ON _{xx} C)	23
2.4.4 Meyer wavelet (Meyer)	23
2.4.5 Battle and Lemarié wavelet (B&L)	24
2.5 Semi-orthogonal wavelets (SO _x O and SO _x D)	24
2.6 Bi-orthogonal wavelets (BO _{xy} O and BO _{xy} D)	25
2.7 Wavelet packets	40
2.8 Wavelet blowups	42
2.9 Phase distribution of the wavelet m_0 function	42

3	The Entropies and the Best Wavelet Basis	59
3.1	The wavelet perspective of an optimum basis	59
3.2	The entropy criteria	61
3.3	Results and discussions	64
3.4	Summary	67
4	Conclusions	74
	APPENDIX A — 中文概述	75
	APPENDIX B — Wavelet 該如何中文稱之？	80
	BIBLIOGRAPHY	82

LIST OF FIGURES

1.1	Phase plane of a wavelet packet's best basis time-frequency windows for a linear chirp signal that is sampled under aliasing condition.	6
1.2	Phase planes of a wavelet packet's best level time-frequency windows using the same linear chirp and wavelet packets as in the previous figure.	7
2.1	The Wavelet translation concept within the scale range of level 3.	16
2.2	The wavelet dilation concept from scale level 0 to level 7 for the BO22O wavelet.	17
2.3	The wavelet dilation concept from scale level 0 to level 7 for the BO22D wavelet.	18
2.4	The wavelet dilation concept from scale level 0 to level 7 for the BO31D wavelet.	19
2.5	The wavelet dilation concept from scale level 0 to level 7 for the BO37O wavelet.	20
2.6	The wavelet dilation concept from scale level 0 to level 7 for the ON66A wavelet.	21
2.7	The mother wavelets of the ON $\chi\chi$ A group originating from the point location of 12.	27
2.8	The father wavelets of the ON $\chi\chi$ A group originating from the point location of 6.	28
2.9	The mother wavelets of the ON $\chi\chi$ S group originating from the point location of 12.	29
2.10	The father wavelets of the ON $\chi\chi$ S group originating from the point location of 6.	30
2.11	The mother wavelets of the ON $\chi\chi$ C group originating from the point location of 12.	31
2.12	The father wavelets of the ON $\chi\chi$ C group originating from the point location of 6.	32
2.13	The mother and farther wavelets of the Meyer wavelet originating from the point location of 12 and 6, respectively, for the boundary point based on level 3.	33

2.14	The mother and farther wavelets of the Battle and Lemarié wavelet originating from the point location of 12 and 6, respectively, for the boundary point based on level 3.	34
2.15	The mother and farther wavelets, as well as their duals, of Chui's semi-orthogonal wavelet.	35
2.16	The mother wavelets of the $BO_{xx}O$ group originating from the point location of 12.	36
2.17	The mother wavelets of the $BO_{xx}D$ group originating from the point location of 12.	37
2.18	The farther wavelets of the $BO_{xx}O$ group originating from the point location of 6.	38
2.19	The farther wavelets of the $BO_{xx}D$ group originating from the point location of 6.	39
2.20	Schematic representation of the tree-like structure of the wavelet packet decomposition.	41
2.21	The blowups of a few wavelets of the $BO_{2x}O$ group.	43
2.22	The blowups of a few wavelets of the $BO_{3x}O$ group.	44
2.23	The blowups of a few wavelets of the $BO_{2x}D$ group.	45
2.24	The blowups of a few wavelets of the $BO_{xy}D$ group.	46
2.25	The blowups of a few wavelets of the $ON_{xx}A$ and $ON_{xx}S$ groups.	47
2.26	The blowups of a few wavelet packets of the $ON_{xx}A$ and $ON_{xx}S$ groups.	48
2.27	The blowups of the $BO_{31}O$ wavelet, noting the vast difference in the ordinate.	49
2.28	The blowups of the $BO_{35}O$ wavelet, noting the difference of the inclinations of the zoom-in curves.	50
2.29	The phase distribution of the m_0 function of the Meyer wavelet.	52
2.30	The phase distribution of the m_0 function of the Battle and Lemarié wavelet, noting the difference from that of Meyer wavelet.	52
2.31	The phase distributions of the m_0 functions of the semi-orthogonal wavelet and its dual.	53
2.32	The phase distributions of the m_0 functions of the wavelets of the most asymmetric group.	54
2.33	The phase distributions of the m_0 functions of the wavelets of the least asymmetric group.	55
2.34	The phase distributions of the m_0 functions of the coiflets.	56
2.35	The phase distributions of the m_0 functions of the bi-orthogonal wavelets.	57
2.36	The phase distributions of the m_0 functions of the dual bi-orthogonal wavelets.	58
3.1	The shift non-invariant property of wavelet transform.	62
3.2	The cumulative probability distribution curves of the transform coefficients using different bases associated with three different transform categories: wavelet, wavelet packet, and Fourier transforms.	70
3.3	Comparison of reconstructed signals using truncated spectral coefficients and semi-orthogonal wavelet coefficients.	71

3.4 The cumulative probability distribution curves of the sorted wavelet and wavelet packet coefficients (L^2 -norm squared, i.e., energy content) for various bases which all originate from a single mother wavelet. 72

LIST OF TABLES

3.1	Entropy of orthonormal and semi-orthogonal wavelet coefficients as well as spectral coefficients under various statistic criteria.	68
3.2	Entropy of bi-orthogonal wavelet coefficients under various statistic criteria.	69

Introduction

1.1 Background

The usefulness of a particular data analysis methodology is highly case dependent; there simply exists neither a full-fledged analyzing function basis nor an all-purpose numerical scheme for all sorts of signals or applications.

Chronically, from the somewhat traditional and well established spectral perspective to the more recent wavelet viewpoints, we have: Fourier transform; Short time Fourier transform or windowed Fourier transform; The Gabor's analytical signal procedure and the relevant Hilbert transform; Various time-frequency transforms associated with individual distributions, such as Wigner Distribution, Page distribution, Choi-Williams distribution, and etc. [5]; The discrete wavelet transform; and, The continuous wavelet transform or the integral wavelet transform. We note here that, unlike discrete and continuous Fourier transforms, which are basically identical in both function bases and formulations, the discrete wavelet transform and continuous wavelet transform are essentially two different categories in that, first, they may use completely different function bases, second, they involve relatively quite independent formulations.

Applying to a one-dimensional time series signal, the Fourier transform yields another one-dimensional data in frequency domain. The transform correspondence is one independent variable to another independent one. For short time Fourier transform, it

yields somewhat localized frequency contents; and, when the capping window is shifted along the time axis, it provides time-dependent spectral information. Through such a multiple processing the correspondence is from the time variable to the time and frequency variables. For Gabor's analytical signal procedure [10], it yields instantaneous frequency and envelop distribution curves along the time line. Here the frequency and the envelop cannot be regarded as independent variables. The independent variable in the two corresponding domains is time. For various time-frequency transforms associated with individual distributions, they also provide time-varying frequency contents that are conceptually identical to the short time Fourier transform, except that the involved analyzing kernels are related to individual distributions rather than the Fourier kernel. For the discrete wavelet transforms, the one-dimensional time series yields directly another one-dimensional coefficient series that contains the information that covers both time and scale (or representative frequency). The correspondence is one independent variable to two in one process. As to the continuous wavelet transform, the one-dimensional time series yields a two-dimensional coefficient series that contains the information that is also varying both in time and in scale (or representative frequency). But here, every time point has a scale distribution components and every scale may play a role at a specific time. And the transform is a multi-process numerical scheme similar to the short time Fourier transform, except the core difference of the capping windows.

1.2 Non-stationary effects

It is well known that Fourier transform is suitable for characterizing stationary signals and not quite satisfactory for analyzing transient local phenomena. The reasons can be illustrated by the following properties of the transform.

- Any Function cannot be both time- and band-limited. If a function is limited (finitely supported) in one domain, then the independent variable of its corresponding function in the other domain stretches the entire real line (\mathbf{R}). In real world

situations, however, signals are almost always limited in time and space; meanwhile, hardware's capability is generally band-limited. This simply implies that there is not going to be a function basis that perfectly matches theory to practice. A slight variation of the Fourier transform is the short time Fourier transform, which is just the Fourier transform of the windowed signal, i.e., the original signal capped with or multiplied by a window function. In short time Fourier transform this property of mutual exclusivity in time and frequency localizations is indicated by the Balian-Low theorem, which basically states that if the window function $g(t)$ of a Gabor type frame

$$g_{m,n}(t) = e^{-2\pi imt} g(t - n), \quad (1.1)$$

in which $m, n \in \mathbf{Z}$, is well localized in time, then the associated Fourier transform window can not be well localized in frequency. The point here sounds a bit abstract, but, in reality, this is conceptually equivalent to the following points.

- The Gibbs phenomenon states that, if there is a jump in signal, then the overshoots, occurring at both sides of the discontinuity when the inverse Fourier transform is implemented, can never disappear and remain at constant. This amounts to say that it takes quite many a spectral components to make up a sharp transient feature and that a local variation affects a broad range of the spectrum just as the Fourier transform of the delta function (more precisely, delta distribution) covers the whole frequency axis.
- Fourier basis functions are periodic and extend bi-infinitely; signals thus studied are better to be periodic and sampled infinitely. The unavoidable side effects for not fulfilling these requirements are many: frequency leakages, smoothing errors, edge effects due to data truncations, aliasing due to under-sampling or non-periodicity (figure 1.1 is actually a case of under-sampling, where a linear chirp is sampled at a rate half of the Nyquist frequency), and, uncontrollable spectral variance due to the finite resolution or histogram processing.

Overall, the syndromes associated with the above listed items can be referred to the non-stationary effects.

1.3 Windowed transforms

Both short-time Fourier transform and wavelet transform try to remedy Fourier basis's deficiencies in characterizing transient phenomena by analyzing the set of localized signals. For the short time Fourier transform this can easily be executed by varying m and n in equation 1.1. For the wavelet transform this can be illustrated through the use of the Morlet wavelet by varying its translation and dilation variables.

Both transforms yield local spectral information – more precisely, local scale information, if the term "frequency", "Hz", or "spectrum" is strictly reserved for sinusoidal functions. However, due to the Balian-Low theorem mentioned above, the waveform associated with short time Fourier transform can never be truly local in time since in reality the frequency domain of discrete Fourier transform is always band-limited by obeying the Nyquist law. In this regard, wavelets can be of exactly local; at least, they must have suitable or better decaying property such that they contain no zero-frequency component.

Let us further outline a few specific properties pertaining to individual transform:

- Both short time Fourier transform and wavelet transform are windowed transforms. In short time Fourier transform there exist two quite distinctive operations. The first operation is applying a suitable time-window to the signal; the second operation is performing the Fourier transform for the capped signal. The corresponding inverse transform (or reconstruction process) of the short time Fourier transform is naturally associated with a frequency-window and involves two similar distinctive operations too. However, in wavelet transform these two distinctive steps are not clearly observable — rather than using the very distinctive "window (either time- or frequency-window)" and "Fourier basis function (i.e., sine or cosine function)", the "window" and the "basis function" are synthesized in an inseparable specific form

called “wavelet”. In fact, one can clearly solidify this notion by comparing the Gabor type frame (equation 1.1) with the Morlet wavelet when the window function $g(t)$ of equation 1.1 is assumed to be a Gaussian bell. The intention for either the combined operation or synthesized operation is completely the same: to provide a mechanism (or kernel) for projecting a signal into modulated or oscillating wave constituents.

- The time-frequency windows in short time Fourier transform keep rigid for different scales since the window function $g(t)$ in Equation 1.1 does not depend on m , i.e., their widths (usually referring to time) and heights (usually referring to frequency) do not change for all frequencies. In wavelet transform, the windows are adjusted to different scales, but the sizes (or areas) of different windows are still fixed, i.e., each window’s height and width are inversely proportional and the product remains constant (either for discrete wavelet transform or continuous wavelet transform). The concept of fixed size windows is illustrated by the fixed area of the gray blocks in the phase planes shown in Figures 1.1 and 1.2, where the discrete wavelet packet transforms are performed for a chirp signal using different bases originating from the same seeding mother wavelet. In the figures, since the bases are orthonormal, all time-frequency windows do not overlap. As for the continuous wavelet transform, various time-frequency windows severely tangle with each others. And we generally do not show the actual sizes and shapes of various windows — rather, each window is represented by a point (or a small area depicting the time-frequency resolution) having coordinates corresponding to its centroids in the time and frequency axes.
- The function basis of the short time Fourier transform is the unique orthonormal Fourier basis comprised of sine and cosine functions; whereas, for wavelet transform, apart from the very loose constrain that the basis function (or the mother wavelet) satisfies the admissibility condition (for continuous wavelet transform) or

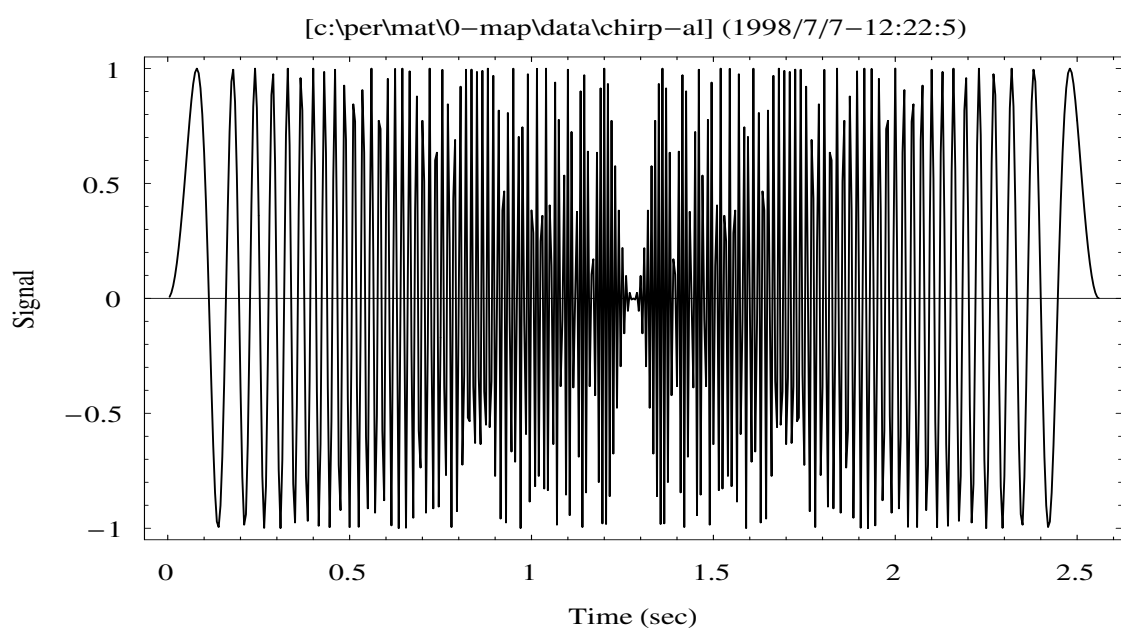
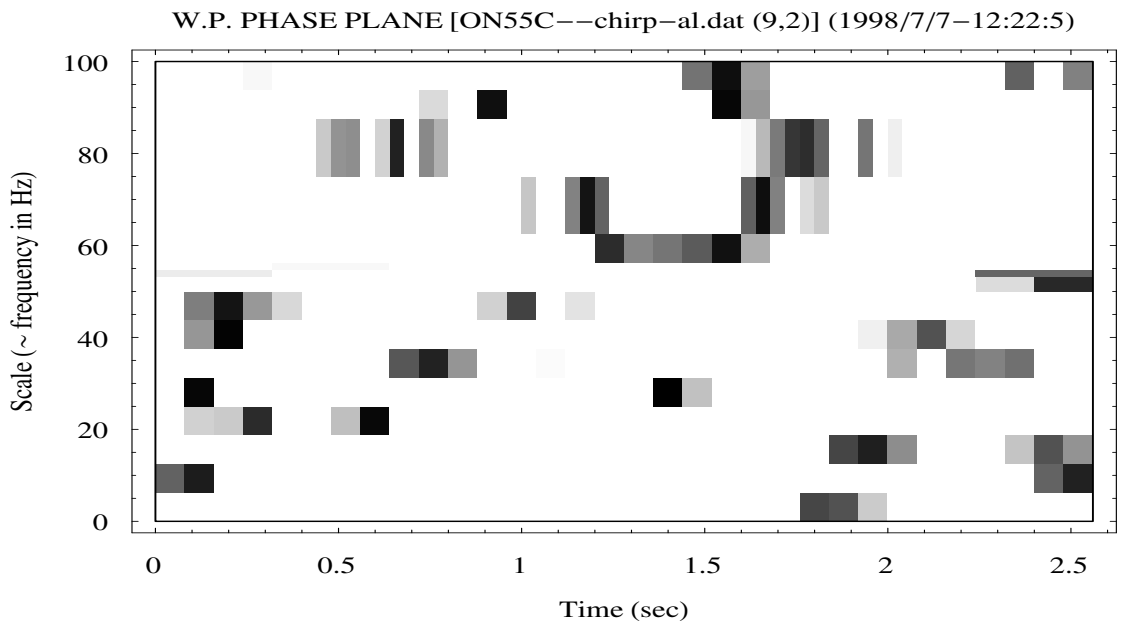


Figure 1.1: Phase plane of a wavelet packet's best basis time-frequency windows (top) for a linear chirp signal that is sampled under aliasing condition (bottom). Here wavelet packets associated with coiflet of 30 convolution weights is used. The original signal, if not under-sampled, has linear instantaneous frequency distribution form 0 to 100 Hz. Note the non-symmetric effects and the scattering of windows due to the composite frequency bands that form the wavelet.

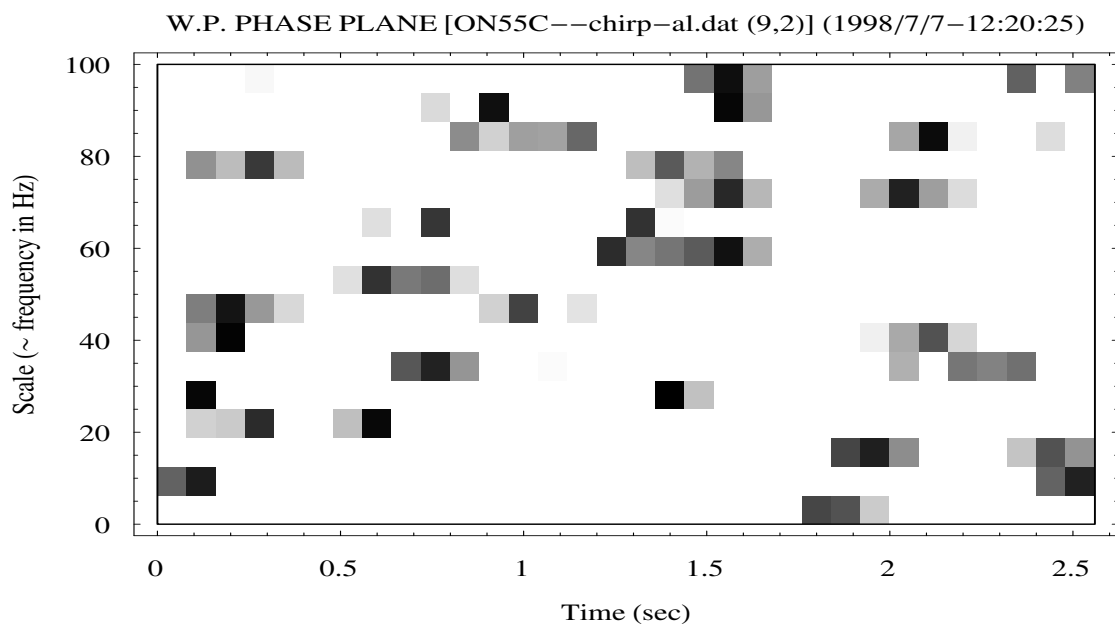
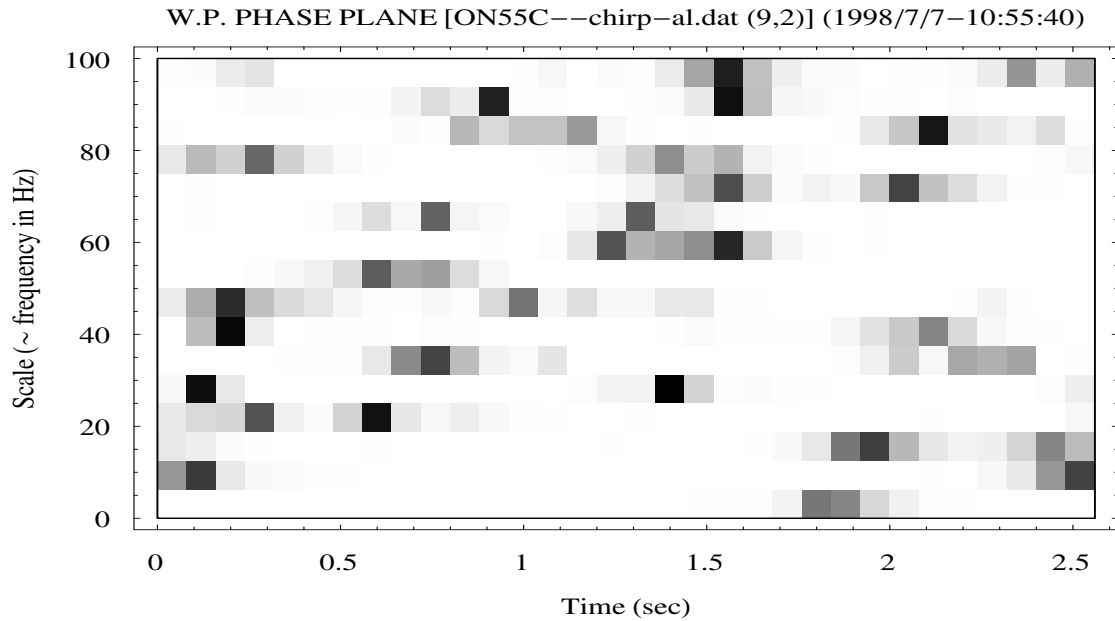


Figure 1.2: Phase planes (top: logarithmic measure; bottom: linear measure) of a wavelet packet's best level time-frequency windows using the same linear chirp and wavelet packets as in the previous figure. In view of the fact that a single orthonormal mother wavelet can yield many different wavelet packet representations, that there are basically infinitely many wavelet bases, and that we may use different graphic renderings, we are easily trapped in the dilemmas of choosing an appropriate basis.

stability condition (for discrete wavelet transform), there is virtually no restriction on the choice of basis functions. The coefficients of short time Fourier transform, which represent local Fourier spectral information, still have the exact meaning of “frequency”. In wavelet transform, wavelet coefficients refer to specific scales rather than “frequencies”. Here, we generally suffer from their physical interpretability due to the following reasons: (1) No unique basis — the analyzing function or mother wavelet can be designed in a plenty of ways, and the basis functions related to the mother wavelet can be either dependent or independent (orthogonal or non-orthogonal); (2) Scale does not have unit — together with the first point, it severely hampers our ability to directly perceive the wavelet’s size and physical shape; and, (3) No fixed algorithm to implement wavelet transform — many techniques and various adaptations exist, such as, the treatment using flexible time-frequency windows for continuous wavelet transform (Lee[9]), multi-voice (Daubechies 1992) or multi-wavelet (Coifman 1992a, b; Wickerhauser 1992) frames, and discrete wavelet transform using different dilation factors other than the most often seen value of 2 (Auscher 1992). Generally speaking, these varieties may not be as disturbing in certain application fields (such as data transmission or signal decomposition and reconstruction) as they are for our studies focusing on the water wave physics.

- In general, the dilation lattice is in logarithmic measure for discrete wavelet transform (e.g., the a_0^j in the stability condition to be mentioned) and in linear measure for discrete short time Fourier transform (e.g., the $e^{-i2\pi mt}$ in the above mentioned Gabor type frame). Continuous transforms do not involve lattice. The concept of lattice is associated with the concept of time-frequency density, which is defined as the inverse of the product of dilation and translation steps (Daubechies 1992). For short time Fourier transform frames, due to Shannon sampling theorem, the time-frequency density must not go beyond the value of generalized Nyquist density, $(2\pi)^{-1}$. For wavelet transform, however, there is no such a clear-cut limit of time-

frequency density. Moreover, Balian-Low theorem depicts that there is no good time-frequency localization for a short time Fourier transform frame if constructed under a strict time-frequency lattice; on the contrary, numerous wavelet bases with good time-frequency localization have been given (Chui 1992a; Daubechies 1992; Meyer 1992). These physically imply that wavelet transform may provide better zoom-in.

- The existence of a lattice structure can be either practical or impractical. For water waves, if we don't anticipate any significant gaps in the scale contents, that is to say, the physical process involves time and spatial scales that are "changing" or "evolving" in a relatively continuous sense, we generally do not appreciate the use of frames. Here a continuous transform may provide better chance of success.
- Both continuous and discrete wavelet transforms implement a process of integral wavelet transform over the real line \mathbf{R} in a continuous sense but they analytically emphasize the use of different integration symbols: \sum and \int . Digitally sampled signals are certainly discrete, but this is irrelevant to the methodology of continuous wavelet transform or discrete wavelet transform. The main difference, from the application point of view, is that there is no practical interest of reconstruction (or inverse transform) for continuous wavelet transform due to the redundant or non-orthogonal nature of its wavelet coefficients. Both methods are capable of decomposing either functions defined over the real line or signals sampled discretely. In reality, applying continuous wavelet transform to sampled data is implemented in a discrete manner; vis-à-vis, doing discrete wavelet transform for an unlimited ladder, such as that of the standard multiresolution analysis of Mallat (1989), can describe any function in infinite detail, i.e., over the whole real line. The concept of unlimited ladder of discrete wavelet transform is illustrated by two examples shown in Figures 2.21 through 2.28 where the blow-ups of individual segments of wavelet curves are shown. The figure also illustrates possible bizarre behaviors of certain

wavelets and indicates that mother wavelets with short support lengths might not be of ideal choices. In addition, a few discrete wavelet transform formulas when generalized in the limit sense are quite helpful in explaining a few continuous wavelet transform characters.

- We note that the present scope focuses on the $L^2(\mathbf{R})$ Banach space, i.e., the Hilbert space, since some of the statements here may not apply to other function spaces or classes (Daubechies 1992; Meyer 1992). Nevertheless, most of the intricacies that differentiate different spaces are only of analytic interest up until now (e.g., on the existence of multiresolution analysis (MRA), on the regularity and differentiability of wavelets and its associated scaling functions). From the practical point of view, it is far enough to restrict to the Hilbert space, i.e., a space of functions with finite energy contents.

1.4 The objectives

The foothold to use localized transforms in our water wave applications can be stated quite simply, as well as intuitively — if we perceive our signal as composed of waves which are limited in both life span and covering distance, i.e., constituent waves are evolving with time and in space, then it is natural to adopt wavelet as our analyzing function; furthermore, in addition to this modulation nature, if we also acknowledge that intrinsic instability due to nonlinear effects or boundary conditions is everywhere to be found for even regular water waves, then it is still quite possible that wavelet decomposition can provide better descriptions of physics for stationary signals than what can be provided by Fourier decomposition. Besides, another advantage of using wavelets is the possible flexibility in adapting their wave forms to our desires; this is related to the modifications of time-frequency windows for better physical implications.

In this study we mainly focus on discrete wavelet categories. And the covered categories should be quite comprehensive — in the sense that they have included all the

extreme analytical properties in wavelet designs. And it is the author's belief that if you ever find an individual wavelet you have great chance to assign it into one of these categories, and if not, you have great reason to say that its properties fall within (or between) the covered characterizations and thus its possible usefulness (or destiny) trapped accordingly. The relevant characterizations and intrinsic properties for all the categories are extensively illustrated through the depictions of their mother and father wavelets, the translations and dilations of wavelets, the zoom-ins or blowups of any kind of wavelets, the linear phase filtering features. Physical counterparts of analytical aspects are provided when possible. Finally the entropy criterion is applied to the whole set of wavelets for signals obtained from wave-tank experiments. And the optimal wavelet basis is judged to be the semi-orthogonal dual wavelet.

The Wavelet Bases Tested and Their Characterizations

2.1 Introduction

In almost all modeling experiments various modeling or scaling laws can at best be partially satisfied. The situation is further complicated for multi-scale and multi-dimensional phenomena. In the introduction chapter we noted the problems of proper scaling for the transient phenomenon that involves diversified scales. For water wave experiments it is acknowledgeable that there may be significant distortions concerning the coupling mechanisms targeted. For example, a limitation in space as well as the lack of scale diversification in the tank may hinder the development of certain mechanisms and impose restrictions upon the evolutions of certain interactions. With these understandings, as well as the cognizance regarding the inadequacy of the Fourier spectral approach in our applications as discussed in the first chapter, it is understandable that, if the modeling of the proposed physics is at all possible, the deployment of an optimized analyzing scheme using sensitive and appropriate basis functions is desired. Specifically speaking, we shall select among a broad array of functional bases the most appropriate one for our signals and describe the proper analyzing method. Akin to the interest of such an attempt, it war-

rants to give more systematical descriptions of different properties of various categories of wavelet function bases. Herein we cover a comprehensive set of discrete wavelet categories that has essentially included all the extreme and opposite analytical properties in wavelet designs.

2.2 The numerical programming

We develop the wavelet numerical analysis and all the relevant data processing from the ground up using the Asyst programming language. It is our desire that the program should provide full coverage of various wavelet bases and it should also be capable of exploring any related characterizations of wavelet relevant functions. Besides, it should be quite flexible yet user-friendly. And it is our belief that any keyboard input of data or information should be minimized to none (cut and paste might in rare cases be unwillingly tolerated). To achieve such goal, several program add-ins and application auxiliaries are integrated; notably, these include:

- The Postfix language — This enables the generation of high quality Encapsulated Postscript figures directly from the core programming, and this much improves the overall code writing efficiency, as well as eliminates the painful task of plotting the numerous figures during testings. Besides, full annotations of parameters for all the figures are much possible and thus analyses are confidently error free.
- The on-screen real time display of PCX format figures — The Encapsulated Postscript figures is mainly for quality printing, but it forms in the background and does not display in real time during the running process of the program; therefore, the on-screen real time display of figures should greatly enhance the debugging efficiency and make possible the writing of a huge and complex program that is also user-friendly, easy to maintain, as well as interactive and extremely flexible.
- The data spreadsheet interface — The input or output of data from and to Excel or

Lotus-123 compatible worksheet is integrated. In cases that articulate figures are desired such a function is readily convenient.

- The data interface to Mathematica programming language — This eliminates human intervention for the transferring of results of Asyst analyses to the post generation of various two-dimensional phase plane figures.
- The WinEdt macro programming language — The language is specifically used to develop the shell environment or the development platform for the Asyst program code writing. With this all the code components are displayed in much a scientifically organized and eye-pleasant way. Missing such an integrated part the editing and the debugging of the programs must be quite painful and exhausting.

2.3 Wavelet bases tested and the relevant notations

The Riesz wavelet bases tested here can basically be divided into four categories: orthonormal (ON), semi-orthogonal (SO), bi-orthogonal (BO), and orthonormal wavelet packets bases. For the orthonormal category it is divided into several different subgroups: Daubechies wavelets (both the most and least asymmetric), Coiflets, Meyer wavelet, and Battle-Lemarié wavelets.

No detail accounts of these wavelets will be given; only the main criteria and core features of each categories will be briefed. Let first state the related notations and conventions needed for the context that follows. Let a function or a signal be denoted by $f(t)$; the two-scale scaling function of a Riesz basis be $\phi(t)$; the associate mother wavelet be $\psi(t)$ and its dyadic wavelets be $\psi_{j,k}(t) = \sqrt{2^j} \psi(2^j t - k)$, where $j, k \in \mathbf{Z}$ and k stands for translation and j for dilation. The concept of translations and dilations are illustrated in Figures 2.1 through 2.6.

The space V_j (formed by $\psi_{j,k}$, $k \in \mathbf{Z}$ for a given j) in the multiresolution ladder are nested in $\cdots \subset V_{-1} \subset V_0 \subset V_1 \cdots$, and the finest and the coarsest scale space, say,

for a 1024-point signal, are V_{10} and V_0 , respectively; the number of filter coefficients or the number of convolution weights be N if the associated wavelet is finitely supported (support length equals to $N - 1$); the dual wavelet and dual scaling function, if exist, be $\tilde{\psi}(t)$ and $\tilde{\phi}(t)$; the inner product be $\langle \cdot, \cdot \rangle$; and the Kronecker delta be $\delta_{j,k}$, $j, k \in \mathbf{Z}$, which is equal to 0 for $j \neq k$ and 1 for $j = k$.

Up until now, all practical wavelets of discrete transform are associated with the theory of multiresolution analysis (MRA) (Mallat 1989; Daubechies 1992). For Riesz wavelets there always exist dual wavelets except for orthonormal wavelets, which are self-dual. Any discrete wavelet transform involves two convolution operations: one yields detail information; another yields smooth information (Press et al. 1992). Convolutions can either be implemented in a direct way in the time domain for compactly supported wavelets or in an indirect way in the frequency domain. We list the basic properties (restricted to real-valued wavelets) and give the symbols of representation for various categories and subgroups as follows.

2.4 Orthonormal wavelets

The orthonormal wavelets covered here include the following categories: Daubechies most compactly supported wavelets (denoted as ON_{xx}A); Daubechies least asymmetric wavelets (ON_{xx}S); Coiflets (ON_{xx}C); Meyer wavelet (Meyer); Battle and Lemarié wavelet (B&L). Here in all the subsequent annotation x is an integer related to support length (physically, the span of mother wavelet curve).

$$\psi = \tilde{\psi}, \quad (2.1)$$

$$\phi = \tilde{\phi}, \quad (2.2)$$

$$\langle \psi_{j,k}, \tilde{\psi}_{l,m} \rangle = \delta_{j,l} \delta_{k,m}, \quad (2.3)$$

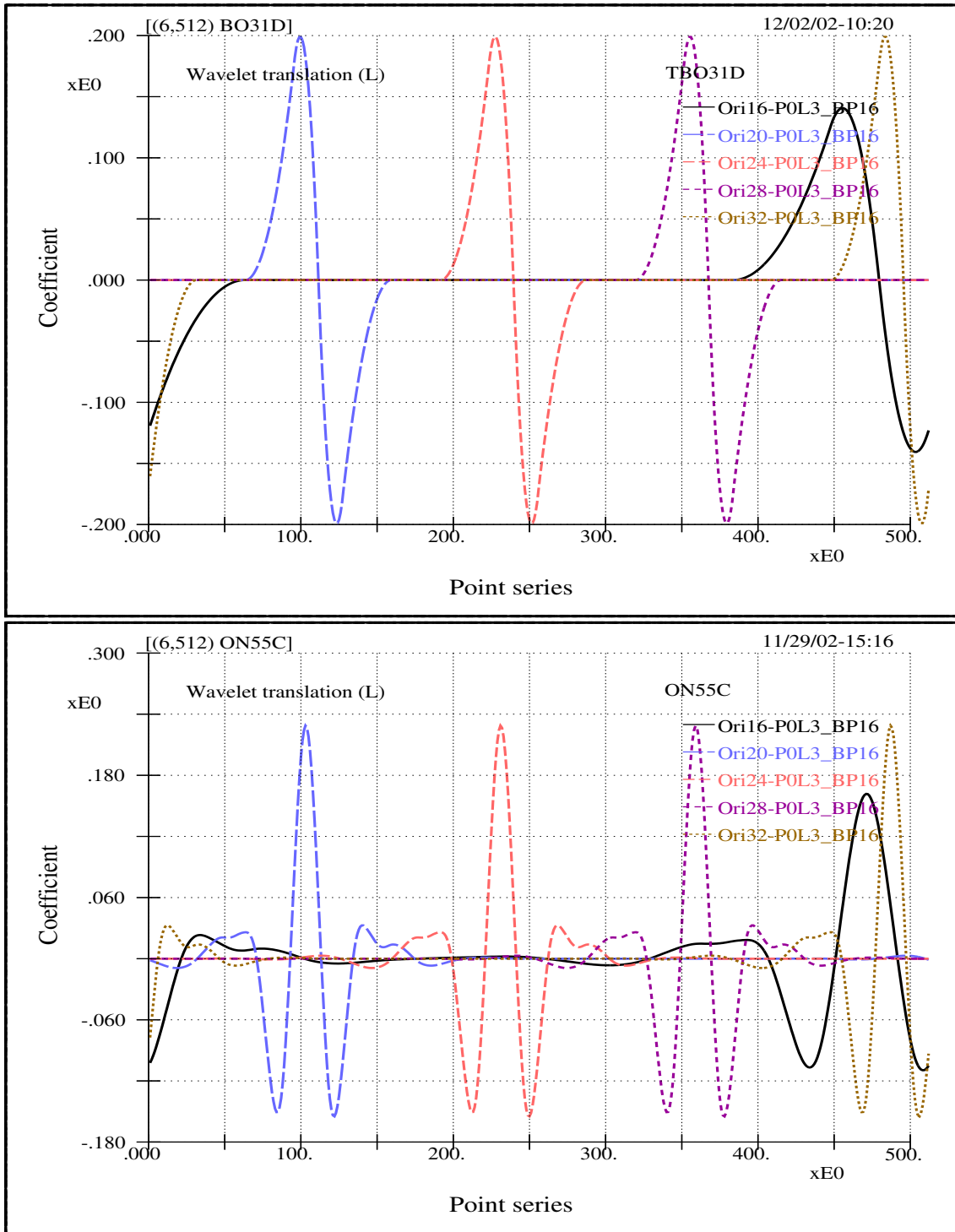


Figure 2.1: The wavelet translation concept within the scale range of level 3.

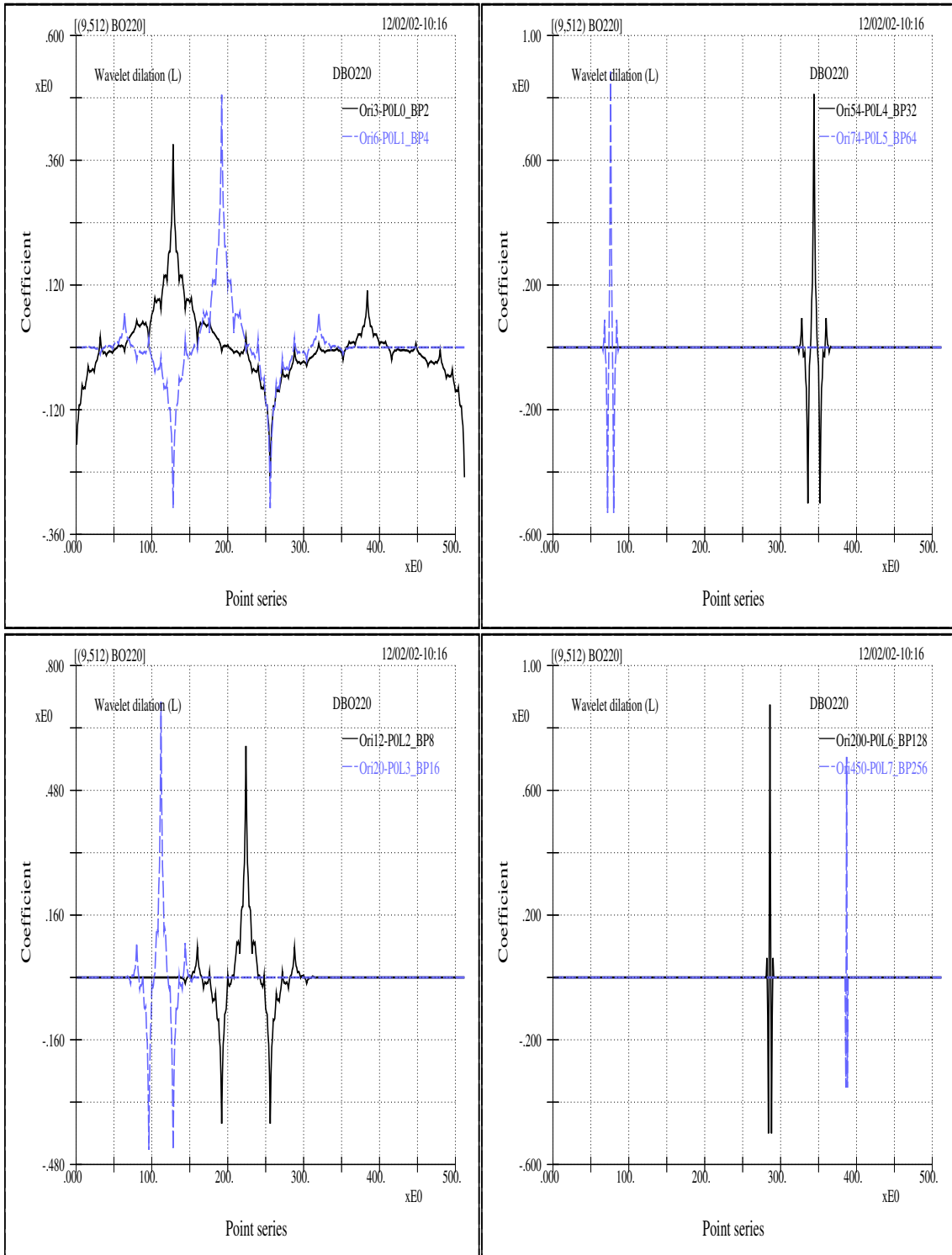


Figure 2.2: The wavelet dilation concept from scale level 0 to level 7 for the BO220 wavelet. Each wavelet curve corresponds to an individual translation location.

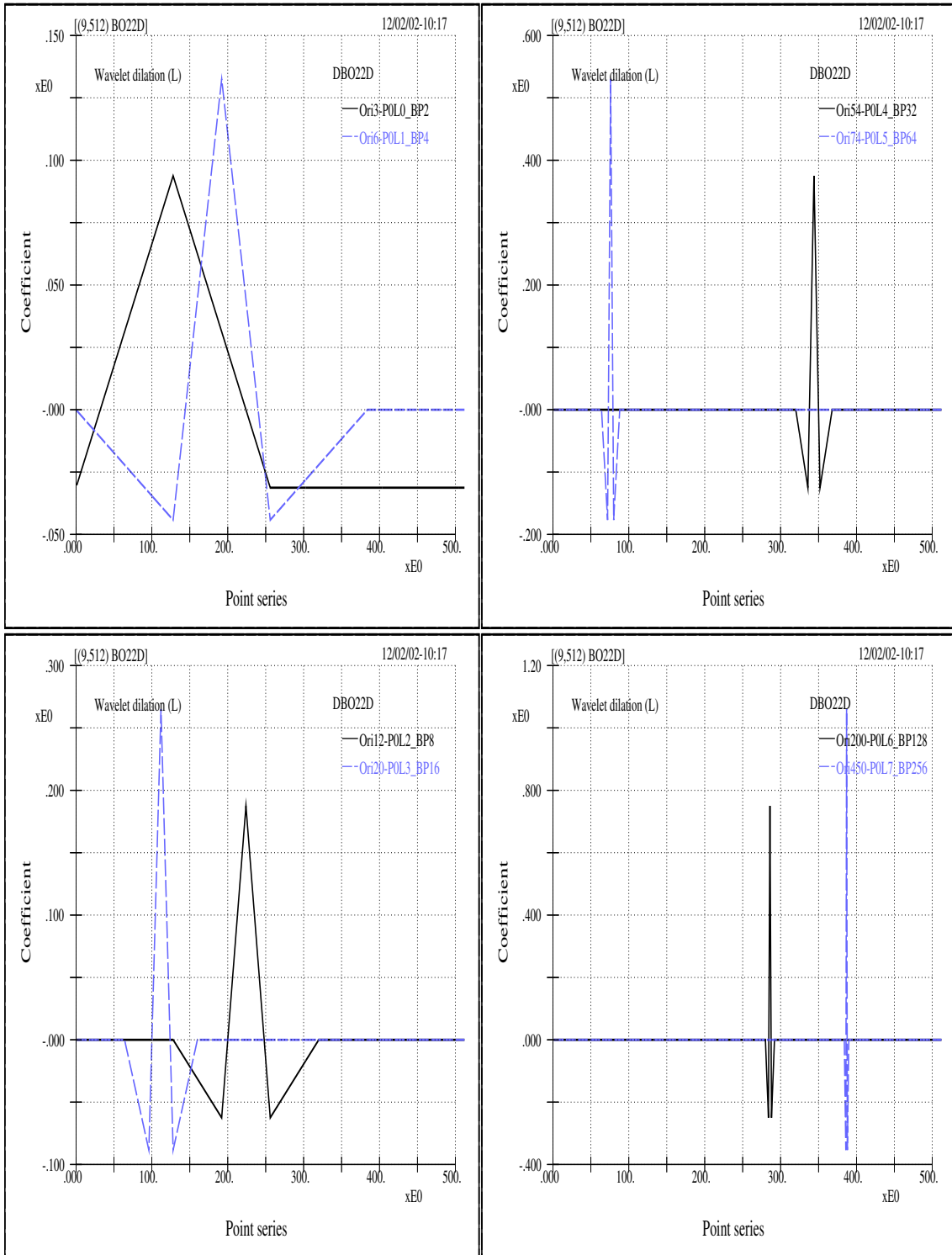


Figure 2.3: The wavelet dilation concept from scale level 0 to level 7 for the BO22D wavelet. Each wavelet curve corresponds to an individual translation location.

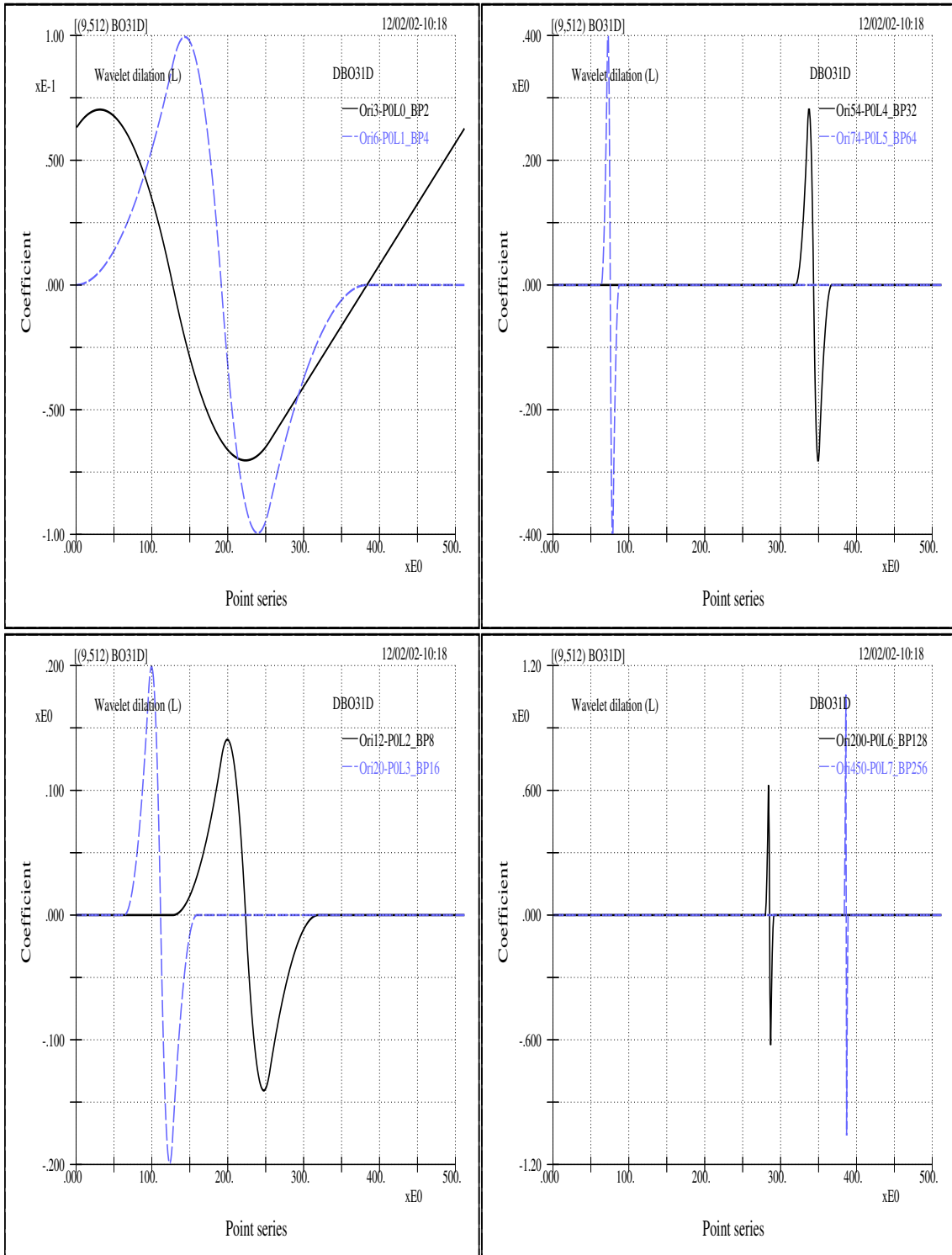


Figure 2.4: The wavelet dilation concept from scale level 0 to level 7 for the BO31D wavelet. Each wavelet curve corresponds to an individual translation location.

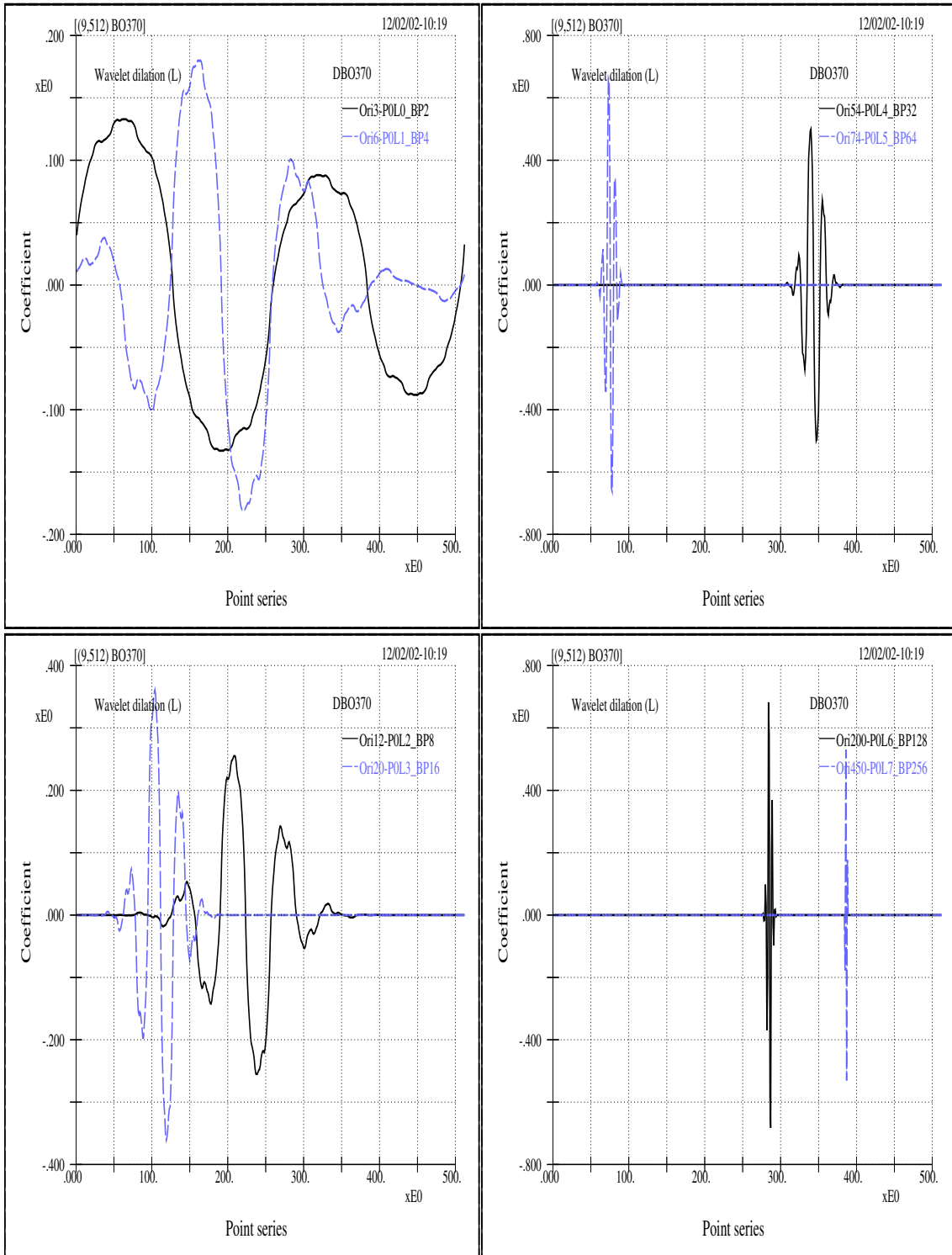


Figure 2.5: The wavelet dilation concept from scale level 0 to level 7 for the BO370 wavelet. Each wavelet curve corresponds to an individual translation location.

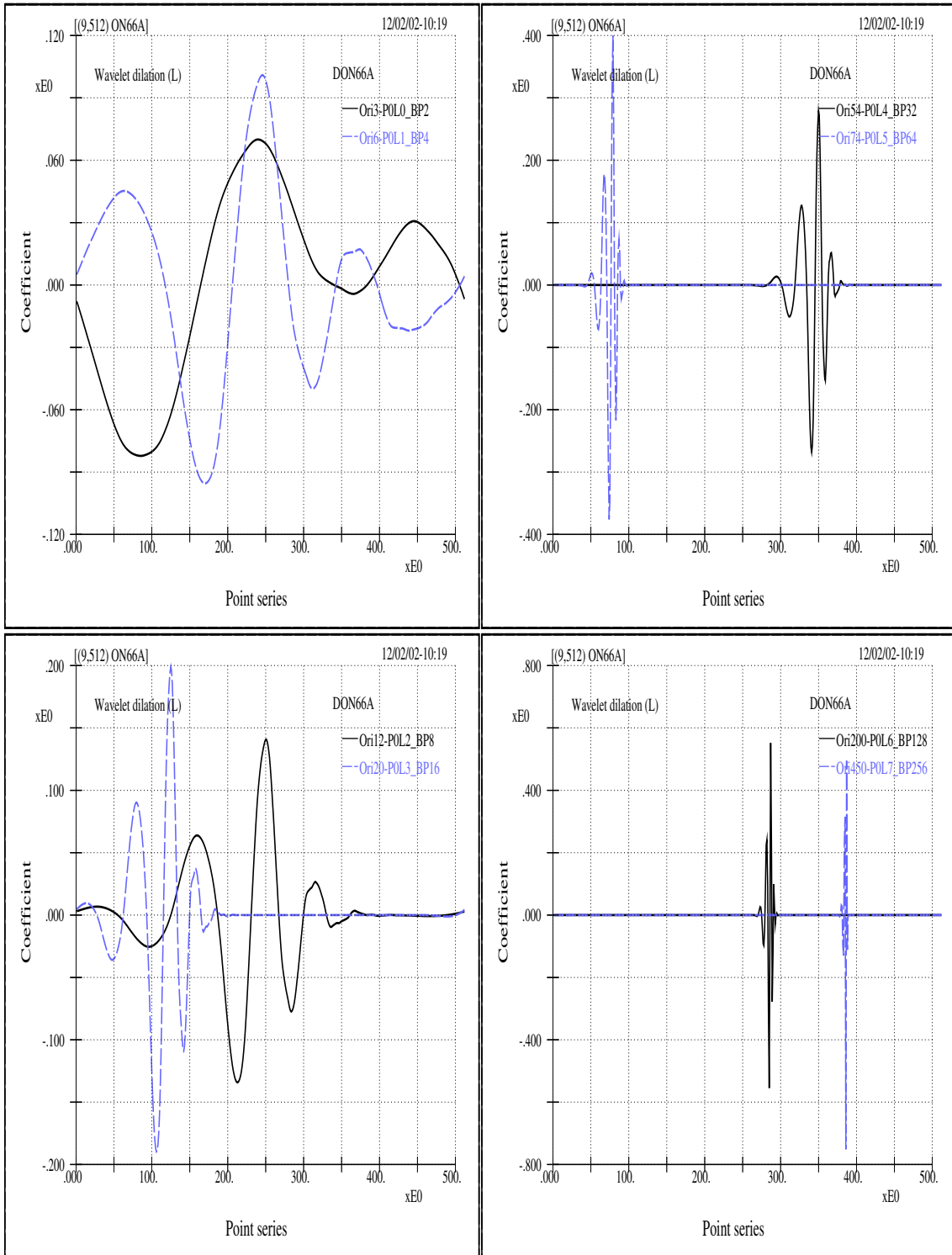


Figure 2.6: The wavelet dilation concept from scale level 0 to level 7 for the ON66A wavelet. Each wavelet curve corresponds to an individual translation location.

$$f(t) = \sum_{j,k} \langle f, \psi_{j,k} \rangle \psi_{j,k}, \quad (2.4)$$

One MRA ladder (single set of frame bounds),

One filter pair (one smooth and one detail).

2.4.1 Daubechies most compactly supported wavelets (ON_xxA)

The wavelets in this group have maximum number of vanishing moments for given compatible support width. Or stated otherwise, they are the most compactly supported wavelets for given compatible number of vanishing moments. The famous most compactly supported continuous wavelet belongs to this group and has only four filter coefficients. These wavelets are quite asymmetry (so, the “A” in ON_xxA). The mother and farther wavelets for the group corresponding to the originating points of 12 (boundary point based on level 2) and 6 (boundary point based on level 3), respectively, for this group are shown in Figures 2.7 and 2.8. The vanishing moments and the number of filter coefficients are, respectively,

$$\int_{-\infty}^{\infty} t^l \psi(t) dt = 0, \quad l = 0, 1, \dots, x, \quad (2.5)$$

$$N = 2x, \quad (2.6)$$

where x is the integer number in ON_xxA. The minimum number of x is 2.

2.4.2 Daubechies least asymmetric wavelets (ON_xxS)

For a given support width, these wavelets, in contrast to those of the ON_xxA subgroup, are the most symmetric ones (so, the “S” in ON_xxS, but still not symmetric). They have the same representations of vanishing moments and number of filter coefficients as those of ON_xxA. But the known minimum number of x is 4. The mother and farther wavelets for this group corresponding to the same originating points as the previous ones are shown in Figures 2.9 and 2.10.

2.4.3 Coiflets (ON_xC)

The Coiflets have vanishing moments for both ψ and ϕ ; therefore, from Taylor expansion point of views (Daubechies 1992), they have high compressibility for fine detail information (i.e., a great portion of the fine scale wavelet coefficients are relatively small); and henceforth, they have simple quadrature rule to calculate the fine smooth information (i.e., the calculation of the inner product of a function and the fine-scale scaling functions is more efficient). Since every discrete wavelet transform involves both smoothing and detailing operations, there may exist some advantages from these two properties for certain applications such as applications that do not stress lossless of signal contents or perfect reconstructions (Coifman et al. 1992a; Wickerhauser 1994). Their vanishing moments and number of filter coefficients are

$$\int_{-\infty}^{\infty} t^l \psi(t) dt = 0, \quad l = 0, 1, \dots, x, \quad (2.7)$$

$$\int_{-\infty}^{\infty} \phi(t) dt = 1, \quad (2.8)$$

$$\int_{-\infty}^{\infty} t^l \phi(t) dt = 0, \quad l = 1, \dots, x, \quad (2.9)$$

$$N = 6x. \quad (2.10)$$

For this group the mother and farther wavelets are shown in Figures 2.11 and 2.12.

2.4.4 Meyer wavelet (Meyer)

The Meyer wavelet (denoted as Meyer or ME in figures) is the wavelet with most compact support in frequency domain (here, if without any specific assignment, “finitely supported” refers to time domain). Therefore, due to contrast properties between the two Fourier domains, the wavelet is infinitely differentiable in time domain, i.e., has an infinite Lipschitz regularity C^∞ and does not have exponential decay. And the support length $N \rightarrow \infty$. The associated mother and farther wavelets corresponding to the same

originating points are shown in Figure 2.13.

2.4.5 Battle and Lemarié wavelet (B&L)

The Battle and Lemarié wavelet (denoted as B&L or LE in figures) of m^{th} order is constructed from the orthonormal scaling function derived by applying the standard orthonormalization trick to the m^{th} order cardinal B -spline N_m (Battle 1992; Chui 1992). For $m = 1$, it is exactly the Haar wavelet. The latter is the only finitely supported wavelet in this group (also the case of BO11O=BO11D to be mentioned below) and is also a discontinuous wavelet with the most compact support. All other wavelets in this group are infinitely supported. These wavelets have an exponential decay and possess C^{m-2} regularity. The mother and father wavelets for the Battle-Lemarié wavelet are shown in Figure 2.14. Compared to the curves of Meyer wavelet (Figure 2.13), they look quite identical even though their constructions, or derivations, or formula involved (including Lipschitz regularity and decay property) are completely different.

2.5 Semi-orthogonal wavelets (SO_xO and SO_xD)

The semi-orthogonal wavelets are inter-scale, but not inner-scale, orthogonal. Their scaling functions are cardinal B -spline N_m and have finite two-scale relations. Although there are two distinctive (independent) filter pairs (one for the decomposition and the other for the reconstruction), there is only one MRA V_j -ladder. It was shown by Chui (1992a, b) that the cardinal B -spline wavelet of an order higher than $m = 3$ is almost a modulated Gaussian (but a modulated Gaussian is not a wavelet). Therefore only the fourth order Cubic B -spline wavelet ($m = 4$) is tested. It has the following characterizations.

$$\psi \neq \tilde{\psi}, \quad (2.11)$$

$$\phi = \tilde{\phi}, \quad (2.12)$$

$$\langle \psi_{j,k}, \psi_{l,m} \rangle = \langle \tilde{\psi}_{j,k}, \tilde{\psi}_{l,m} \rangle = \delta_{j,l}, \quad (2.13)$$

$$f(t) = \sum_{j,k} \langle f, \psi_{j,k} \rangle \tilde{\psi}_{j,k} = \sum_{j,k} \langle f, \tilde{\psi}_{j,k} \rangle \psi_{j,k}, \quad (2.14)$$

$$N = 3x - 1 \quad \text{for SOxD}, \quad (2.15)$$

$$N \rightarrow \infty \quad \text{for SOxO}. \quad (2.16)$$

One MRA ladder ,

Two filter pairs ,

The mother and father wavelets of the fourth order and the associated dual wavelets are shown in Figure 2.15.

2.6 Bi-orthogonal wavelets (BO_xyO and BO_xyD)

The wavelets in this category are constructed also by Daubechies, and are sometimes called non-orthogonal wavelets. As is well known all real-valued orthonormal compactly supported wavelets, except the Haar wavelet, are not symmetrical. However, from the point of view of reconstructing a signal from its partially truncated wavelet coefficients, the symmetry is a desired property of the filter when a more natural perception or smoother variations is important. There is a very practical implication here: if non-symmetrical function bases are used, then a small change in the wave form causes significant variations of scale information. In other words, to have minor impacts to the data analysis, it is desirable to have bases as symmetrical as possible. Moreover, when considering that random errors, or noise, or uncontrolled factors are present, we should be able to comprehend the significance of this property. In fact many of the figures given in this study indicate such a feature. The symmetry can be achieved by sacrificing orthogonality; if this is the case one has dual pairs for both wavelets and scaling functions. It is obvious that conditions for semi-orthogonal cases are more general than those of orthogonal ones,

and the bi-orthogonal cases are even more general. This situation is clearly indicated by the additional freedom of dual scaling function, as is reflected by the two parameters x and y in the notations of BO_{xy}O and BO_{xy}D . Nevertheless, the wavelets in this category involve only one pair of independent filters for both decomposition and reconstruction even though there involve two different MRA ladders that are associated with their own individual sets of Riesz bounds. This is quite opposite to the case of semi-orthogonal wavelets where they involve one MRA ladder but with two filter pairs.

$$\psi \neq \tilde{\psi}, \quad (2.17)$$

$$\phi \neq \tilde{\phi}, \quad (2.18)$$

$$\langle \psi_{j,k}, \tilde{\psi}_{l,m} \rangle = \langle \phi_{j,k}, \tilde{\phi}_{l,m} \rangle = \delta_{j,l} \delta_{k,m}, \quad (2.19)$$

$$f(t) = \sum_{j,k} \langle f, \psi_{j,k} \rangle \tilde{\psi}_{j,k} = \sum_{j,k} \langle f, \tilde{\psi}_{j,k} \rangle \psi_{j,k}, \quad (2.20)$$

$$N = 2y + x - 1 \quad \text{for } \text{BO}_{xy}\text{O} \text{ and } x \text{ odd}, \quad (2.21)$$

$$N = 2y + x - 2 \quad \text{for } \text{BO}_{xy}\text{O} \text{ and } x \text{ even}, \quad (2.22)$$

$$N = 2y + x - 1 \quad \text{for } \text{BO}_{xy}\text{D} \text{ and } y \text{ odd}, \quad (2.23)$$

$$N = 2y + x - 2 \quad \text{for } \text{BO}_{xy}\text{D} \text{ and } y \text{ even}. \quad (2.24)$$

Two MRA ladders,

One filter pair,

The mother and father wavelets for this group and the associated dual wavelets are shown in Figures 2.16 through 2.19.

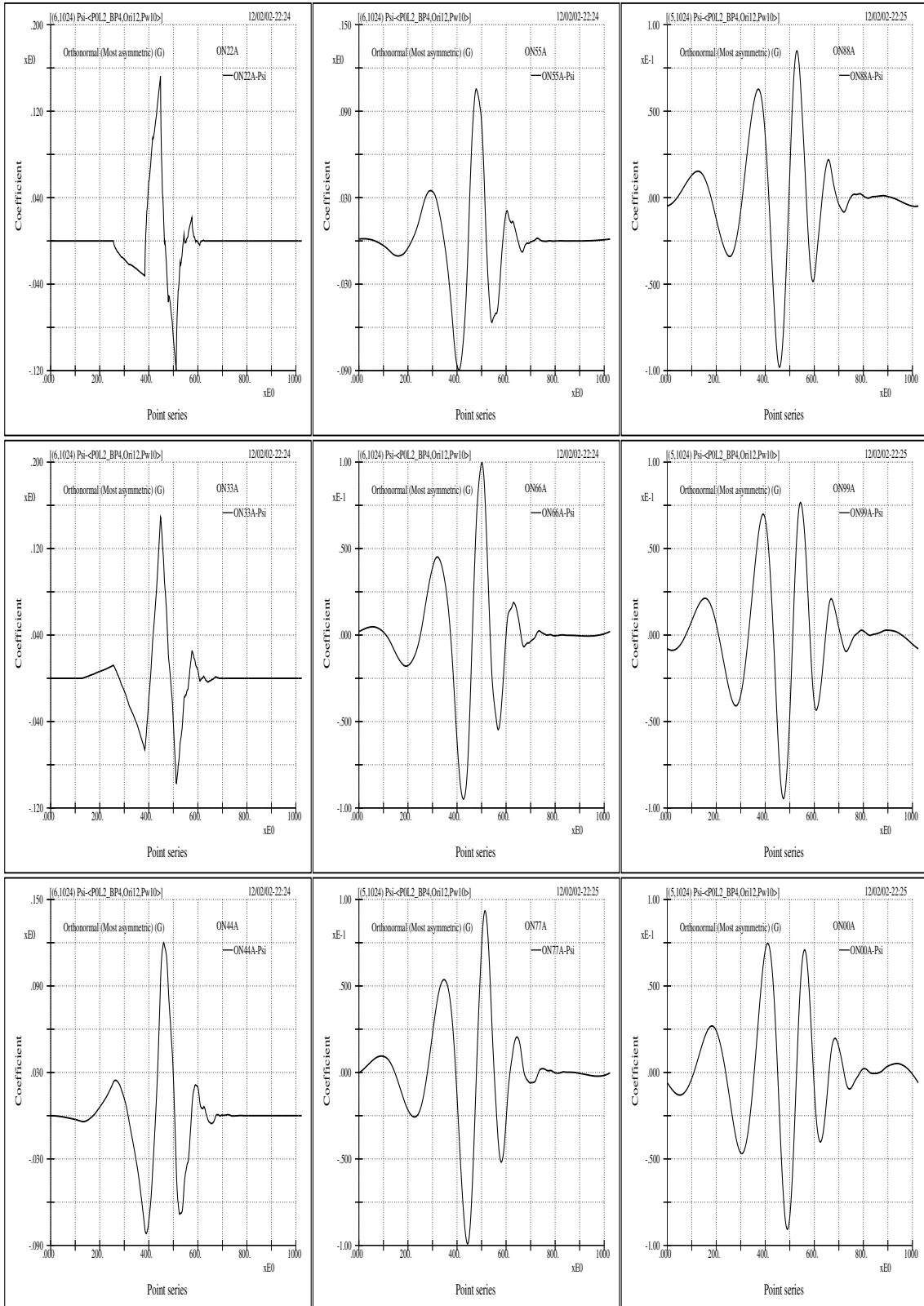


Figure 2.7: The mother wavelets of the ONxxA group originating from the point location of 12. Here the boundary point should be based on a level less or equal to 3.

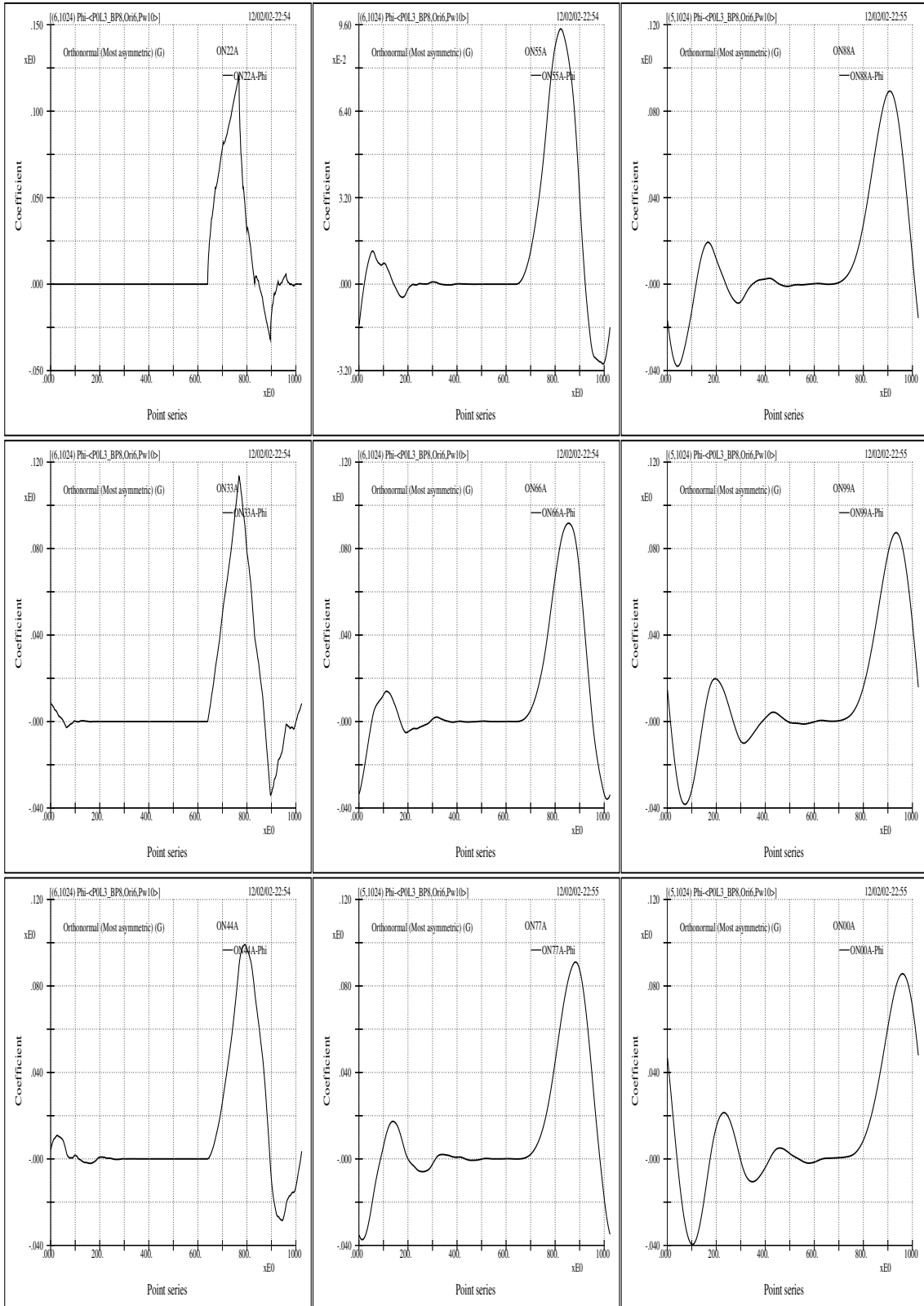


Figure 2.8: The farther wavelets of the ON xx A group originating from the point location of 6. Here the boundary point should be based on a level higher or equal to 3.

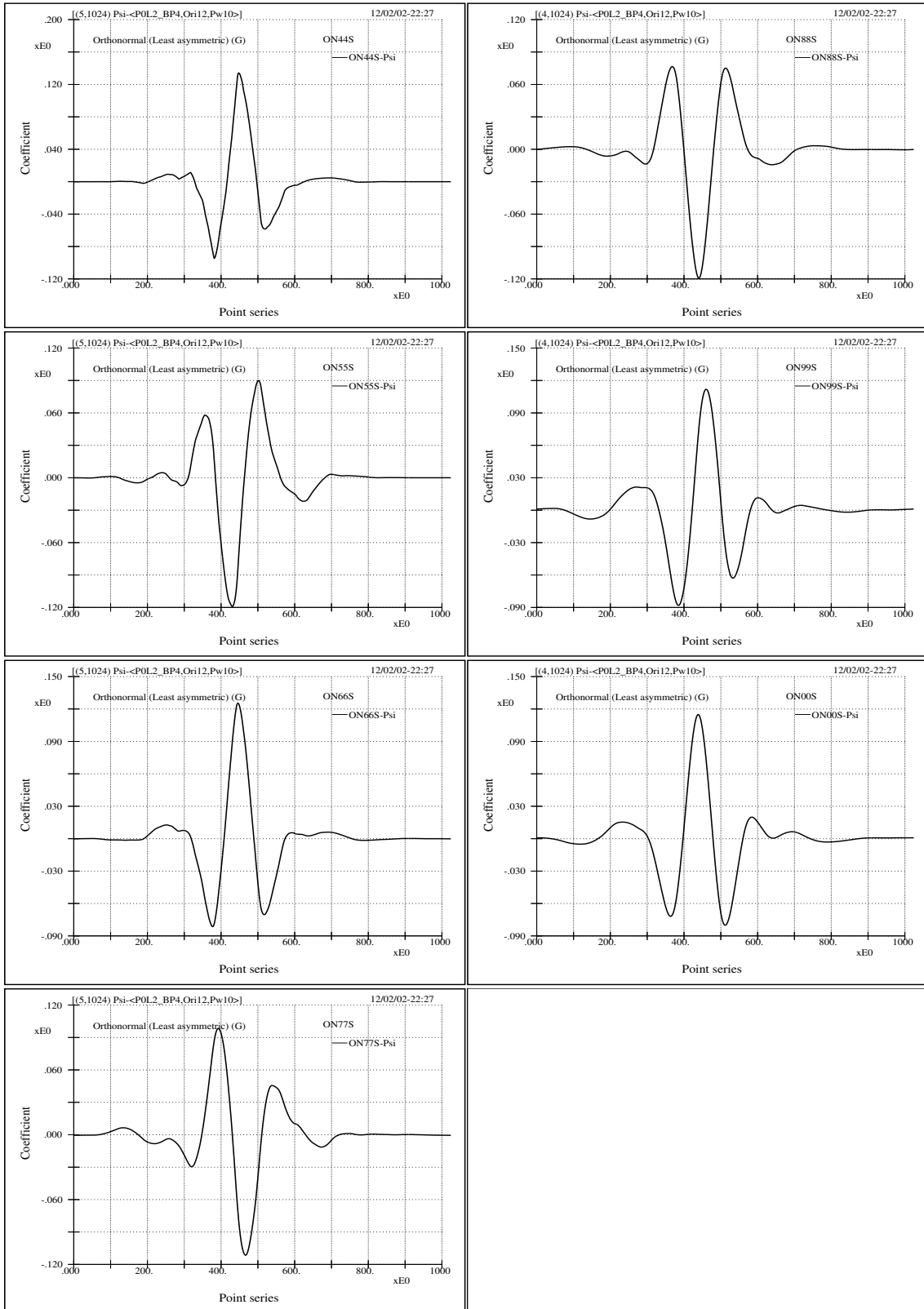


Figure 2.9: The mother wavelets of the ON x x S group originating from the point location of 12. Here the boundary point should be based on a level less or equal to 3.

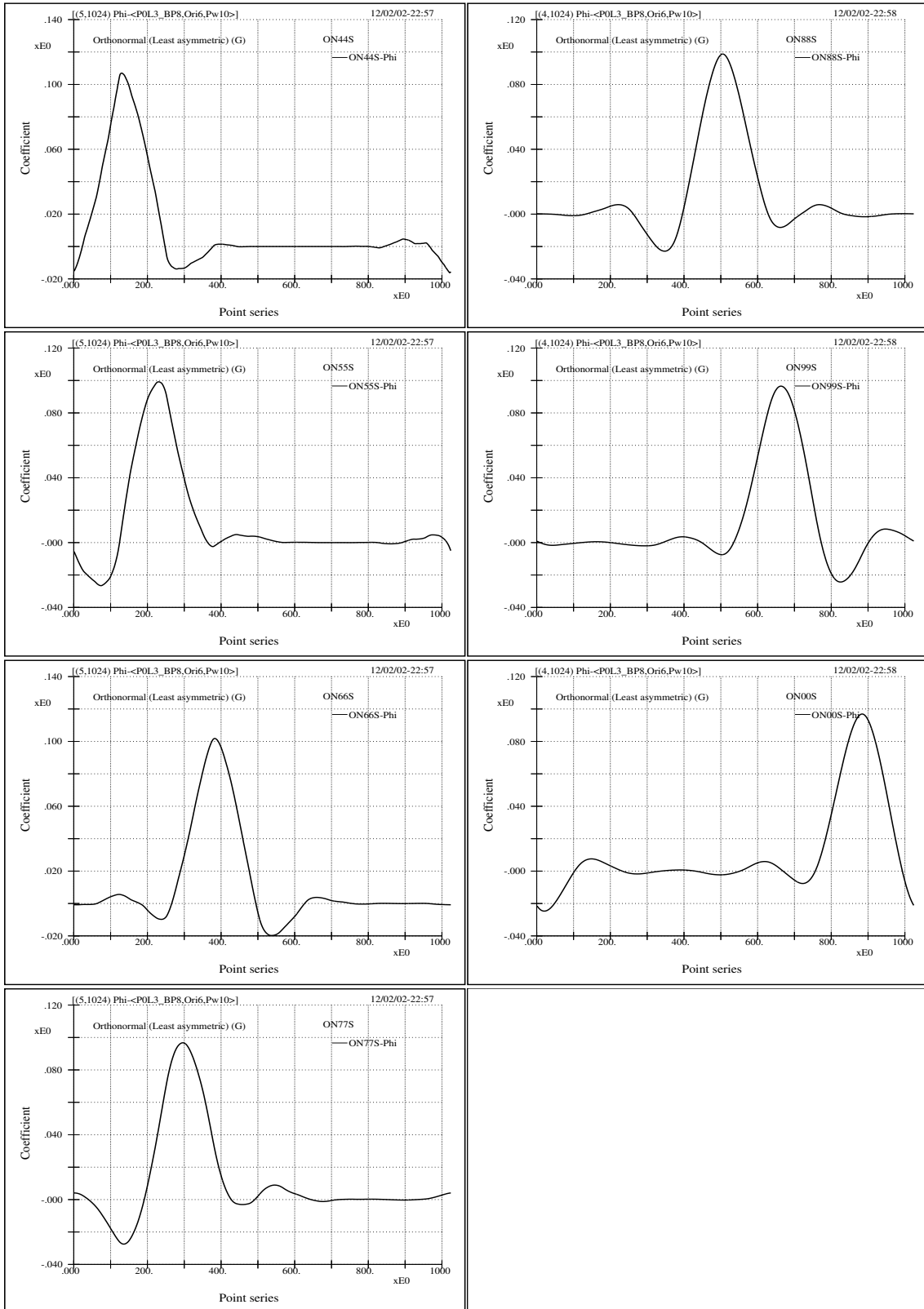


Figure 2.10: The farther wavelets of the ON x xS group originating from the point location of 6. Here the boundary point should be based on a level higher or equal to 3.

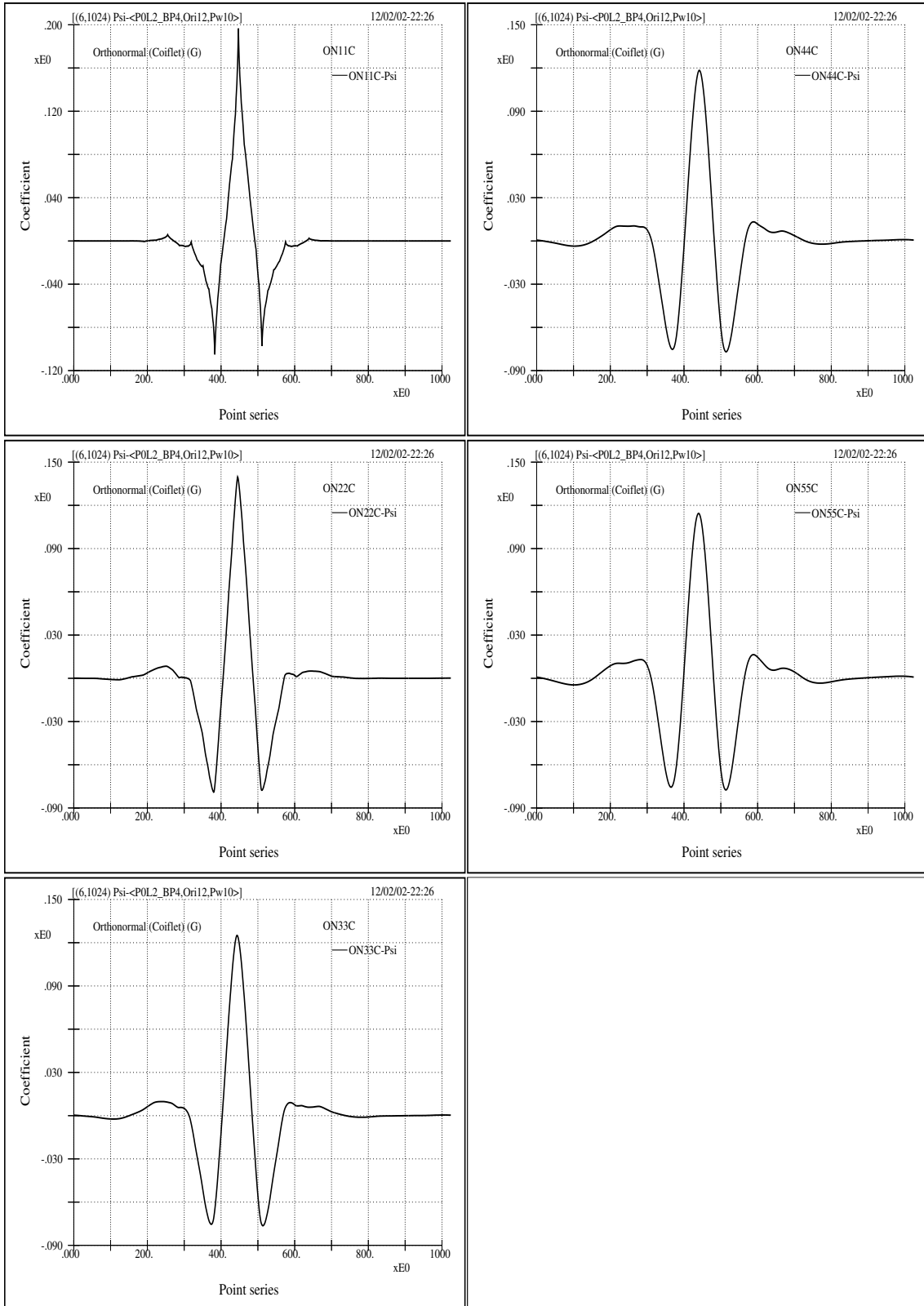


Figure 2.11: The mother wavelets of the ON xx C group originating from the point location of 12. Here the boundary point should be based on a level less or equal to 3.

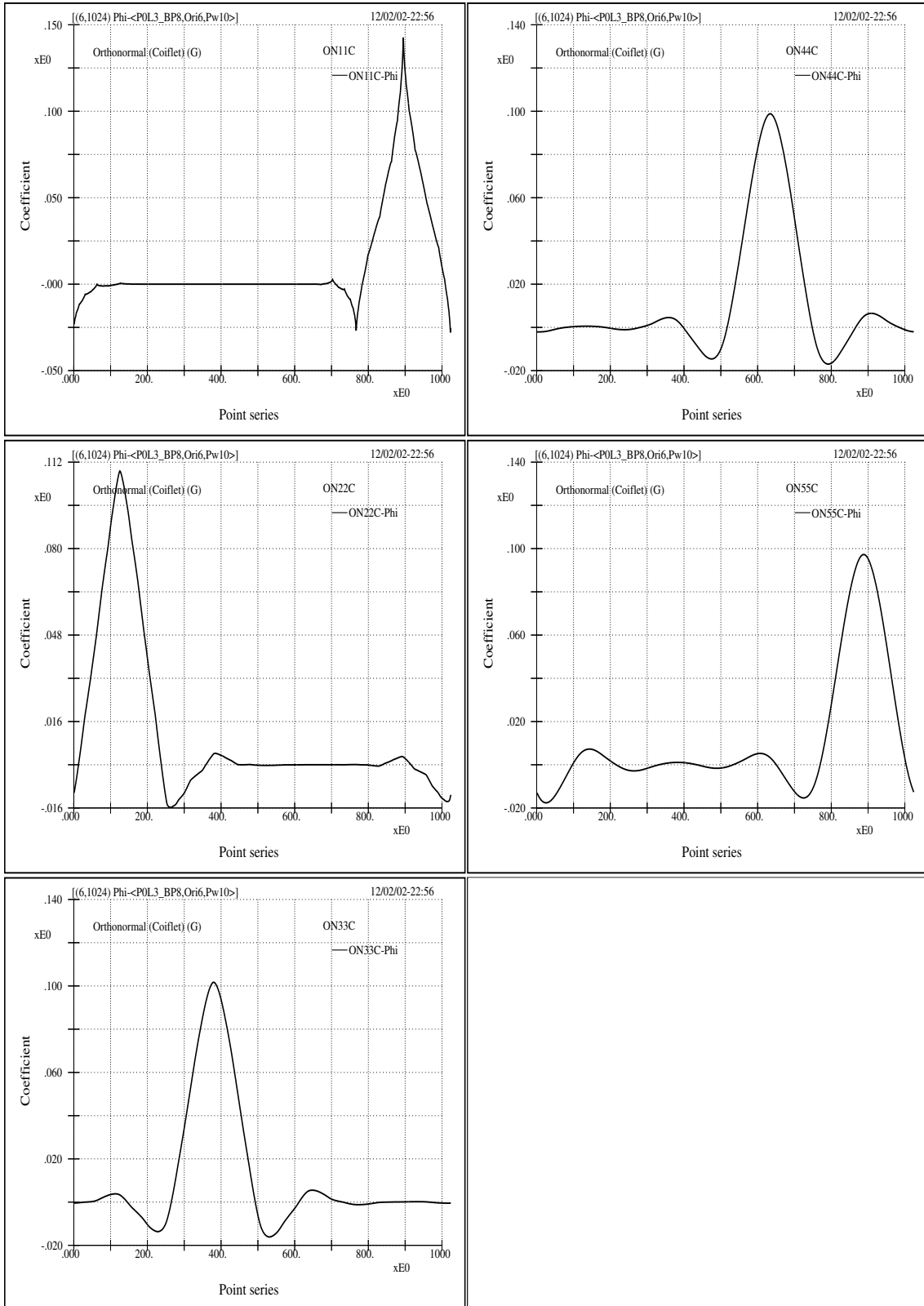


Figure 2.12: The farther wavelets of the ON_x.x_C group originating from the point location of 6. Here the boundary point should be based on a level higher or equal to 3.

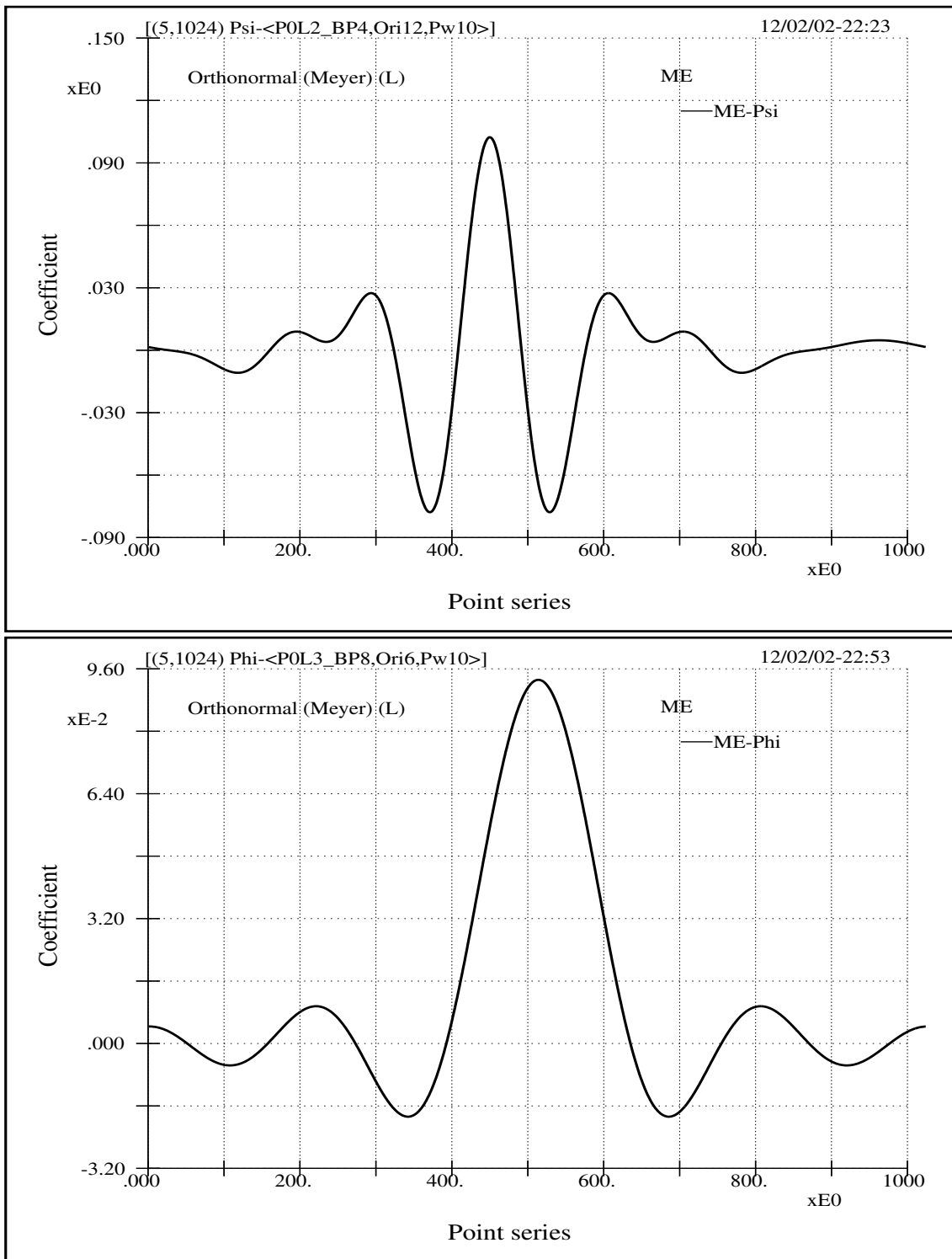


Figure 2.13: The mother (top) and father (bottom) wavelets of the Meyer wavelet originating from the point location of 12 and 6, respectively, for the boundary point based on level 3. This figure is to be compared to the next one.

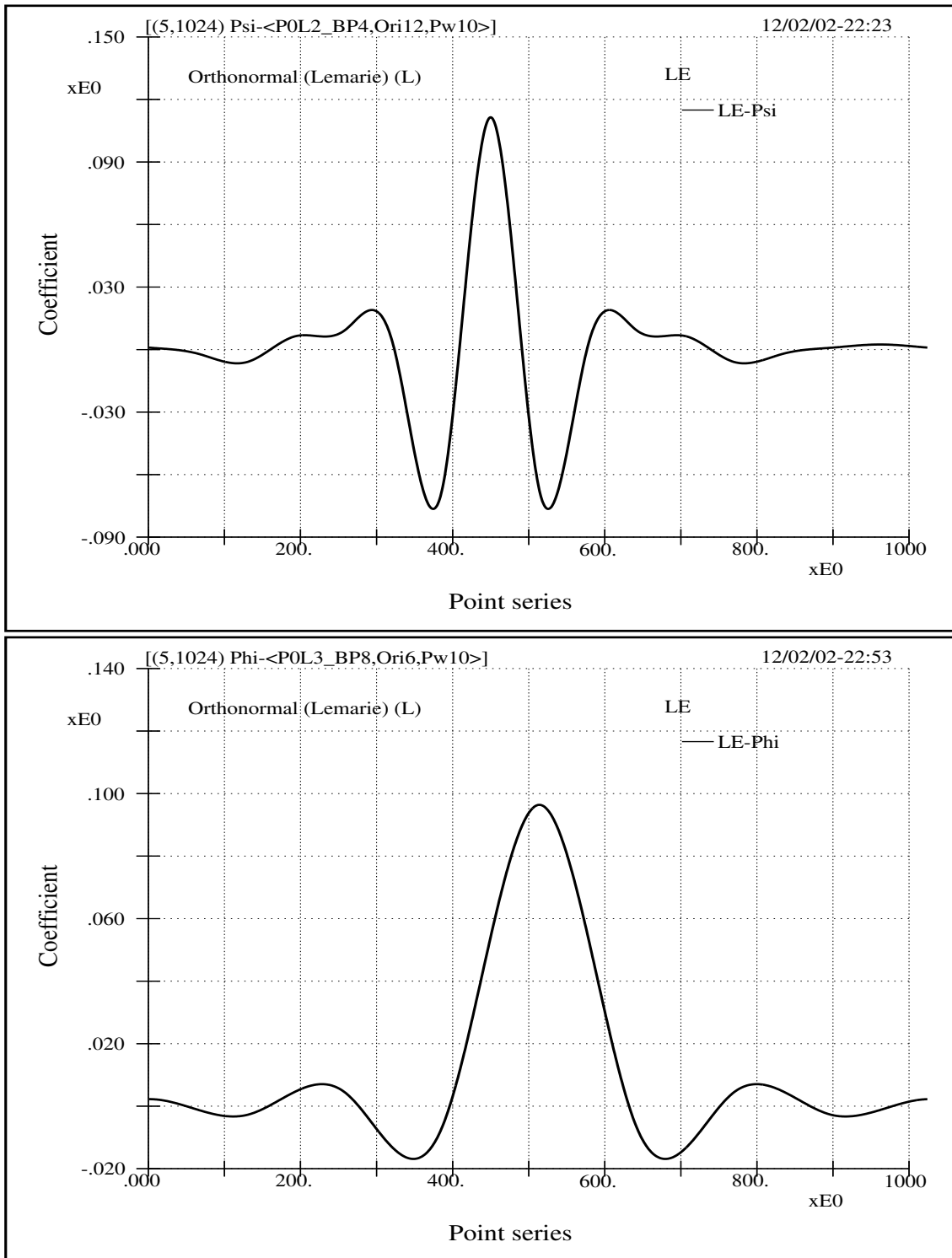


Figure 2.14: The mother (top) and farther (bottom) wavelets of the Battle and Lemarié wavelet originating from the point location of 12 and 6, respectively, for the boundary point based on level 3. Comparing the wavelet functions shown here with those shown in last figure (Figure 2.13), we see that two wavelets of similar looks but with quite distinctive constructions and analytic properties (such as regularity, differentiability, rate of decay, support length, etc.) It therefore gives rise the concerns that many complicated aspects of discrete Riesz wavelet seem not to reflect their associations with practical concerns.

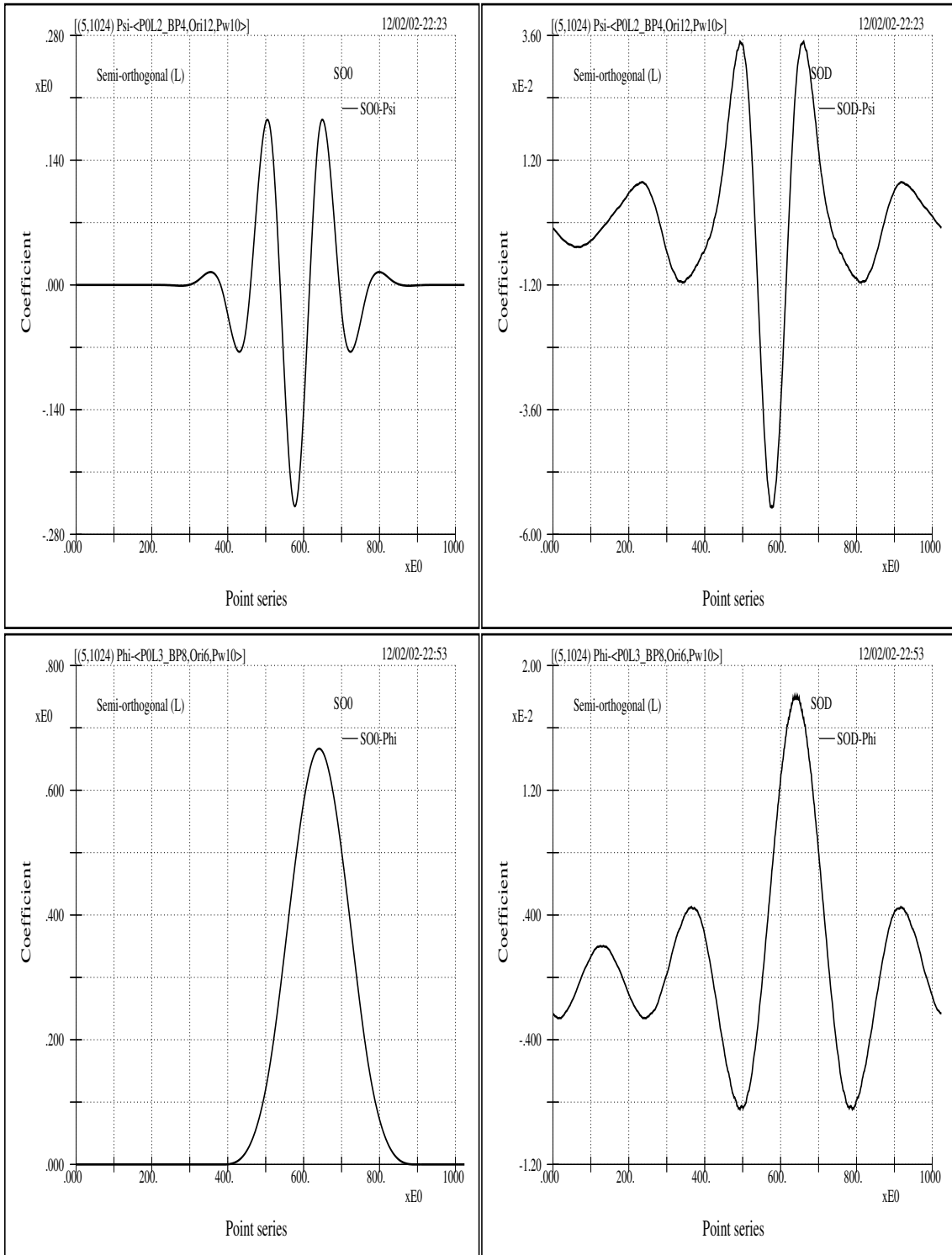


Figure 2.15: The mother (top left) and farther (bottom left) wavelets, as well as their duals (right), of Chui's semi-orthogonal wavelet [3, 4] originating from the point location of 12 and 6, respectively, for the boundary point based on level 3.

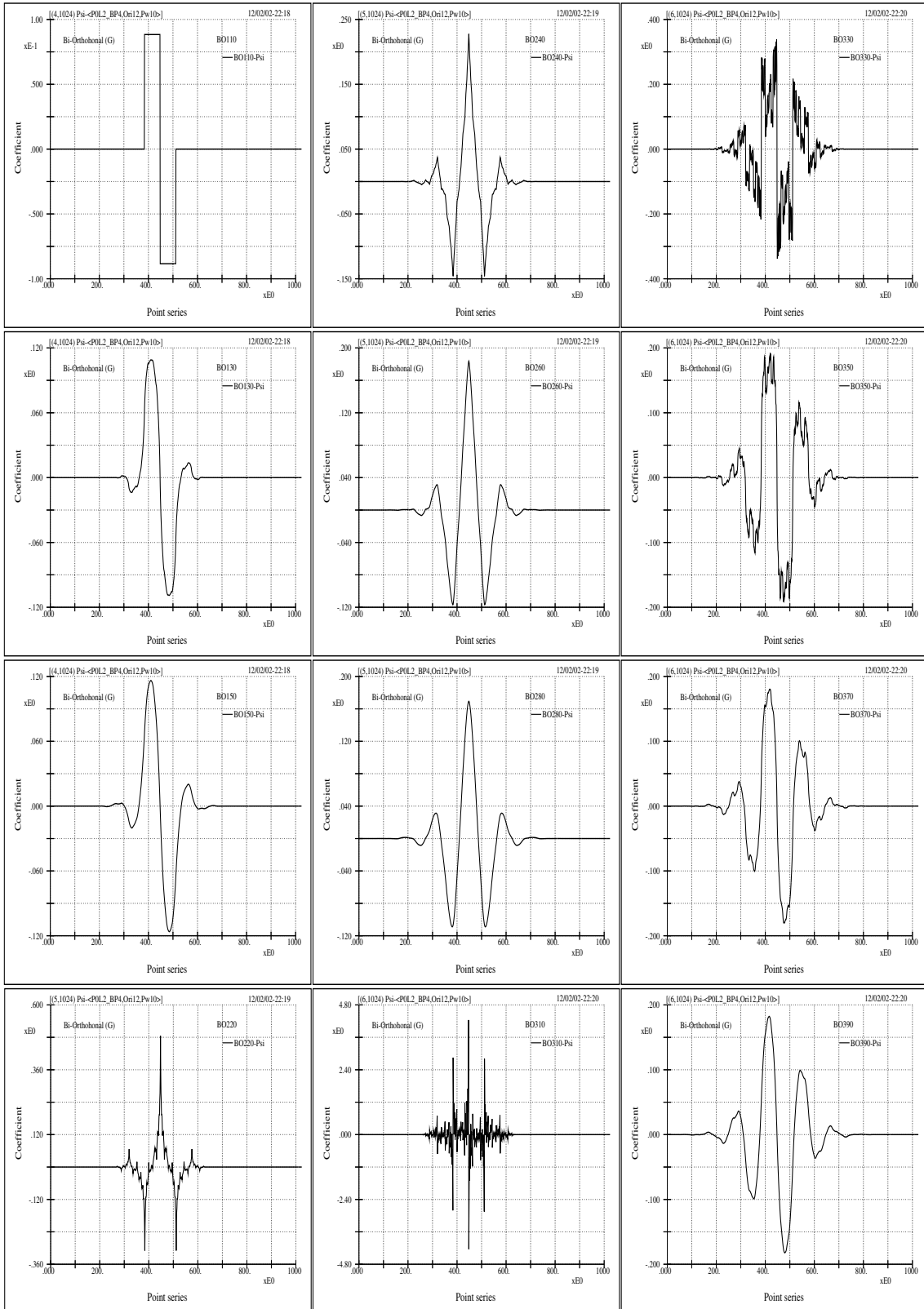


Figure 2.16: The mother wavelets of the BO x xO group originating from the point location of 12. Here the boundary point should be based on a level less or equal to 3.

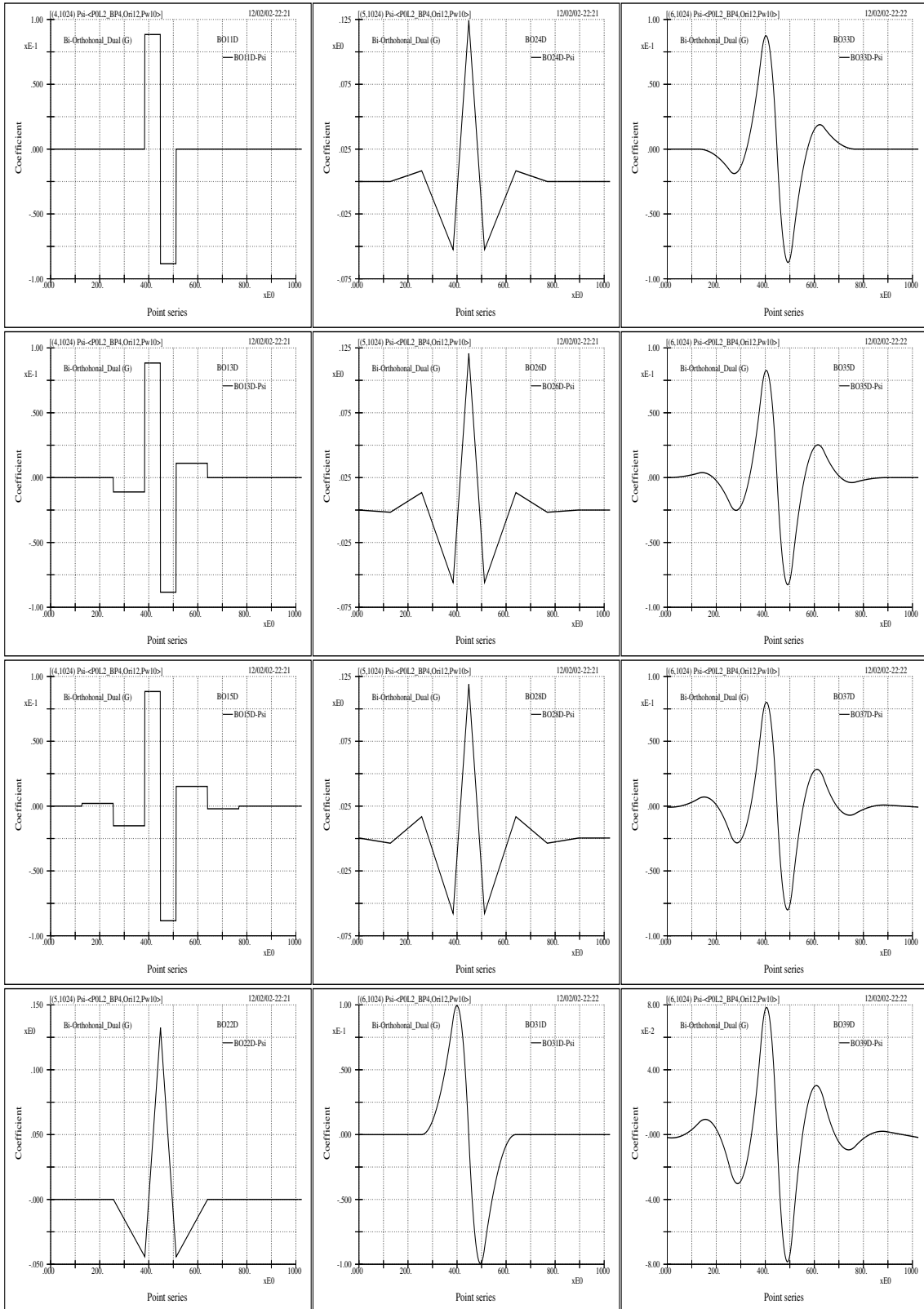


Figure 2.17: The mother wavelets of the BOxxD group originating from the point location of 12. Here the boundary point should be based on a level less or equal to 3.

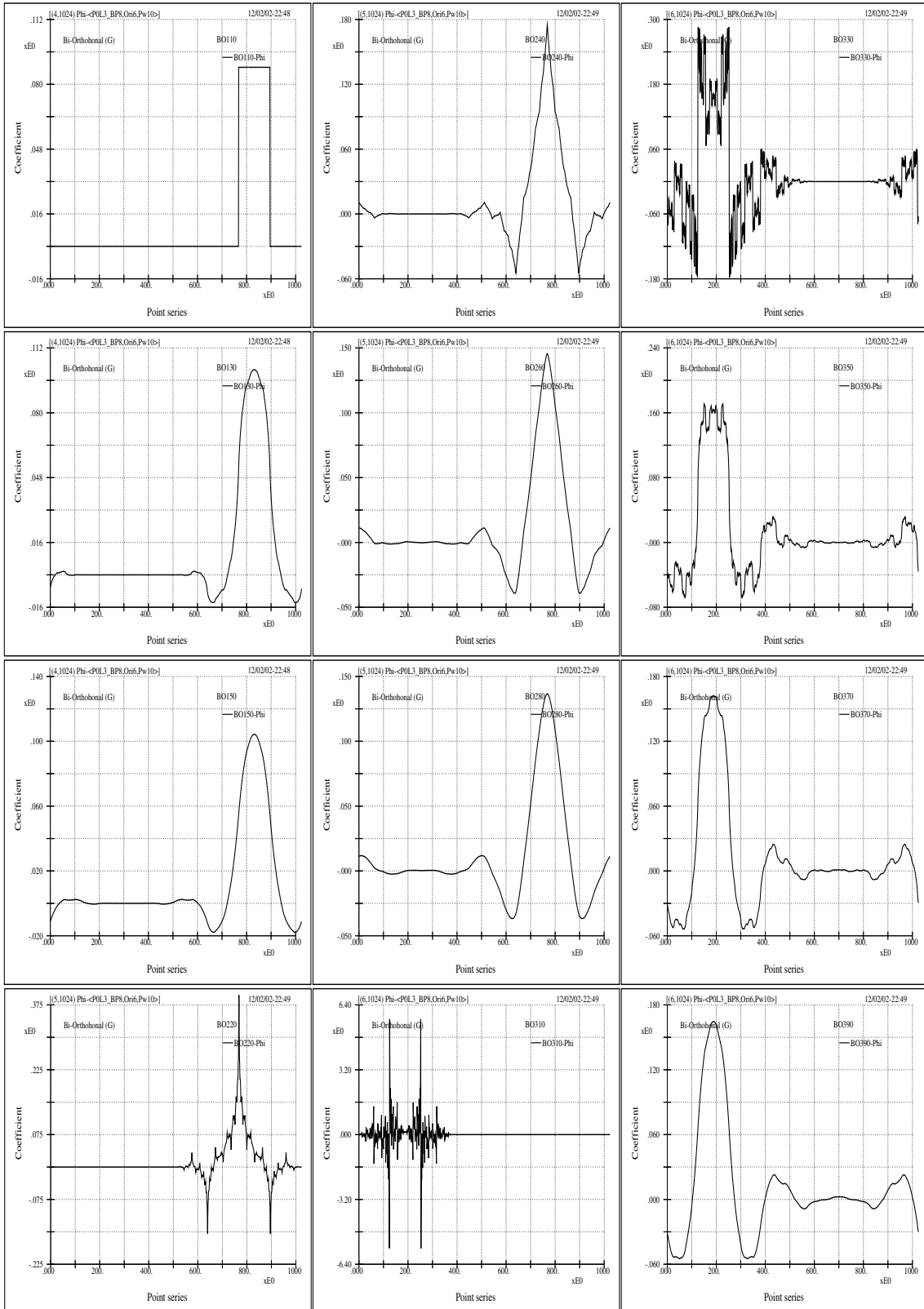


Figure 2.18: The farther wavelets of the BO_{xx}O group originating from the point location of 6. Here the boundary point should be based on a level higher or equal to 3.

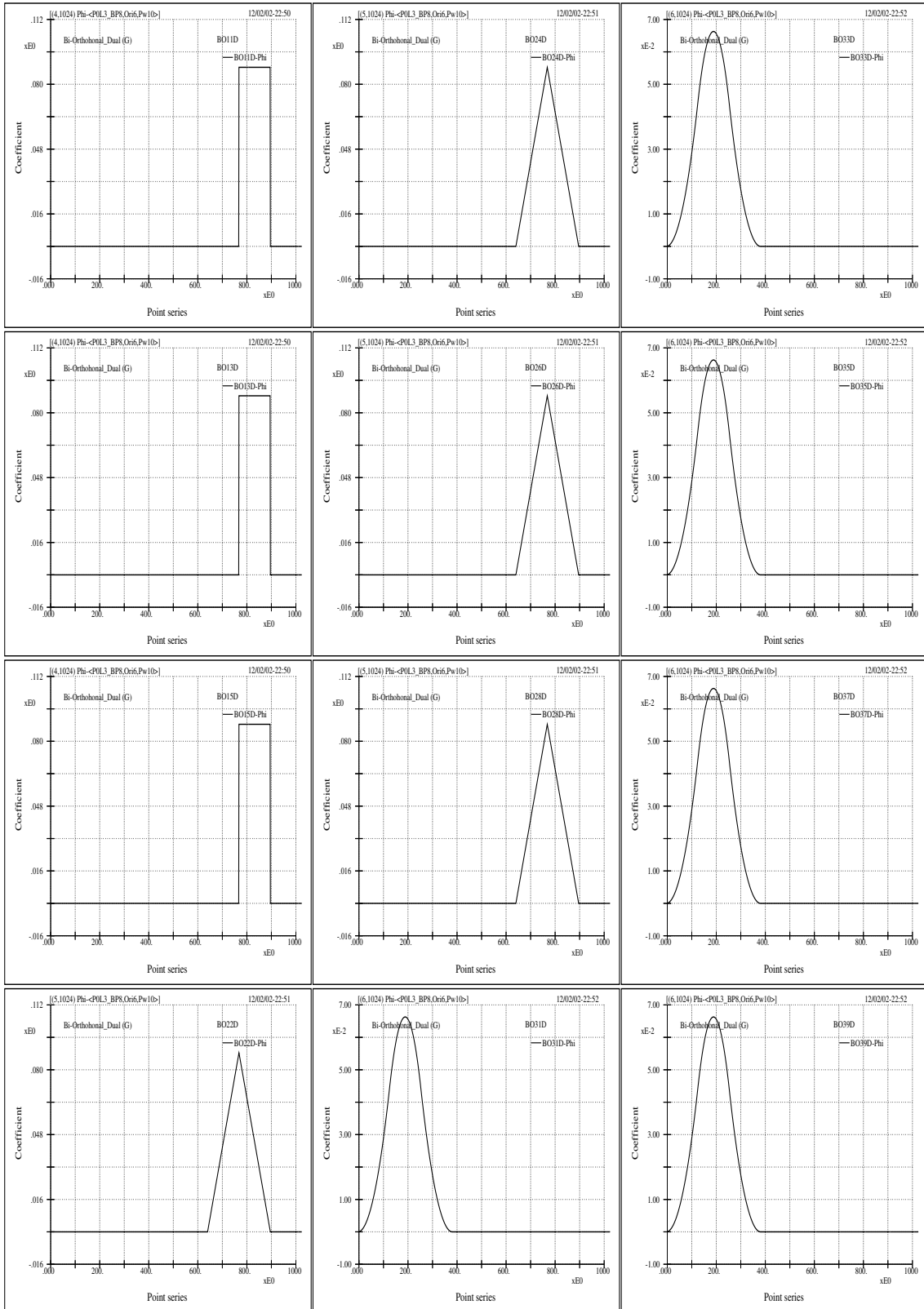


Figure 2.19: The farther wavelets of the $BO_{xx}D$ group originating from the point location of 6. Here the boundary point should be based on a level higher or equal to 3.

2.7 Wavelet packets

The wavelet coefficients derived from an orthonormal wavelet decomposition can be further decomposed by using either the set of filter coefficients (called two-scale sequence in Chui (1992a)) associated with the original wavelet, or different sets of filter coefficients associated with other orthonormal wavelets. Therefore, basically there can be infinitely many wavelet packet decompositions. These further decompositions are of a tree-like refinement process and are called the wavelet packet transform. The wavelet packet coefficients give better frequency resolutions with longer time supports. There are no simple formulas to describe the tree-like decompositions, but a schematic plot help elucidate the mechanism shown in Figure 2.20. The branch patterns and the number of branches can be chosen in any way so long as there is no repeat occurrences within any column under the stretch of the coefficients. That is to say, any column, wide or narrow, must have one and only one contribution from all levels (rows). Due to the tree-like process the computational works are dramatically increased.

For this category we have two criteria for selecting our best basis. One is still called the “best basis”; another “best level basis”. Take for example, for a 1024-point signal, the finest level occurs at $j = \log_2 1024 = 10$ and there are 2^{10} different choices of bases. And within these 2^{10} choices the one which yields the minimum entropy is called the “best basis”. And if we enforce the restriction that all wavelet packets be at the same level j , then we have 10 levels (0 to 9) to choose from; the level that yields minimum entropy is called best level basis. The indexes of a wavelet packet coefficient, i.e., the subscript and superscript of U labeled in the figure determine the time of occurrence of that coefficient and also indicate the associated support length and frequency resolution, i.e., the shape and location of the coefficient’s time-frequency window within the phase plane. Concepts regarding the wavelet packet transform can be seen in Figure 1.1. Again we also see the effects of non-symmetrical filtering. One specific feature is that the areas of all individual windows are all equal.

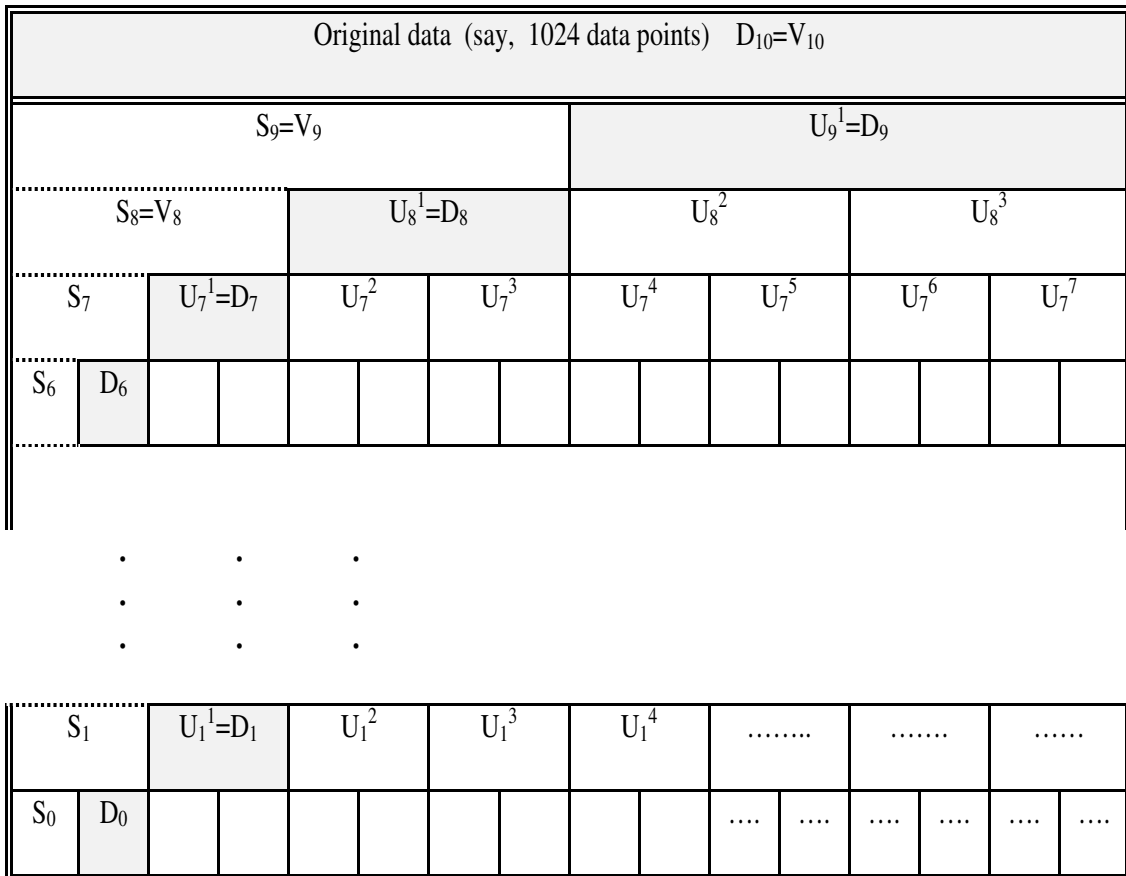


Figure 2.20: Schematic representation of the tree-like structure of the wavelet packet decomposition. $S(=V$ in the text) and D stand for smooth and detail information, respectively. U with superscript larger than 1 stands for further decomposition of D by wavelet packets. All subscripts mean scale levels. All superscripts mean relative locations of the frequency bands for compatible subscripts.

2.8 Wavelet blowups

Wavelets are fractal in nature, that is to say, no matter how detail we zoom into the wavelet curve its blowups all show similar characterization, and this is related to the wavelet differentiability, regularity, support length, and decaying property.

The Asyst program is written to be able to blow any wavelet constructions, such as mother and father wavelets, wavelet bases and wavelet packet bases at any point on any level. A few examples are shown in Figures 2.21 to 2.28.

Her we note that wavelets with fancy analytical properties are often of bizarre wave forms and not of our choice for studying water wave related physics — either judging from they entropy values to be given in the next chapter or from their stability conditions.

Moreover, this blowup exercise hints the behaviors of several numerical and theoretical aspects of wavelet analysis, such as the edge effects, the possible differences of function curves due to finite resolution, and the convergent or error propagation property.

Figures 2.27 and 2.28 show the blow-ups of bi-orthogonal wavelet BO310 and BO350, respectively. Relevant data for BO310 is: Origin of wavelet curve: level 2, position 12 (i.e., element U_2^{12} in figure 2.20); Blow-up point: 150; data length: 512. Each sub-figure shows successive blow-up scale of 2^6 . Here the blow-ups diverge rapidly, i.e., the wavelet fails to identify itself numerically in the refinement cascade. Relevant data for BO350 is: Origin of wavelet curve: level 2, position 12 (i.e., element U_2^{12} in figure 2.20); Blow-up point: 225; data length: 512. Each sub-figure shows successive blow-up scale of 2^6 . Here the blow-ups converge but go with peculiar inclinations.

Figure 2.26 also exhibits the grouping tendency of wavelet packets.

2.9 Phase distribution of the wavelet m_0 function

It is out of the present scope to give a full description of the wavelet related function $m_0(\xi)$ [8] studied here. Suffice it to say that it is comprised of the summation of the wavelet construction convolution constants (or coefficients corresponding to the support

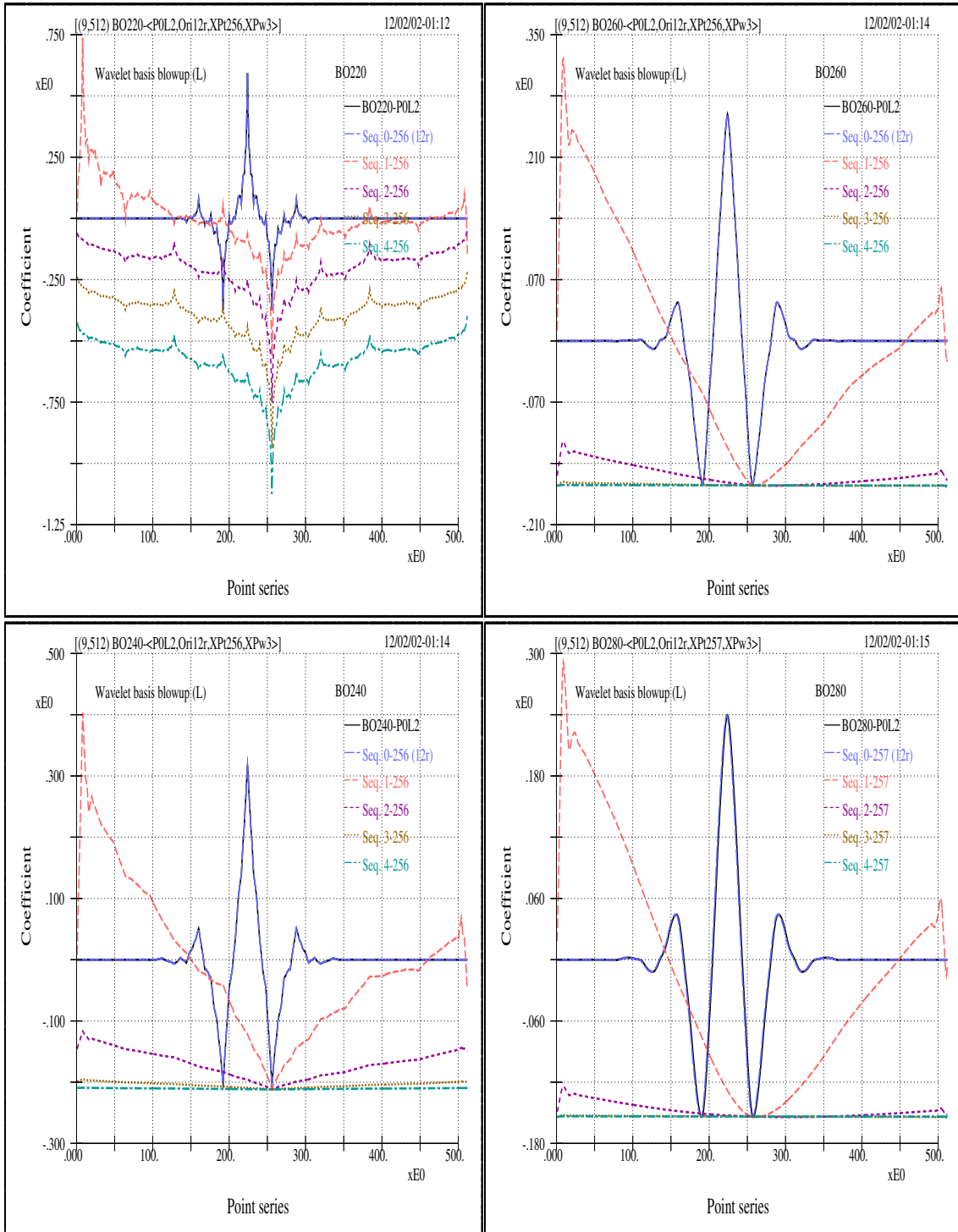


Figure 2.21: The blowups of a few wavelets of the BO2xO group. Each successive blowup scale is 2^3 . The originating point of the wavelet function and the blowup location point are labeled in individual sub-figure.

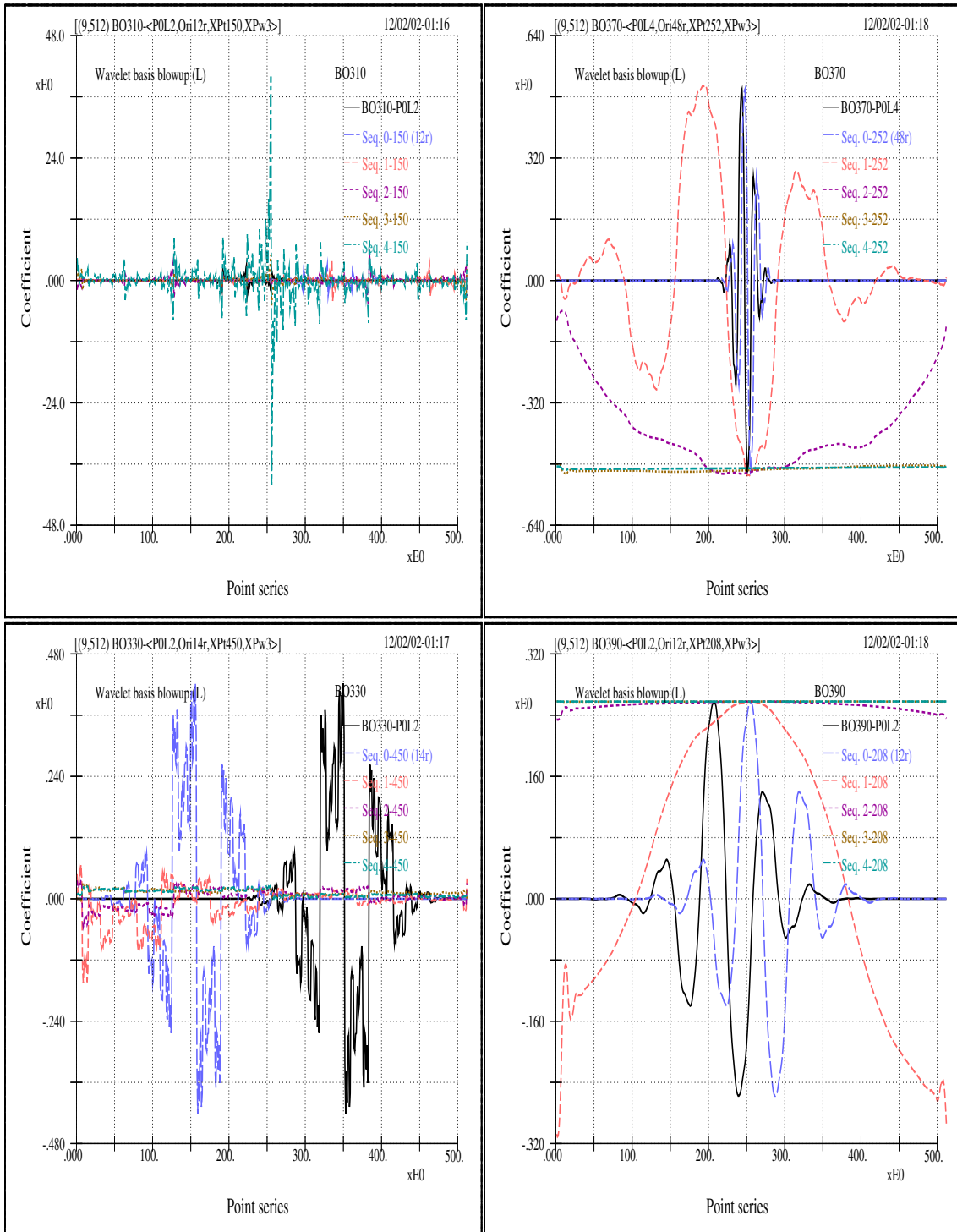


Figure 2.22: The blowups of a few wavelets of the BO3xO group.

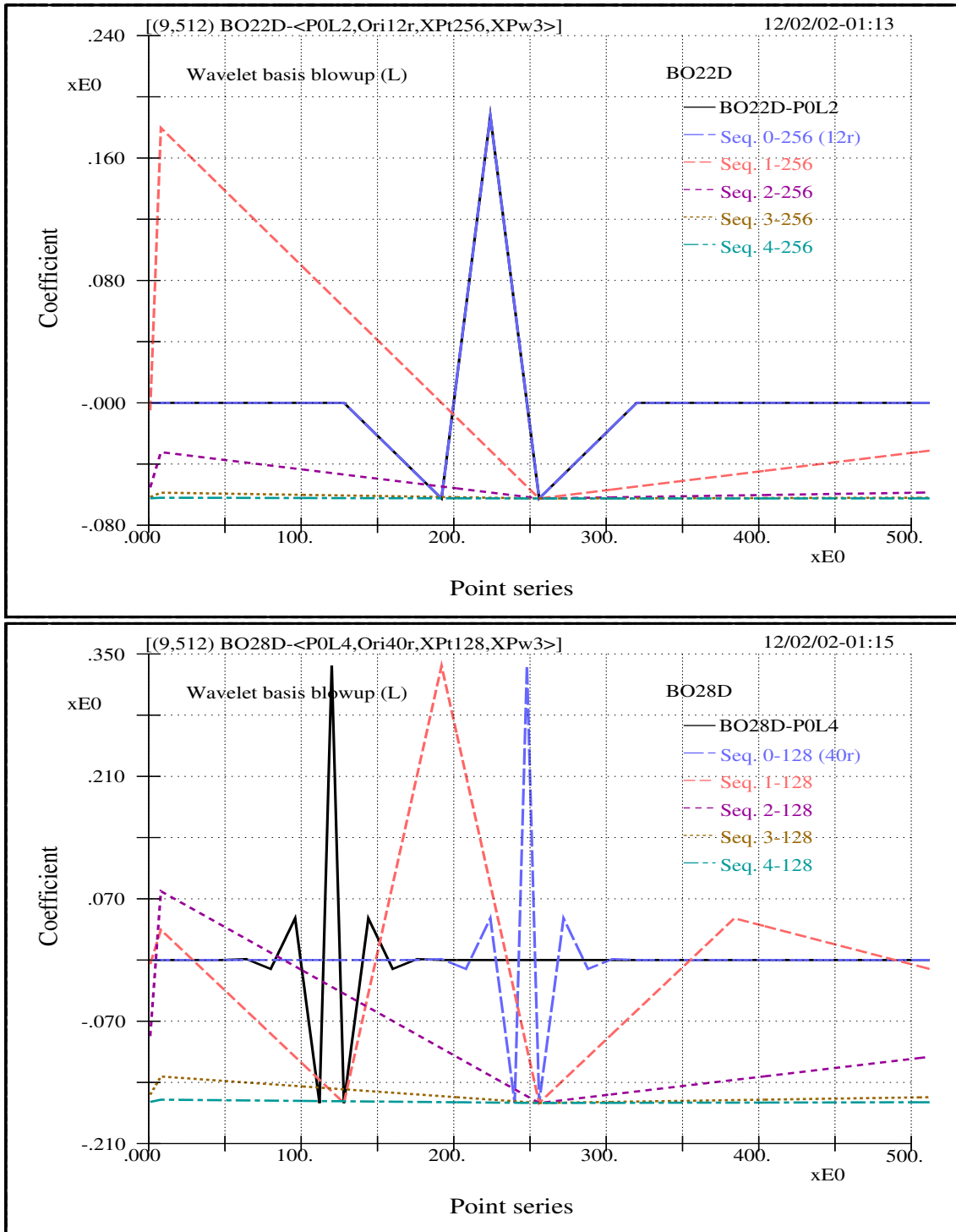


Figure 2.23: The blowups of a few wavelets of the BO2xD group.

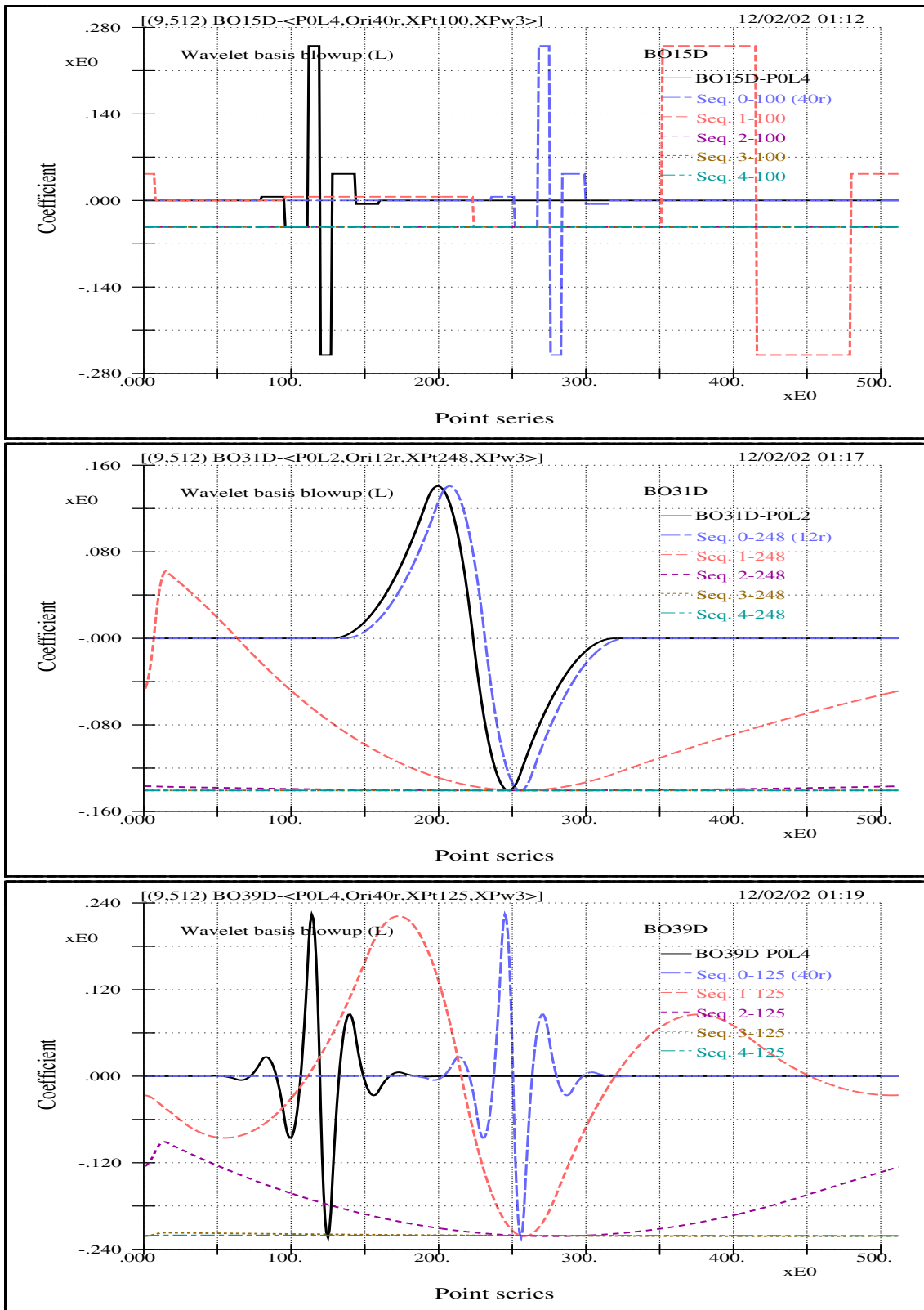


Figure 2.24: The blowups of a few wavelets of the BOx yD group.

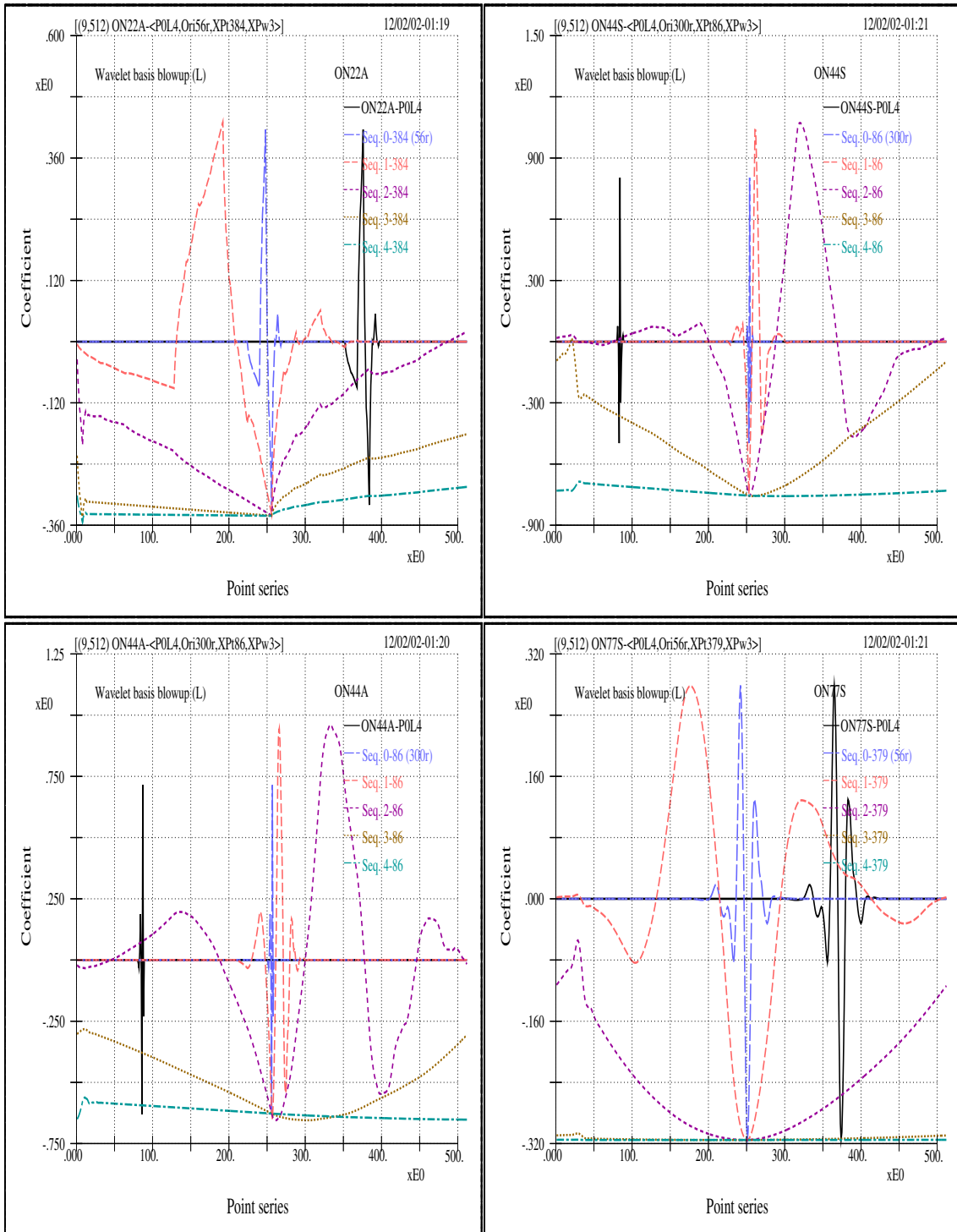


Figure 2.25: The blowups of a few wavelets of the ONxxA and ONxxS groups.

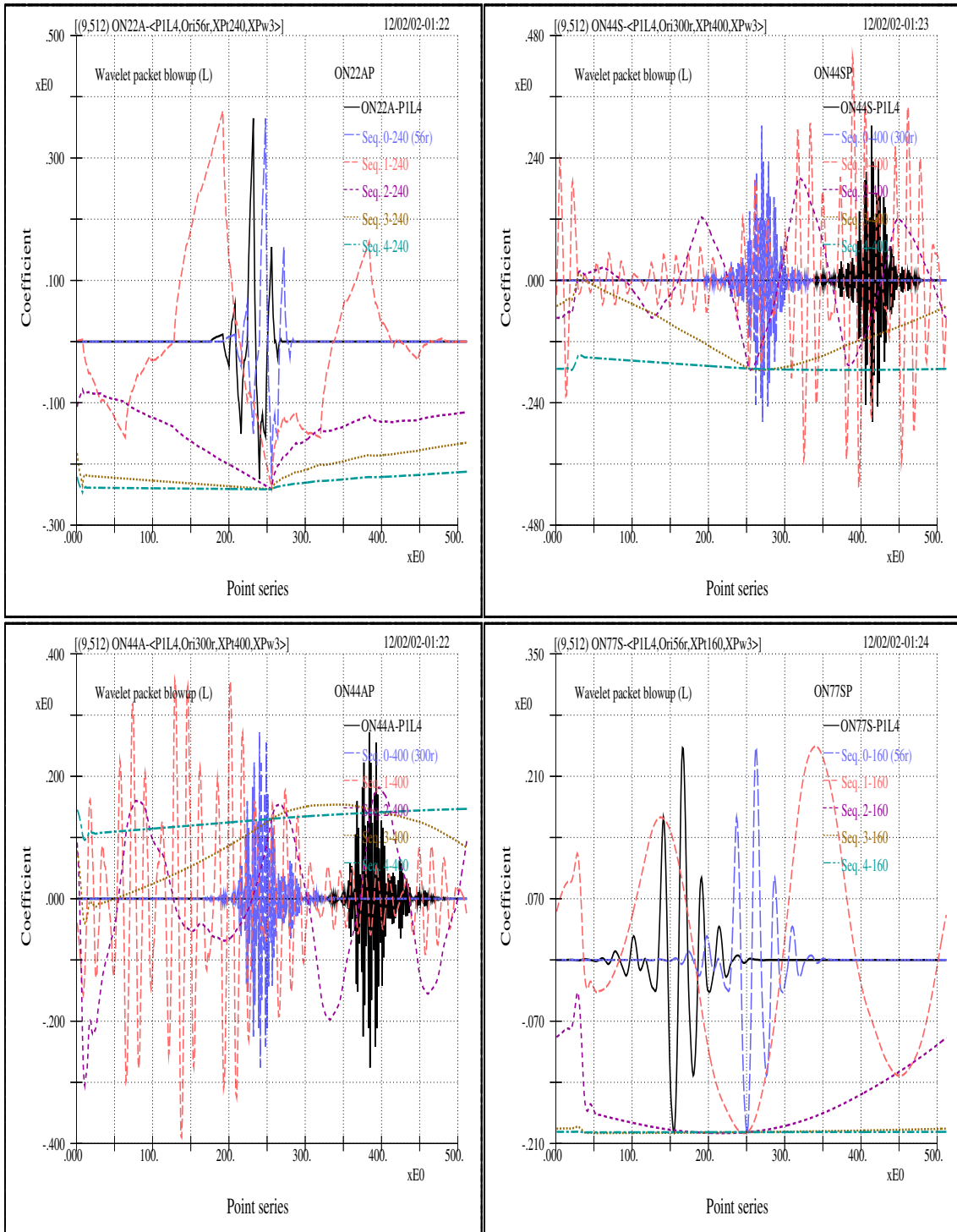


Figure 2.26: The blowups of a few wavelet packets of the ONxxA and ONxxS groups. Note the grouping tendency of the wavelet packets.

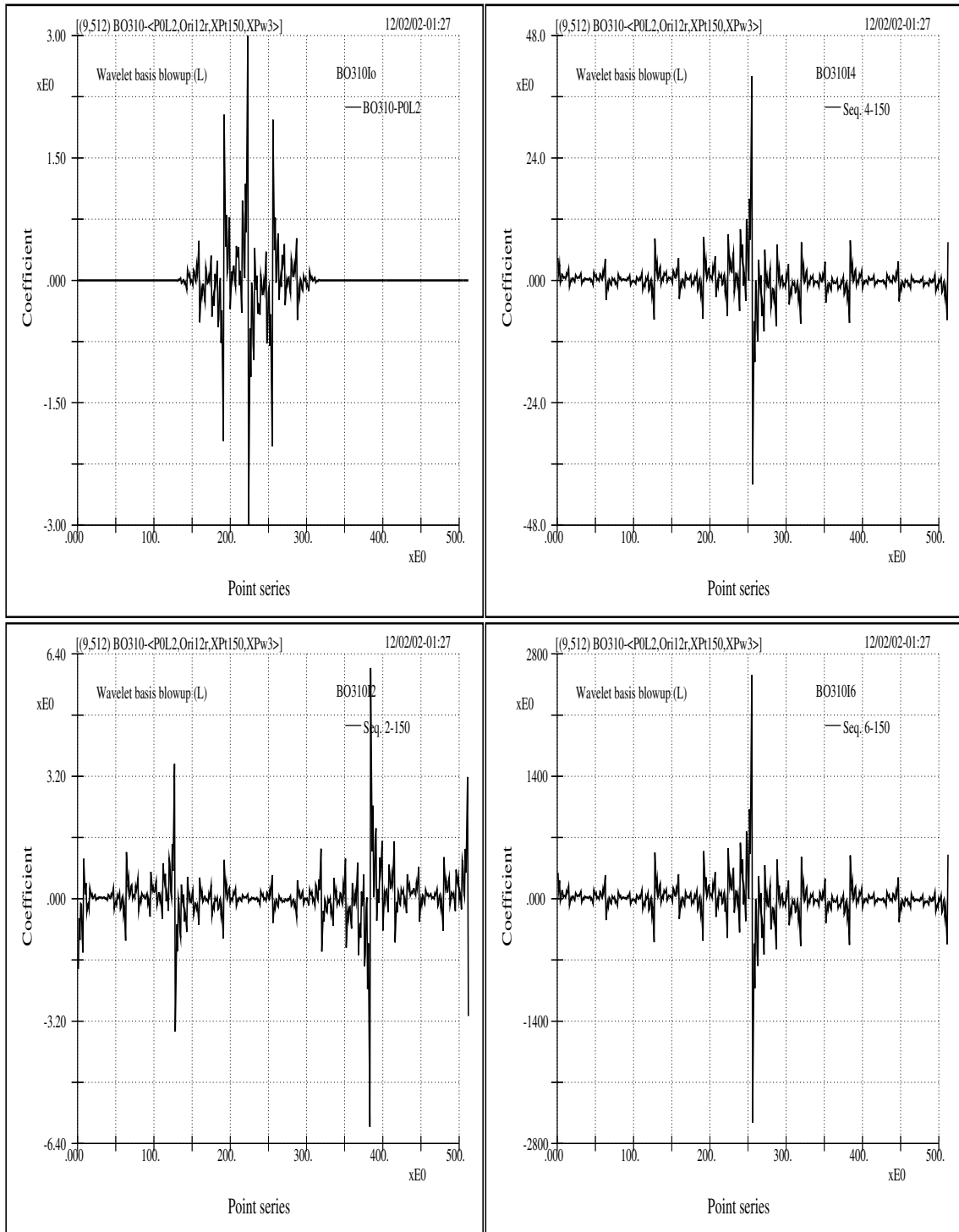


Figure 2.27: The blowups of the BO310 wavelet, noting the vast difference in the ordinate. Here successive blowup scale is 2^6 .

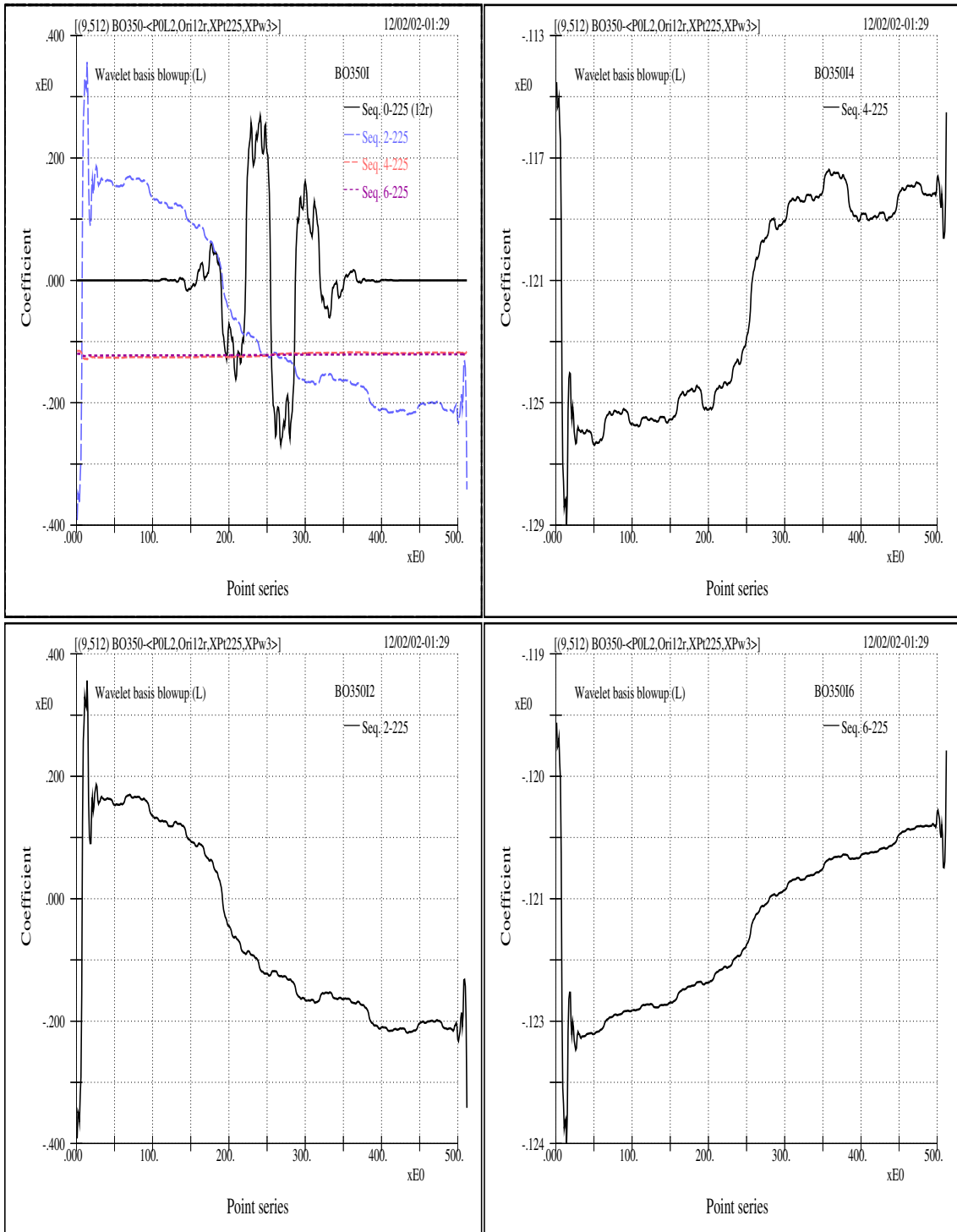


Figure 2.28: The blowups of the BO350 wavelet, noting the difference of the inclinations of the zoom-in curves. Here successive blowup scale is 2^6 .

length of a wavelet) times the complex exponential functions of various scales and that it is intrinsic to the transcendental formulations of the mother and father wavelets. The $m_0(\xi)$ function is linked to the linear phase filtering effects, which is generally a desirable property for filtering efficiency.

Figures 2.29 to 2.36 show the phase distributions of all the covered wavelet categories. A few notable points are given below.

- Wavelets with similar visual appearance may show extremal phase difference, such as those shown in Figures 2.29 and 2.30.
- In view of the entropy results given in the next chapter, as well as the phase distributions of all the wavelet considered, we see that linear phase distribution is not sufficient to guarantee a best performer for the water wave signals – and it seems that a constant phase is required. The semi-orthogonal wavelet (Figure 2.15) is the one with such a property (Figure 2.31).
- Most of the phase distribution curves for the bi-orthogonal wavelets and their duals are the same not only within their subgroups but also crossing the subgroups. This proves that lengthening the support length of the wavelet of this category provides no benefit.
- The lengthening of support length of the orthonormal wavelets may still yield more irregular phase distribution curves. Again this disproves any possible benefit that may arise from further expanding the construction of these orthonormal wavelets.
- Judging from the last point, since two extremal categories of orthonormal wavelet have been covered, we therefore don't see any possibility that there exists other orthonormal wavelet that may provide suitable and better characterization for water wave physics.

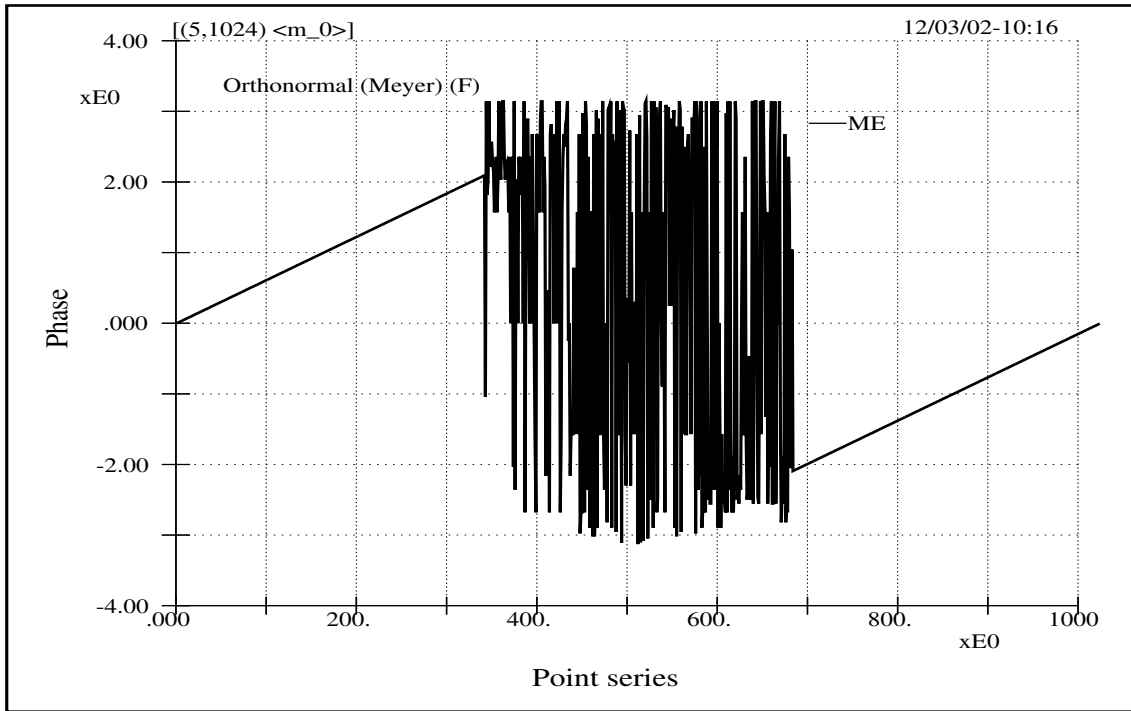


Figure 2.29: The phase distribution of the m_0 function of the Meyer wavelet.

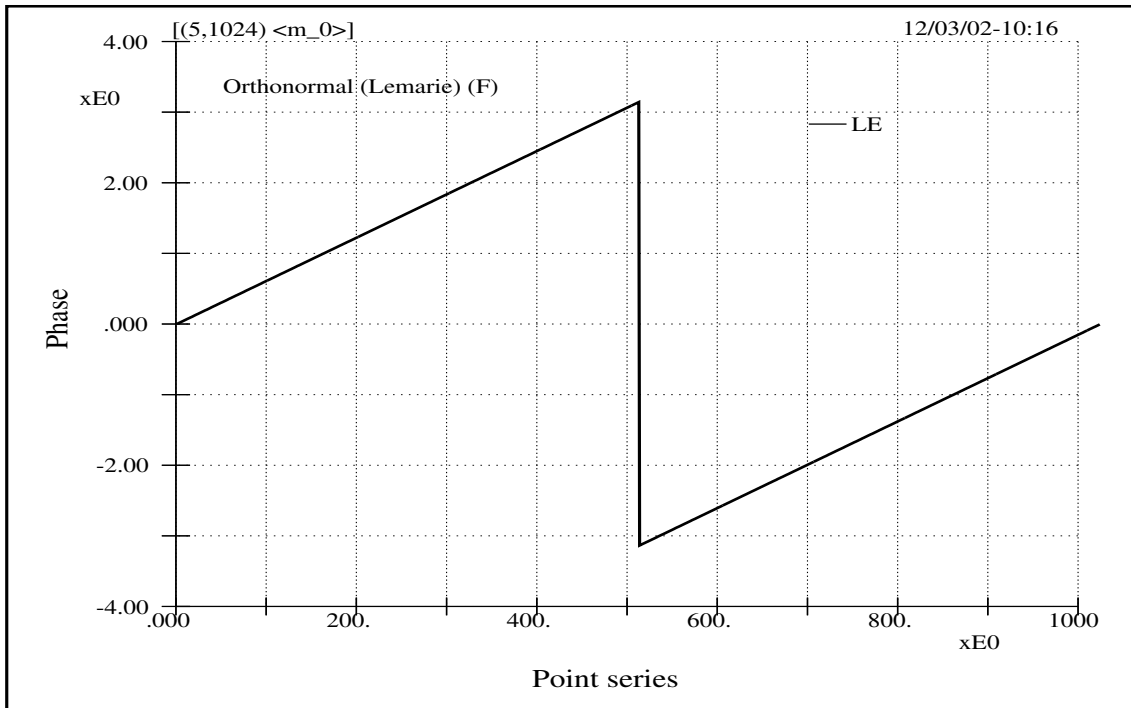


Figure 2.30: The phase distribution of the m_0 function of the Battle and Lemarié wavelet, noting the difference from that of Meyer wavelet.

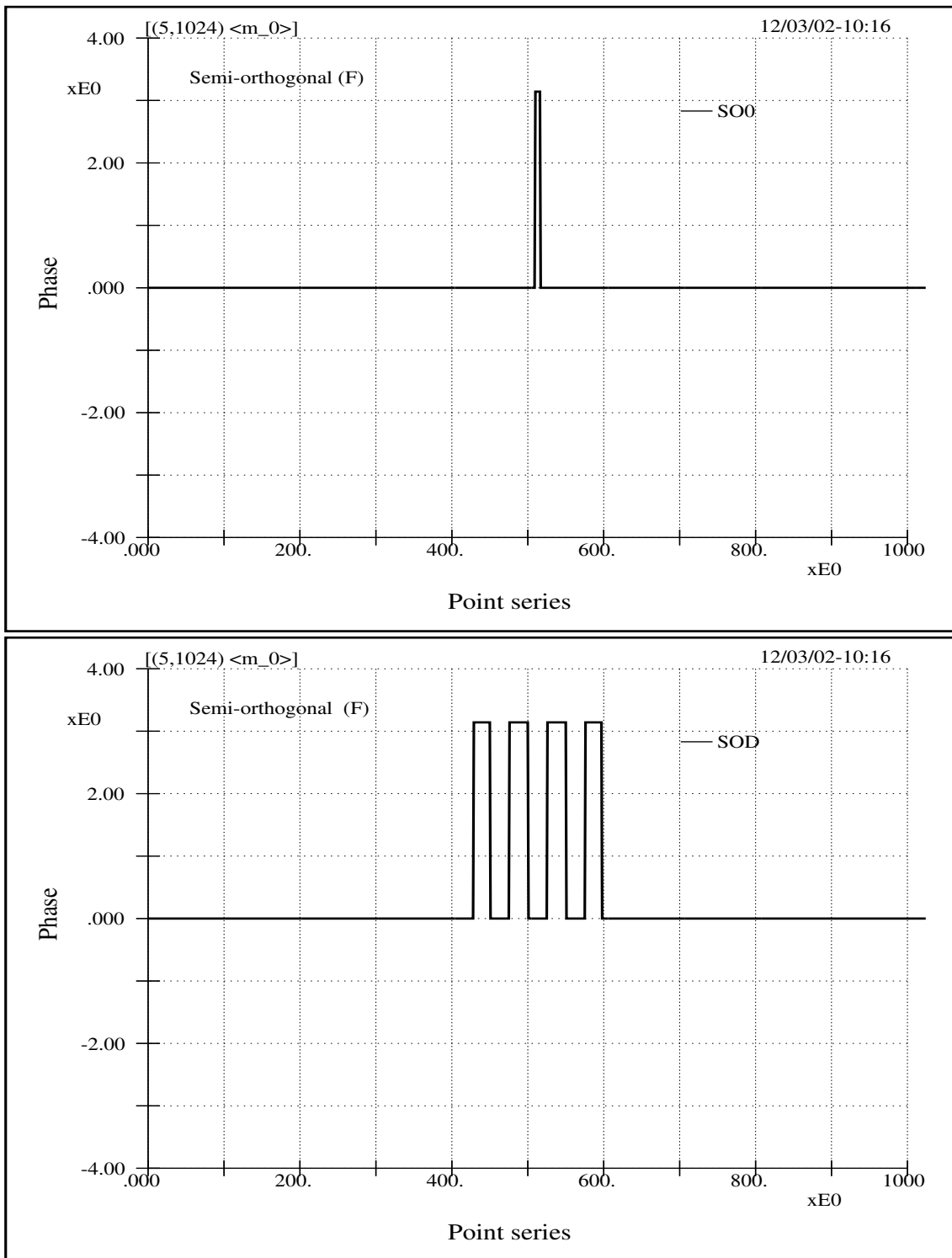


Figure 2.31: The phase distributions of the m_0 functions of the semi-orthogonal wavelet and its dual.

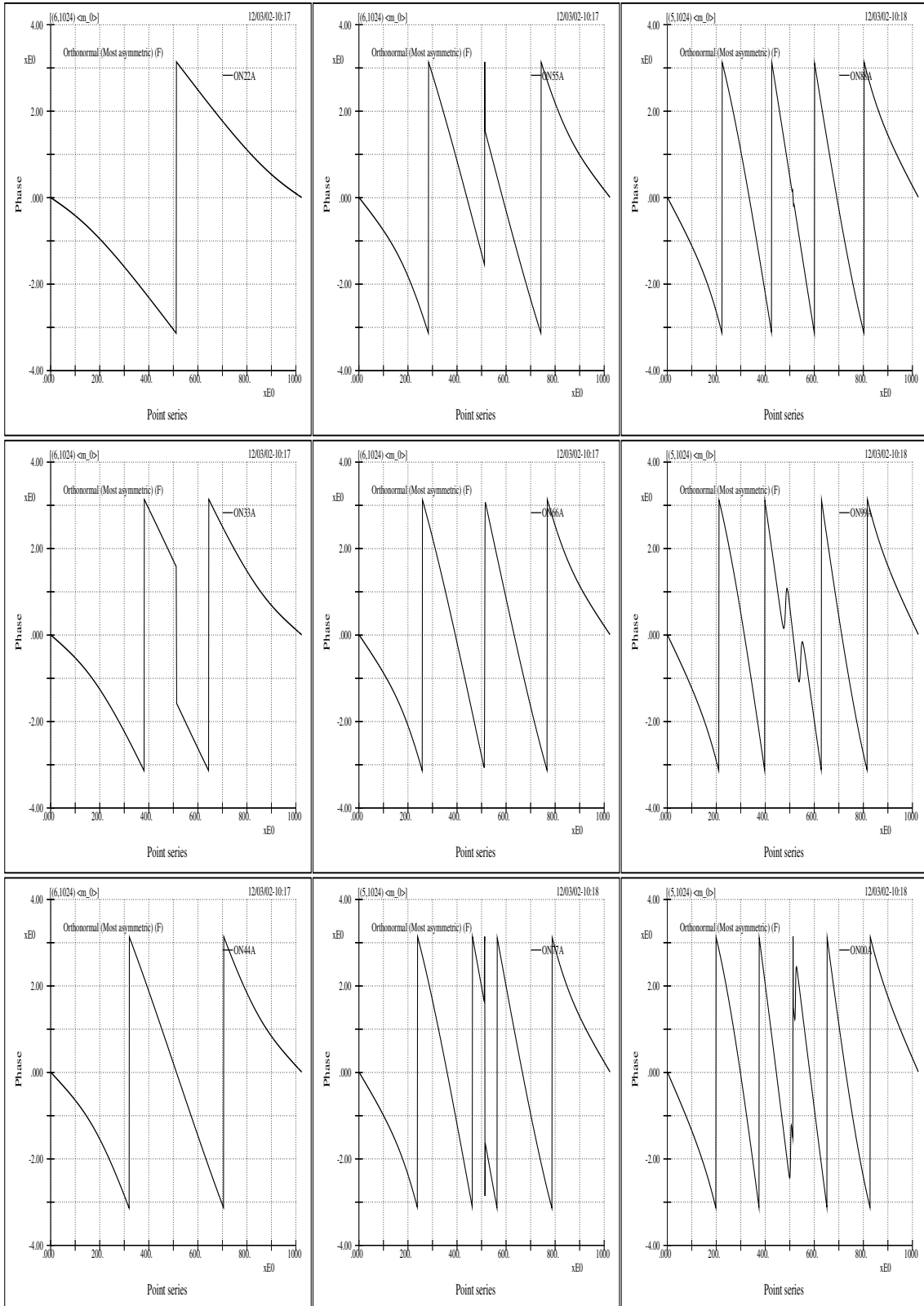


Figure 2.32: The phase distributions of the m_0 functions of the wavelets of the most asymmetric group.

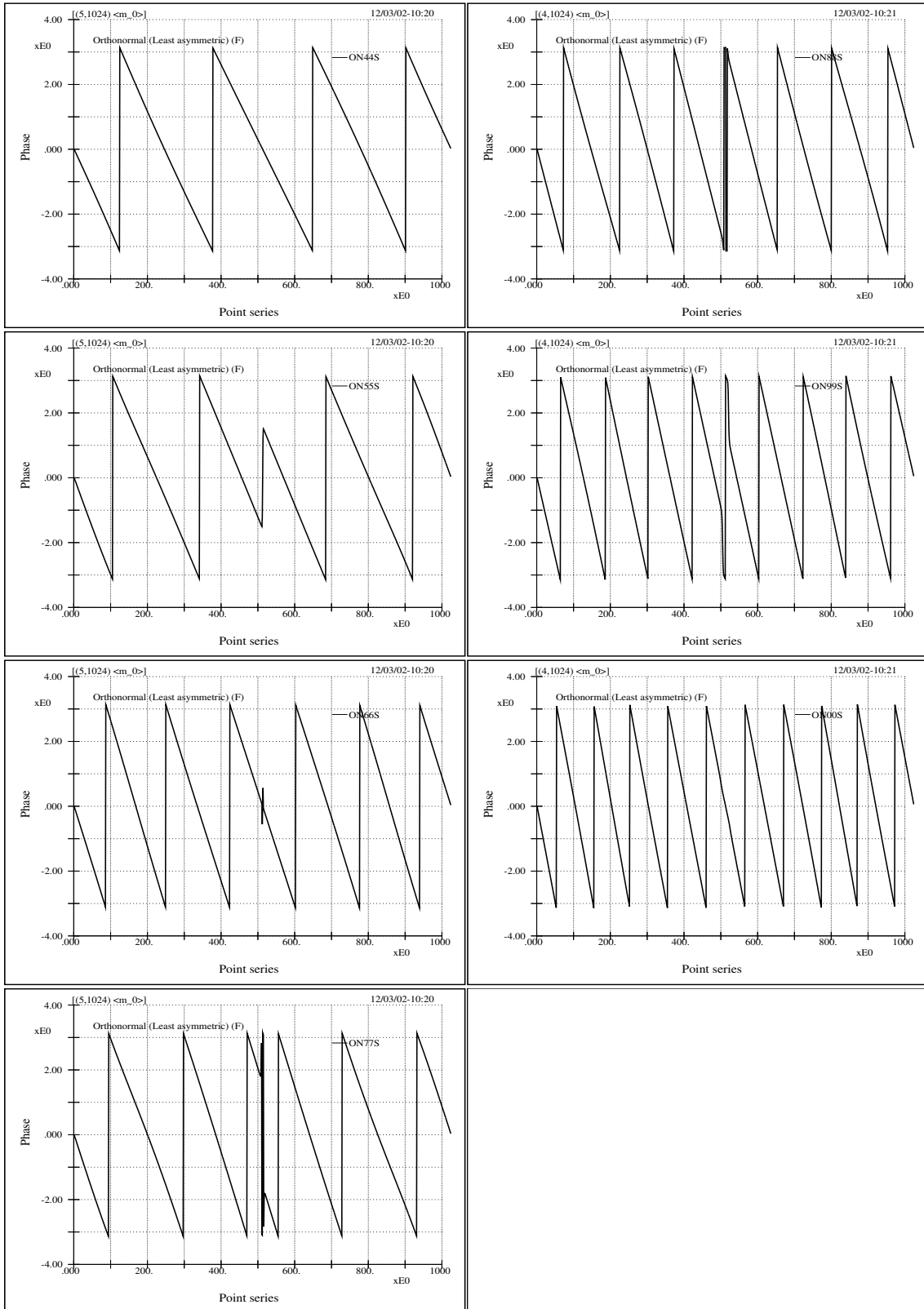


Figure 2.33: The phase distributions of the m_0 functions of the wavelets of the least asymmetric group.

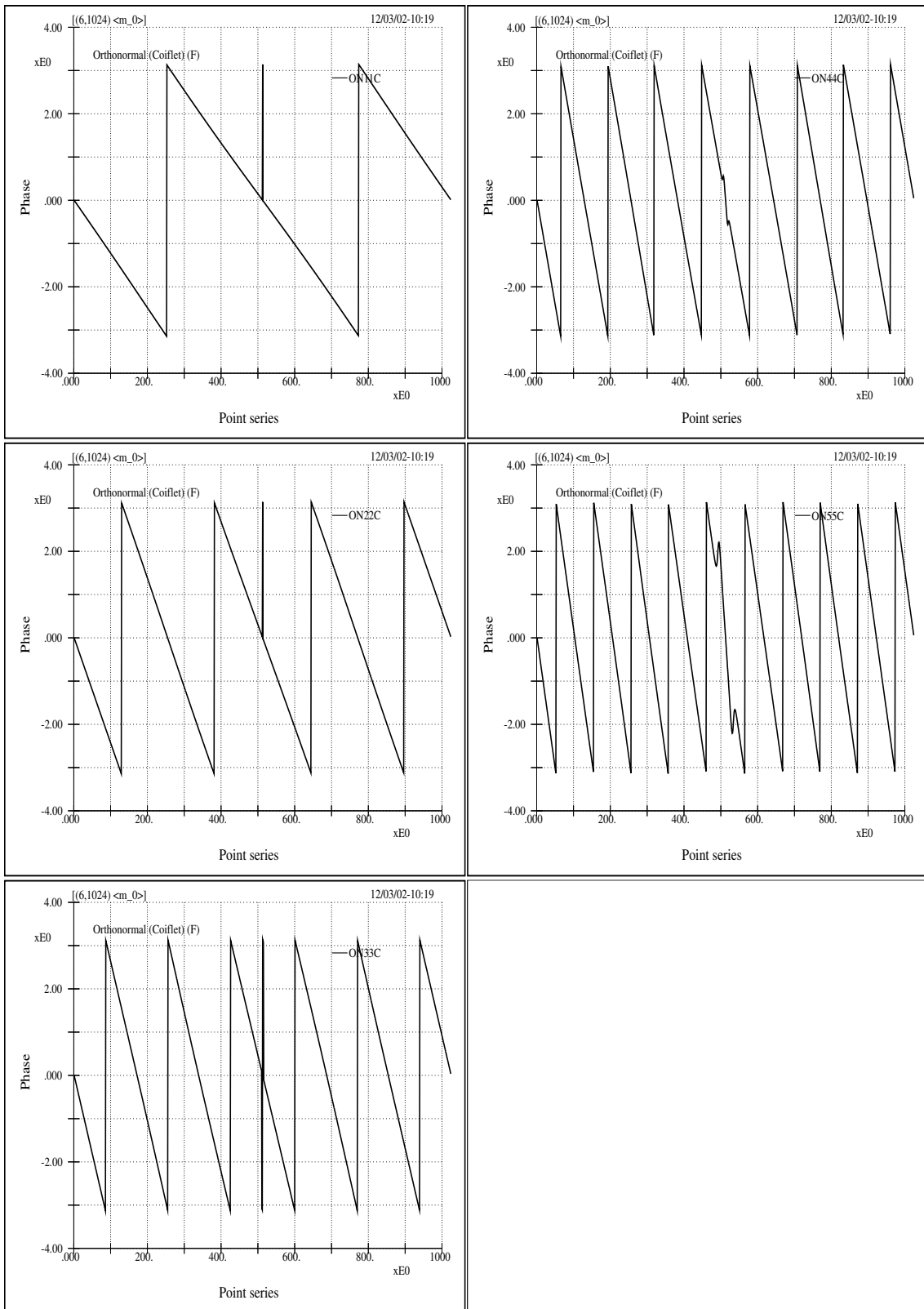


Figure 2.34: The phase distributions of the m_0 functions of the coiflets.

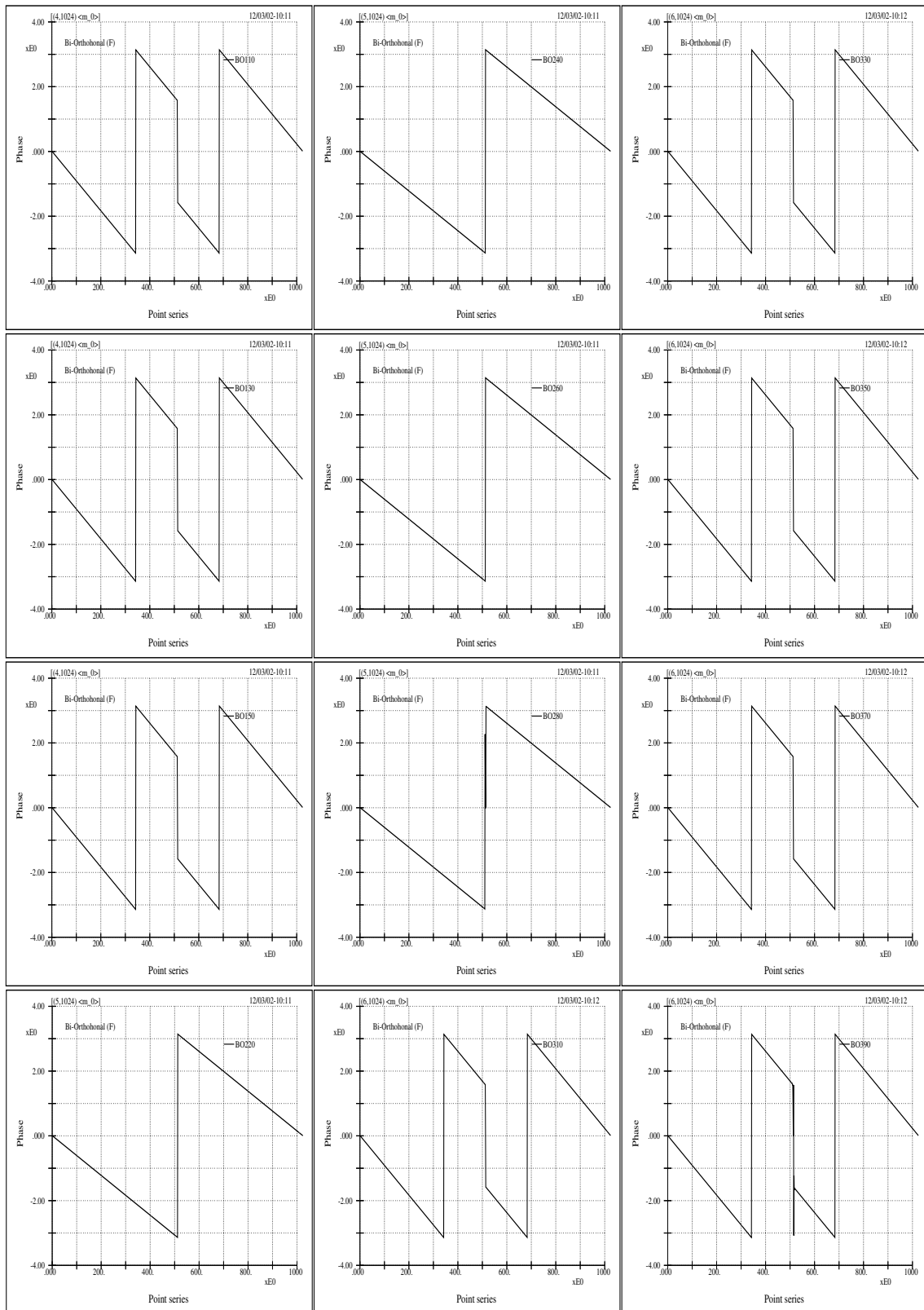


Figure 2.35: The phase distributions of the m_0 functions of the bi-orthogonal wavelets.

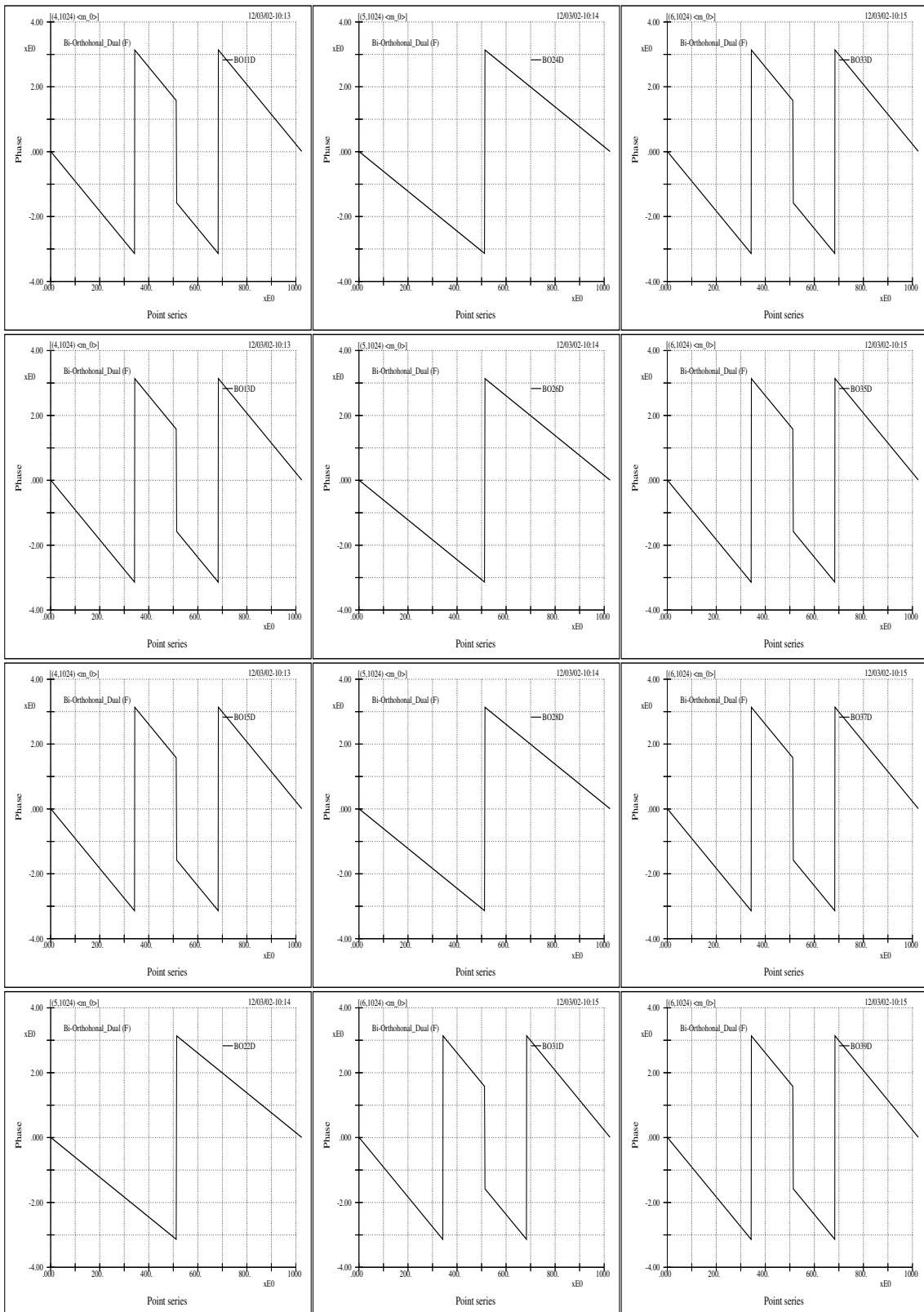


Figure 2.36: The phase distributions of the m_0 functions of the bi-orthogonal wavelets.

The Entropies and the Best Wavelet Basis

3.1 The wavelet perspective of an optimum basis

Many of the points stated in the previous two chapters hint a core concept of wavelet analysis: the decaying properties of the basis functions both in time or frequency domains are at the heart of all sorts of function bases, and different intricate analytical properties of wavelets are just manifestations to these decaying features. And since two decay properties that are analytically quite differentiable may only have very minor visual differences in their wave forms such as those shown in Figures 2.13 and 2.14, in which, the Meyer and the Battle and Lemarié wavelets, as well as their corresponding scaling functions, are shown. one generally feels that the bearing of wavelets' physical implications is not proportional to their analytic interests.

Nevertheless, we still can benefit from the wavelet approach due to its flexibility in devising the analyzing wavelets as well as its adaptability in forging the algorithms. But versatility does not come without the price of ambiguity. For example, the power spectra of a function are shift-invariant; whereas, wavelet spectra are highly shift-variant (Mallat and Zhong 1992). Figure 3.1 shows such a property and it gives us the idea of how significant the phase effects may be. And this property should be regarded as the wavelet counterpart to that of the ambiguity effect due to the add-up of constituent wave compo-

nents or shift versus convolution effects of the Fourier analysis. Note that these figures indicate the possible usefulness associated with the uses of non-orthonormal or redundant function bases.

In studying the physics of certain phenomena using wavelets one of the most intriguing questions is how to choose the analyzing wavelet(s). The concern here is quite in contrast to those studies where they are mainly numerically or analytically oriented. For example, in coding of images or acoustic signals the goals are straightforward: the maximum compression with minimum handling and the highest effectiveness with least distortion; under such circumstances mathematical relevance between signal and wavelet can be materialized much more explicitly than physical pertinence needs to be unfolded for our applications.

From this point of view, for our interests in characterizing the physics of water-wave related phenomena, it seems, at first, that the aspiration is not on “efficiency” or “compactness”. However, with the understanding that the compactness of a coding means the closeness between signal component(s) and analyzing function(s) along with the conception that wave forms which do not look like our signals (or signal components) are obscured from intuitive perceptions of physics, it is justified to find the wavelets that provide the most efficient or most economical representations for our signals. And this viewpoint is related to the concept of entropy — seeming to converge to the same objective for what are emphasized in different disciplines.

The works in this chapter are mainly numerical experiments on measuring the “distances” between our signals and various Riesz wavelet bases given in several wavelet treatises (Chui 1992; Daubechies 1992; Meyer 1992; Press et al. 1992). No attempt to make new constructions of bases or to extend the existing constructions is made. Nevertheless, we have tried to include various categories of Riesz wavelets. We will come to realize that there is really no need to extend the existing constructions if the associated two-scale scaling function or father wavelet is not changed, and that a few sparse fractal-oriented wavelets (Massopust 1994) are just as impractical as they may be in our

applications.

The wavelets tested are dyadic wavelets with “mathematical sampling rate” 1 (no unit). They are of most practical interests in applications for discretely sampled signals. Furthermore, we restrict our scope to laboratory water waves. The criteria used are the entropy statistics of discrete transform coefficients, including Fourier coefficients.

3.2 The entropy criteria

Entropy is a terminology in the statistical physics, thus it gives indication without assurance. The entropy can be viewed as a measure of the “distance” between a signal and its reconstructed signal using partially truncated transform coefficients. To avoid the somewhat mystified notions as one might get from some of the readings, it may be better to give straightforward descriptions by going through the actual numerical process first and returning to its statistical implication later. Let suppose that we have a 1024-point sampled data, then there is a set of 1024 wavelet coefficients ($C=\{c_i\}$). Take the absolute or squared value of these coefficients, sort them, and then divide the sequence into M (say, 100 or 200 or 300) divisions which are equally spaced from 0 to the maximum value of the coefficients. Then we have the statistics of occurrence for each division, and the distribution of these normalized occurrences is the probability density distribution or probability density function (denoted by pdf), say $\{p_1, p_2, \dots, p_{M-1}, p_M\}$. The entropy is

$$H(p) = - \sum_i p_i \log p_i. \quad (3.1)$$

Where, when $p_i = 0$, it is assumed that $0 \log 0 = 0$, since in reality one can assumed that there exists an almost zero probability in that interval without affecting the total sum of probability, after all it is only a statistics and the modification virtually has no influence on the norm value. If absolute values of c_i are taken, $H(p)$ is the L^1 -norm entropy; if squared values are taken, it is squared L^2 -norm entropy. Of course another power can be

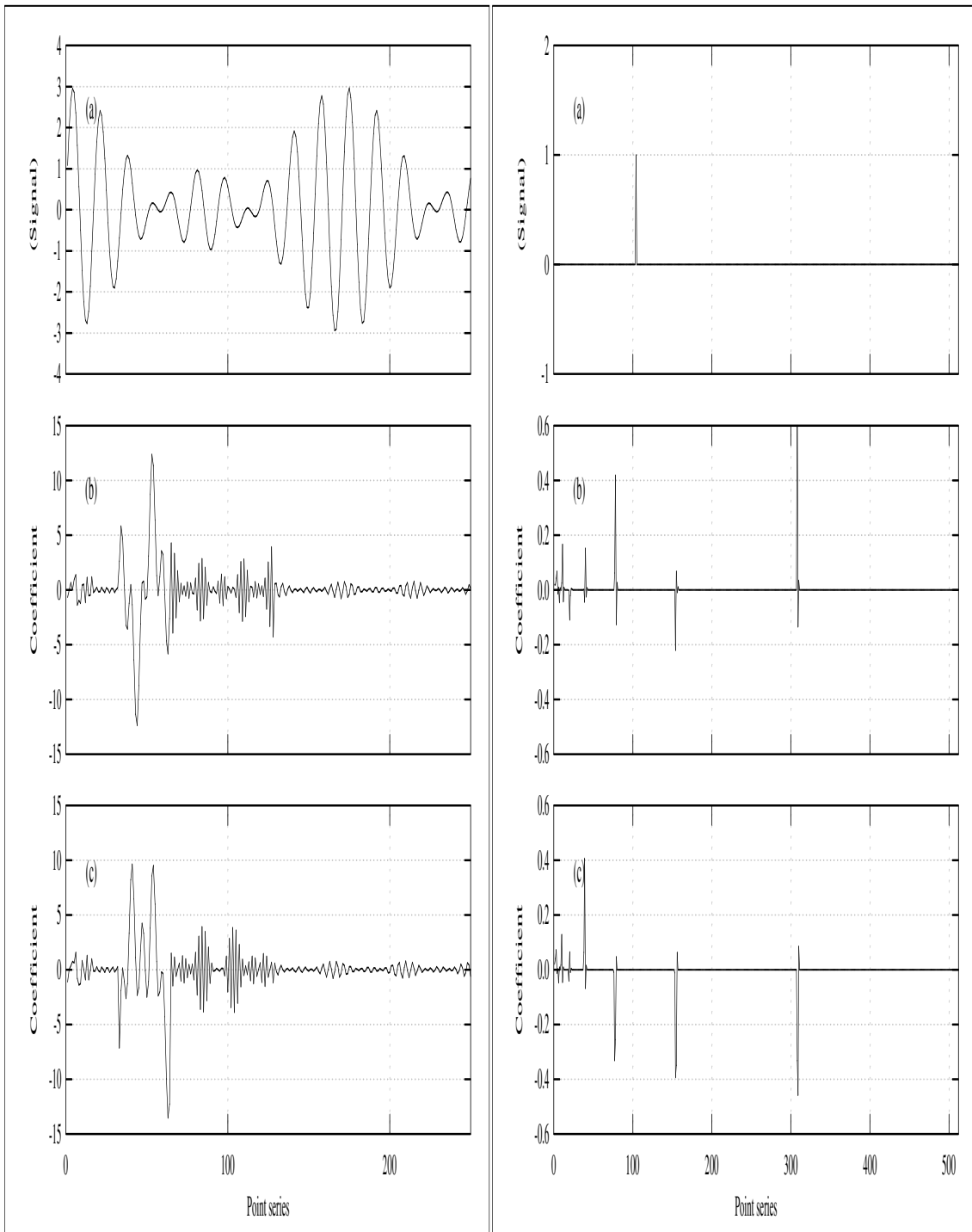


Figure 3.1: The shift non-invariant property of wavelet transforms. Top figure in each column shows individual signal. The middle one shows the wavelet coefficients. The bottom one shows the wavelet coefficients for the shifted signal (right column: 20 points to the left (using BO22D); left column: 3 points to the left (using ON33A)). Note that even though Fourier power spectrum is shift-invariant, Fourier spectral coefficients (without the second power) is still shift-variant. This property is linked to the poor performances of coherence analyses using orthonormal bases.

used, but the squared L^2 -norm, being the energy, is physically the most significant. The practical aspect of this definition of entropy is: let suppose two probability distribution functions sorted in a decreasing order are p and q , if p decreases faster than q , then $H(p) \leq H(q)$ (Wickerhauser 1994). The above inequality of entropy is only one-way correct and the reverse is not always true, but smaller entropy implies that more energy is concentrated within a smaller number of wavelet coefficients. Therefore, if only a fixed percentage of coefficients is kept, the truncated error, i.e., the distance from the total sum, is likely to be smaller for set of coefficients with smaller entropy

There is another notion, sometimes referred as the geometric notion (Wickerhauser 1994), for calculating the entropy. Again, the procedures is given first and the simple physical interpretation next. By setting the number of divisions to be the same as the number of coefficients and by defining probability density to be the normalized (with respect to the total power) value of the squared wavelet coefficient, that is to say, the total energy is $\|C\|^2 = \sum_i |c_i|^2$ and the probability density is $p_i = |c_i|^2 / \|C\|^2$, we get the alternative form of entropy by substituting P_i into Equation 3.1:

$$H(p) = \log \|C\|^2 - \frac{\sum_i |c_i|^2 \log |c_i|^2}{\|C\|^2}. \quad (3.2)$$

The notion here is simple: if one just put more weight on coefficients of small energy and less weight on coefficients of large energy (all coefficients being normalized), then the weighted energy is an indication of entropy. And since taking the log of a value is sort of a weighting operation and since the total energy is finite, small entropy therefore means that the number of significant coefficients is small, or stated otherwise, more energy is concentrated in fewer coefficients.

One equivalent indicator of entropy of a pdf is the theoretical dimension $D(p)$ and is defined as (Wickerhauser 1994)

$$D(p) = e^{H(p)} = \prod_i (p_i^{-p_i}). \quad (3.3)$$

As was stated, entropy does not tell how conclusive the result is. But our numerical results yield little ambiguity regarding the judgement that we can make.

3.3 Results and discussions

To increase the definiteness of the comparisons, we calculate entropy based on several setups: direct coefficient entropy related to L^2 -norm based on Equation 3.3 (column 1 in Tables 3.1 and 3.2), pdf entropy related to L^2 -norm with 300 (column 2) and 200 (column 4) divisions, and pdf entropy related to L^1 -norm based on Equation 3.1 (column 3). Theoretical dimension for one of the setups is also given (column 5). The tables show the results using a wind-wave signal from a wave tank experiment. It is noted that if the peak frequency (or the primary scale) of other signal is significantly different, then, to be consistent in comparison, the analyzed signal lengths and the sampling rates should be properly adjusted according to its peak frequency. This is because in the discrete wavelet transform we need to keep track of the actual physical size of translation so as to have physical perception of the wave forms. Table 3.1 give results from all orthonormal wavelets (including B&L, Meyer, ONxxA, ONxxS, and ONxxC), semi-orthogonal wavelets (Cubic B -spline, SO3O and SO3D), as well as from Fourier spectrum. Table 3.2 give results from bi-orthogonal wavelets. Many distinctive features can be derived from the tables.

- The dual wavelet always gives much smaller entropy than as given by their counterpart wavelet. This certainly verifies that, for our water-wave signals, using

$$f(t) = \sum_{j,k} \langle f, \tilde{\psi}_{j,k} \rangle \psi_{j,k} \quad (3.4)$$

provides a much better efficiency in decomposition and reconstruction than using

$$f(t) = \sum_{j,k} \langle f, \psi_{j,k} \rangle \tilde{\psi}_{j,k}. \quad (3.5)$$

This also points out that dual wavelets rather than their counterpart wavelets should always be used as the decomposing basis for either better physical implications or improved computational efficiency. It may also be worth noting that the practical shapes of all the listed bi-orthogonal wavelets, especially those with small x and y values, are visually quite unrealistic (such as those shown in Figures 2.27 and 2.28). Furthermore, for these bi-orthogonal wavelets, it can be concluded that there is going to be very little improvement by further extending the support width related to y without extending the support width related to x ; since increasing the width (y) from some point on gives no effect on the shape of dual wavelets (such as $y = 7$ or 9 for $x = 3$) and since it is the dual, rather than the counterpart, wavelet that matters for better approximation.

- Entropy values of all orthonormal subgroups do not fall to the level of non-orthogonal ones. Besides, difference in entropy values of long and short supports can barely be differentiated, even though there seems to be a very slight indication that entropy values related to longer support are somewhat smaller. Here the property reflects the role of linear phase filtering as mentioned earlier.
- Among all the orthonormal wavelets none distinguishes itself from the others. And we see no clear tendency within any subgroup. However, from the analytical point of view, the Meyer wavelet is infinitely differentiable or smooth, the B&L is second order differentiable, and the others have various degrees of differentiability or regularity (Daubechies 1992). It is therefore understandable that at the present stage many analytical properties of orthonormal wavelets are of little practical interests for our signals.
- The most striking result is that the dual Cubic B -spline wavelet yields a far smaller entropy value, even lower than that of the spectral coefficients. Figure 3.2 shows the comparisons of the cumulative probability distribution curves for several wavelet bases as well as for Fourier basis. This striking feature is reflected by the extreme

flatness of the SO3D curve, nearly horizontal up until 90 percent of energy ratio. At about 96 percent of the energy ratio there is a crossing between spectral curve and the SO3D curve. These features practically imply that semi-orthogonal wavelet coefficients are better than Fourier coefficients in describing the details of the signals. Figure 3.3 shows the reconstructions of a section of a signal from its spectral and SO3D wavelet coefficients of which 35 percent are kept. It is seen that the wavelet basis yields truer details than does Fourier basis. Again, the reasons for the SO3D's strong performance can be attributed to the following characters: total positivity of the scaling function and complete oscillation of the wavelet. That is to say, the scaling function has no oscillation or zero-crossing; the corresponding wavelet has no unnecessary oscillation, or no oscillation that is without zero-crossing. Physically, the two characteristics hint that our laboratory water waves are far less transient when compared with orthonormal or bi-orthogonal wavelets, and also imply that the description of waves based on suitable support length or life span is more likely to adhere to the physics.

- For the wavelet packet category we have the best basis and best level criteria. It may not be difficult to gain a prior idea that the chance is slim for getting better results using either of the bases. The obvious reason is due to the inherent limitation of wavelet packet transform — wavelet packet transforms are associated only with orthonormal bases. Since the primitive analyzing functions are orthonormal and since orthonormal wavelets perform poorly as just given above, it is therefore hard to anticipate the same strong performance as that of semi-orthogonal wavelets. Nevertheless, both wavelet packet criteria do show improvements when compared with the original orthonormal basis, and the performance of the best basis is certainly better than that of the best level. Figure 3.2–(b) gives the wavelet packet best bases and best level curves for B&L and Meyer's wavelets; they do show improvements when compared with the corresponding curves in Figure 3.2–(a) using regular wavelet transforms. It is quite certain that the improvement is not to the

degree of semi-orthogonal wavelet or that of the Fourier spectrum.

- Figure 3.4 shows cumulative distribution curves of the best level, best basis, and a few different levels bases wavelet packet coefficients, as well as the curve for the corresponding regular wavelet transform coefficients; here, all the curves are associated with ON77S. The curve for the best level comes close to that for the best basis. Again, wavelet packet best basis and best level yield lower entropy values than other relevant wavelet bases, but still their curves are far away from that of SO3D.
- Among orthonormal wavelets, we do not see clear differences arising from different degrees of symmetry (least asymmetric ON x x S or most asymmetric ON x x A); however, semi-orthogonal and bi-orthogonal wavelets are symmetric or antisymmetric, and their entropy values (concerning dual wavelets) are comparatively lower. It therefore indicates that the linear phase filtering is desired since symmetry or anti-symmetry implies linear phase of the two-scale sequence (Chui 1992; Daubechies 1992). Without the linear phase filtering visual impairment may occur. The non-symmetric distribution of time-frequency windows shown in Figures 1.1 illustrates such a significant impact. Though symmetry is desired, it is hard to describe its influence since there are other factors that need to be considered (such as the support length and regularity, e.g., Meyer and B&L wavelets are also symmetric but their entropy values are not comparable to that of the ideal one).

3.4 Summary

Using various criteria of entropy statistics of transform coefficients we identify among a vast array of Riesz bases the best basis for our signals. It is found that, except the B -spline

Table 3.1: Entropy of orthonormal and semi-orthogonal wavelet coefficients as well as spectral coefficients under various statistic criteria.

Wavelet	<u>L**2 coefficient</u> entropy (0 division)	<u>L**2 probability</u> entropy (300 divisions)	<u>L**1 probability</u> entropy (300 divisions)	<u>L**2 probability</u> entropy (200 divisions)	<u>Theoretical</u> dimension (L**2 300 divisions)
B&L	4.691	1.330	3.417	1.179	3.782
Meyer	4.647	1.294	3.365	1.132	3.646
SO3O	4.833	1.669	3.756	1.488	5.307
SO3D	1.823	0.219	1.306	0.172	1.245
Spectrum	2.809	0.270	3.044	0.244	1.310
ON22A	4.993	1.761	3.891	1.516	5.815
ON33A	4.773	1.384	3.499	1.225	3.975
ON44A	4.790	1.517	3.596	1.363	4.559
ON55A	4.819	1.553	3.631	1.367	4.727
ON66A	4.790	1.373	3.456	1.203	3.946
ON77A	4.675	1.355	3.461	1.203	3.877
ON88A	4.645	1.229	3.283	1.082	3.418
ON99A	4.719	1.412	3.501	1.252	4.106
ON00A	4.787	1.423	3.511	1.244	4.149
ON44S	4.835	1.461	3.557	1.281	4.311
ON55S	4.758	1.492	3.576	1.298	4.426
ON66S	4.754	1.402	3.501	1.225	4.065
ON77S	4.751	1.336	3.331	1.188	3.804
ON88S	4.714	1.366	3.481	1.224	3.918
ON99S	4.755	1.469	3.570	1.288	4.345
ON00S	4.635	1.278	3.378	1.134	3.591
ON11C	4.938	1.696	3.832	1.457	5.452
ON22C	4.827	1.468	3.520	1.284	4.342
ON33C	4.756	1.488	3.573	1.333	4.427
ON44C	4.690	1.297	3.337	1.157	3.658
ON55C	4.644	1.309	3.405	1.154	3.703

Table 3.2: Entropy of bi-orthogonal wavelet coefficients under various statistic criteria.

Wavelet	<u>L**2 coefficient</u> entropy (0 division)	<u>L**2 probability</u> entropy (300 divisions)	<u>L**1 probability</u> entropy (300 divisions)	<u>L**2 probability</u> entropy (200 divisions)	<u>Theoretical</u> dimension (L**2 300 divisions)
BO110	5.395	2.623	4.502	2.299	13.777
BO11D	5.395	2.623	4.502	2.299	13.777
BO130	4.943	1.806	3.883	1.627	6.084
BO13D	5.266	2.371	4.373	2.053	10.708
BO150	4.866	1.678	3.755	1.495	5.357
BO15D	5.227	2.291	4.327	1.987	9.882
BO220	5.282	2.362	4.363	2.083	10.609
BO22D	4.434	1.181	3.284	1.034	3.257
BO240	4.963	1.862	3.985	1.634	6.438
BO24D	4.359	1.090	3.220	0.962	2.975
BO260	4.881	1.703	3.835	1.492	5.490
BO26D	4.332	1.064	3.174	0.940	2.899
BO280	4.857	1.624	3.782	1.452	5.073
BO28D	4.318	1.069	3.157	0.941	2.914
BO310	5.824	3.174	4.741	2.835	23.894
BO31D	4.377	1.058	2.655	0.936	2.880
BO330	5.084	2.001	4.062	1.756	7.393
BO33D	4.205	1.102	2.827	0.965	3.011
BO350	4.850	1.697	3.847	1.506	5.457
BO35D	4.125	1.026	2.776	0.908	2.789
BO370	4.790	1.658	3.821	1.442	5.247
BO37D	4.106	0.986	2.737	0.873	2.679
BO390	4.776	1.660	3.835	1.432	5.258
BO39D	4.098	0.967	2.713	0.866	2.629

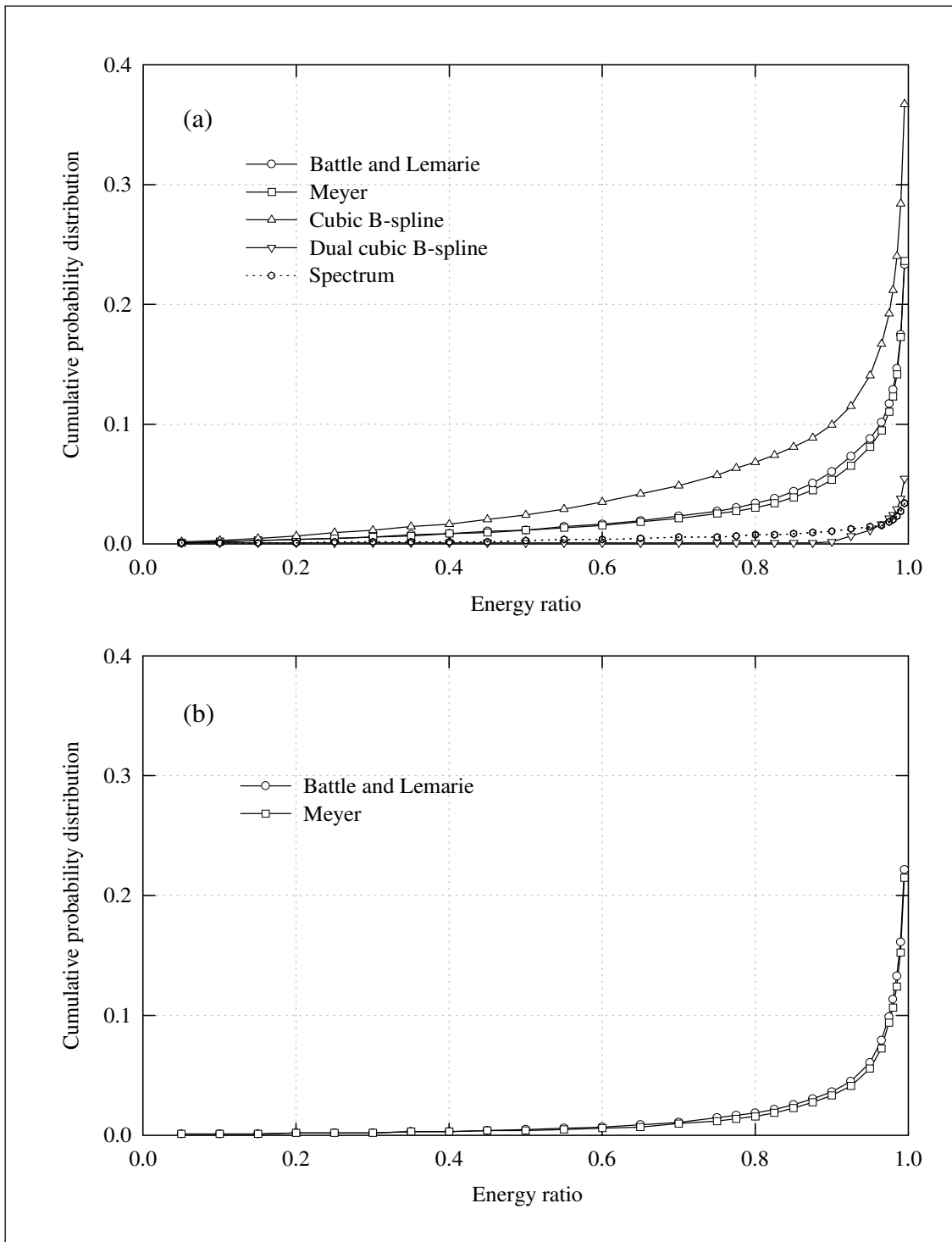


Figure 3.2: The cumulative probability distribution curves of the transform coefficients using different bases associated with three different transform categories: wavelet, wavelet packet, and Fourier transforms. Individual function bases are labeled in the figure. The top figure shows those of the wavelet group as well as a curve for spectral coefficients; the bottom figure shows those of wavelet packets best bases based on two orthonormal bases used in the top figure.

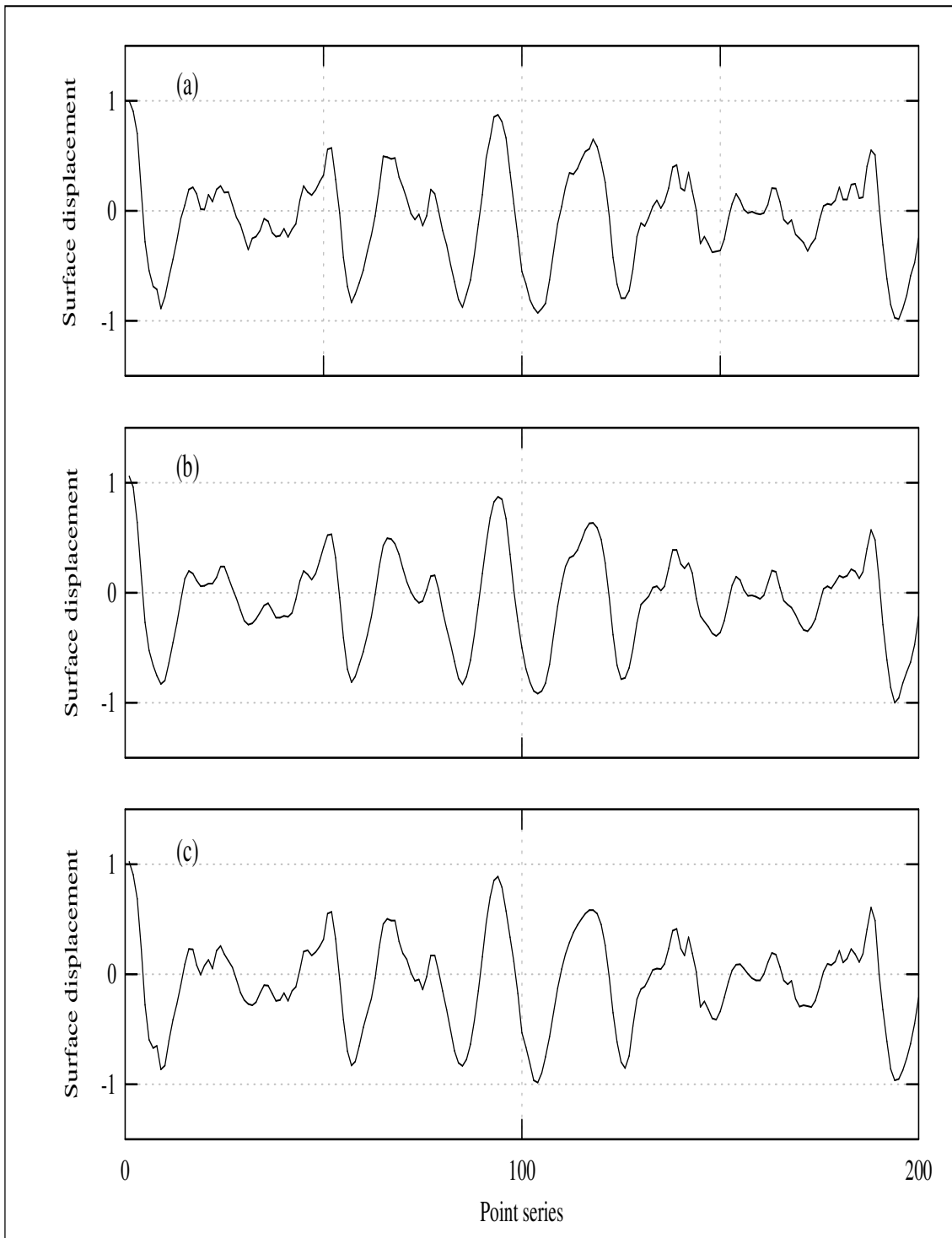


Figure 3.3: Comparison of reconstructed signals using truncated spectral coefficients and semi-orthogonal wavelet coefficients. Here 35% of the coefficients are kept. The original signal is shown in (a), signal reconstructed from spectral coefficients in (b), and that from SO3D wavelet coefficients in (c). The semi-orthogonal wavelet is seen to better portrait the original signal, especially the small scale transient features.

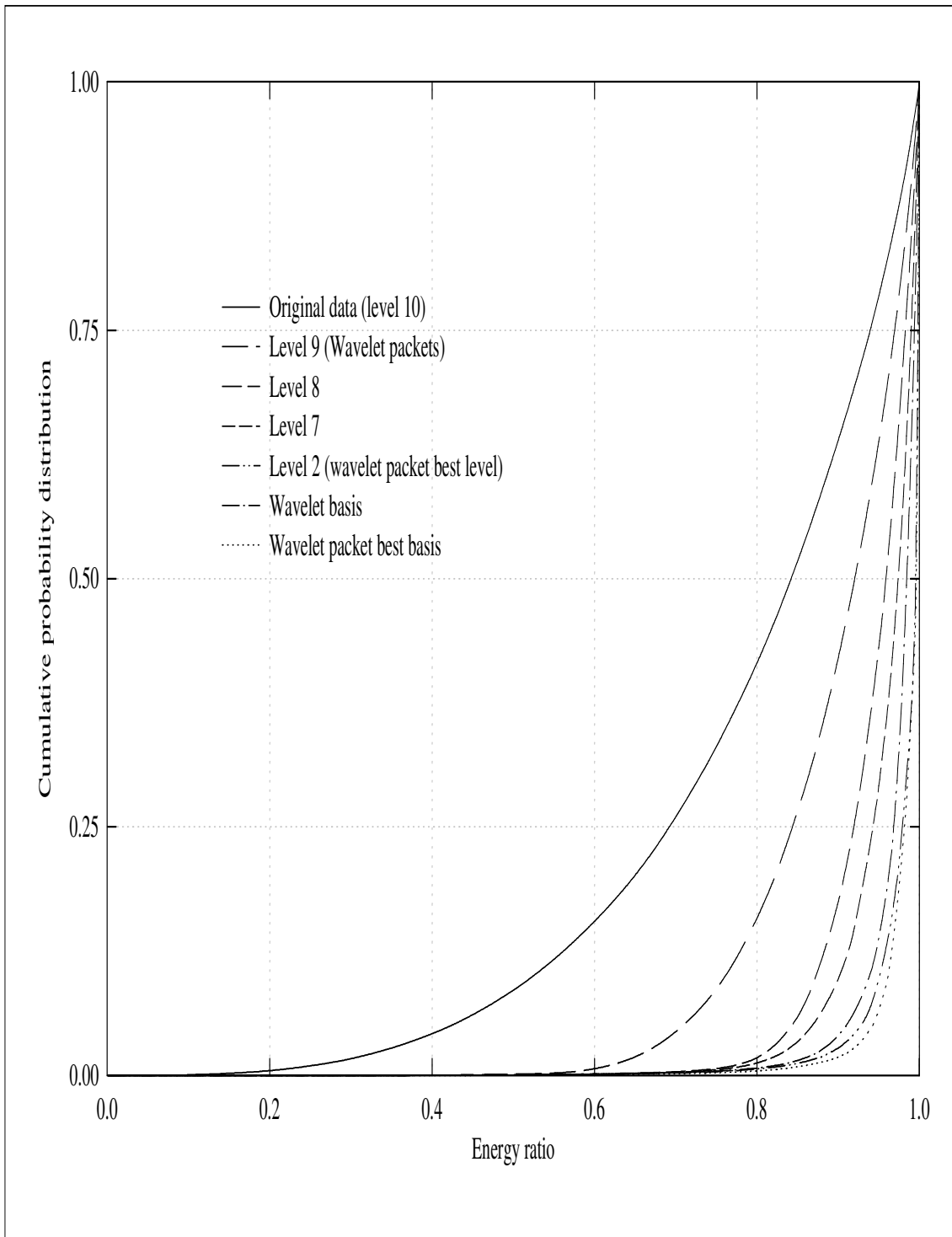


Figure 3.4: The cumulative probability distribution curves of the sorted wavelet and wavelet packet coefficients (L^2 -norm squared, i.e., energy content) for various bases which all originate from a single mother wavelet. These bases include those of various wavelet packet levels, wavelet packet best basis, as well as the seeding wavelet basis ON77S; as are indicated in the legend.

semi-orthogonal wavelets, no wavelet basis tested here can reach the level of approximation given by Fourier spectra. Still, many of the properties of the wavelets studied here are more of analytical interests and hard to be physically significant. The strong performance of the semi-orthogonal wavelet indicates the usefulness of modulated Gaussian wavelets (or the Morlet wavelets) for our applications. Coupling with a few additional features that are specific to continuous wavelet transforms – such as its redundancy nature, the flexible time-frequency resolutions, and the desirable conciliatory segment of interest – promising uses in future applications might be anticipated. ❖

Conclusions

A comprehensive set of discrete wavelet categories is studied for the interests of the water wave related physics. The relevant characterizations and various specific or intrinsic properties are illustrated. The wavelet numerical analyses and the associated data processing are developed from the ground up using the Asyst programming language, as well as several add-in components. Using such a tool we provide extensive depictions of the wavelet natures, such as their mother and father wavelets, the translations and dilations concepts, the zoom-ins or blowups of any kind of wavelets, and the linear phase filtering features — more importantly, their possible physical implications, their practical usefulness, as well as their advantages and disadvantages in water wave applications

Various criteria of entropy statistics are applied to the whole set of wavelets for signals obtained from wave-tank experiments. Results fully identify that the sole optimal wavelet basis is the dual semi-orthogonal cardinal spline wavelet.

And the author firmly believes that if you ever find an individual wavelet you have great chance to assign it into one of these categories; and if not, you have great reason to conceive that its properties must fall within (or between) the covered characterizations and thus, in water wave applications, its fate or possible usefulness is decreed accordingly.



APPENDIX A

仔波時頻分析及其於水波應用之研究

中文概述

第一章 引言

不同的訊號分析法有其不同的專善與優缺點。從典型而用途廣泛亦且成功的傳統波譜分析法以迄較近之仔波分析，我們有傅立葉分析、加窗富立葉分析、蓋博解析訊號分析法或希伯轉換、各種基於不同設計基核分佈函數的時頻分析法、以及離散仔波分析暨與離散仔波法可說不相同的連續仔波轉換分析法。

在這一章中我們說明了各種分析法的特性與大概區別、長處與短處，主要並闡述非穩態下物理與解析之相應表徵。事實上，所有的時頻分析法都可以歸之為加了罩窗的轉換，只是不同分析法對如何加窗是有極其不同的設計。此處我們以仔波轉換與加窗的富立葉轉換例舉他們的加窗特質，並引出何以仔波分析對非穩態與穩態的適用性都有其可能用途。

第二章 各類屬離散仔波函基探討

在幾乎所有的試驗模擬中，幾乎無可避免的是模擬尺度有其限制，而對一個牽涉多尺度、多維向的複雜問題，最重要的就是要能表徵它的非穩態性或突變性，若我們的數值分析鑑取方法無法比較全面性的掌握當中的尺度，那一些互作用現象即無法顯現或正確描述，因此，尋找一個適用於多尺度、並具備最佳化的模擬函基是為必然的訴求。針對這一訴求，在這一章中，我們選取了類屬含蓋廣泛而完整的離散仔波函基加以比較詳細地研究。

我們由基本起、原始性地開發一完整、亦且相當彈性化的仔波數值分析程式，並加入一些輔助功能，期使得以深入瞭解仔波。數值模擬之內容包括母仔波與父仔波、仔波包、仔波相關函數之相位與線性濾波特性、各種仔波相關函數局部展開行為等。經由這種最根本的瞭解，得以說明一些應用分析的表徵，也就是說將解析特質與其於水波數值分析之表現關聯在一起，並藉此判定不同仔波類屬的相對有用性。

第三章 熵值與最適函基之鑑取

在仔波的應用上，有一些研究是可以不牽涉仔波的物理義涵，例如在電子學訊號傳輸、影音壓縮、圖像邊界鑑選等，它們可以只強調效能最佳、速率最快、誤差最小；可是我們水波研究則主要著眼在物理上，而不在數值效能與速度。在前者應用研究中，為達到所要目的，則其函基之不同尺度仔波與訊號成分波必需相近。不夠，話說回來，針對我們水波用途，如果我們所選取的函數分佈形狀與我們訊號構成成分之形狀差異甚多，那我們如何可以安心地認為它可以模擬我們所要的物理。也如是乎，殊途同歸，速度與效能自然地成為我們的鑑取規範。這一規範也就是所謂的最小熵值。

熵值基本上是為一統計物理量，一般物理上它的最簡單（或普遍）的義涵是為無用之能量，也常代表一種亂度。在此處，它最簡明的意義可以表示為一種距離，也就是說，我們是要求取一個無用資訊最少、而與原始訊號距離最短的函基。而更具體的說，我們是從各個仔波轉換（包括仔波包轉換）所取得的係數中，判定那個轉換可以用最少的係數，以反轉換取得與原來訊號最近似之結果。

此處我們應用各種熵值統計規範於水槽風生水波訊號，從而一致判定最適離散仔波是為半正交仔波。其它相關說明項目有：不同熵值定義與實際數值處理手法：訊號重建概念；各類屬仔波於內於外的表現趨勢；暨這些表現與仔波解析之對應因子等。

第四章 結論

爲了鑑取得一個水波分析應用上最適化的離散仔波，我們由源頭、最根本起，開發了一個相當徹底的仔波分析程式並發展其相關套件。研究內容含蓋相當廣泛而完整的離散仔波類屬及其衍生類屬。所探討的包括解析與數值行爲，並將其可能之對應物理表徵與可能之使用性加以闡明。我們應用各類熵值定義一致判定水波分析應用之最適化函基是爲半正交仔波。

最後作者謹表示：或許你會看到一些零散而有點默生的離散仔波，但吾人深信，大部分情形下，它將可以被含蓋在這篇文章所探討的類屬中；如果不是，則吾人亦深信，你也大概可以把它的屬性歸納於介於我們所探討的仔波類屬之間，也如是乎，它於水波物理上的應用性、或是可使用性將不超乎本文之認定。

APPENDIX B — Wavelet 該如何中文稱之？

【摘自本所「研究計畫簡訊第一季」】

值此計畫之伊始，就讓我們來討論一個比較有趣、也是最根本的話題，那就是英文的wavelet 該如何中文稱之？也藉此順便涉略wavelet 的一些相關概念。

Wavelet 如今似乎最常見的翻譯是「小波」，而本人則習慣叫它為「子波」，然而個人認為最貼切的譯法應該是「仔波」。話說當年，約莫是1993年初，是我在國外初次接觸wavelet，而比較大規模的自我研習則大概又在一年之後。因為先前在國內並無接觸，自然對它的中文譯法也無從得知。另一方面也因wavelet 的主要理論與應用學門並不在海洋科技領域，就我所知，學校內並無wavelet 的課程（包含當時數學系及各研究所所開課程），所認識之老中也無人從事這一課題，所以也無人相詢。如是「子波」的稱呼就建立在我的習慣上了。如果當時有如現在這樣發達且簡易而方便的Internet，或許也就可以查到它的叫法，從而附會主流。

言歸正傳，也讓我們來說說為何仔波的譯法最為貼切。從英文字義講-let 是一個名詞附尾，比如我們所常聽到droplet、piglet。這個附尾代表小、年輕、局部，而有活蹦亂跳的含義。但把英文的wavelet 稱之為「小波」，我認為最大的致命傷就是中文的「小」跟「波」形成一種非常泛濫的概念，容易讓人聯想它是小小的波（small wave），也不免讓人想起是否有個相對應的大波？它缺乏一種像英文wavelet 那樣的專有名詞的氣度：另一方面，從數學內涵而論，wavelet 的精神絕對不是在大小方面，它主要的觀念是在強調一種局部性分佈的波，你要它多大就可多大，要多小就多小。此外小波的叫法也缺乏wavelet 的一些內涵，如多元性（無窮多種）、變異性（各形各色）、勁暴性（奇奇怪怪）。再者，小波的叫

法也很難讓人把它與函基（function basis）構成函數作一些關聯連想，而wavelet的重要用途無不肇始於它所衍化形成的函基。另外值得一提的是，實際上，數學的分析可以完全不涉單位，而沒有單位，也就無所謂的絕對大小；而在實用上，一般離散數值解析的整個處理流程可說也可完全不涉單位（只涉及序列），只需於最後的結果適當的考慮加入單位即可。如是，這種大小的區別比較就非核心問題所在。

至於第二種稱法「子波」，個人認為，相對於小波，它比較有專有名詞的氣度，不會像小波有著那樣泛濫的意義。事實上子本身就有小的含義，再者它影射仔的年輕與動力，而它似乎亦表示可成長、演化。不過有個缺點，那就是，wavelet的學門無不在訴說mother wavelet，可是這mother wavelet的中譯法「母子波」，可能給門外漢一種「霧煞煞」的感覺，或者會讓人聯想到跟「子」有相對應的意涵（同樣的，father wavelet「父子波」也容易有所混搖），事實上此處的「母子」並非比照倫理上或家庭上的長幼關係，這裡「母」跟「子」必需完全分離，「母」在此處的主要意涵是源頭，也就是說母子波最貼切的說法是源頭子波（用以製造或生成其它子波以便形成一個函基）。

有了上面的論述，似乎「仔波」叫法的優點也已不述自明了。「仔」者小也、子也，但卻毫無小或子的泛泛，「仔波」很自然地形成一個專有的名稱。再者仔也，傑放不遜、有活力、也可能不按牌理出牌-這顯示它的多元性、變異性、奇特性。而仔也有一種容易呼朋引友，自我膨脹，形成一種特立獨行的群體-這顯示它與函基的意涵有如是密切的關聯。至於「母仔波」、「父仔波」，與「母子波」、「父子波」的差異，我想大概也是不說而自可分明。

BIBLIOGRAPHY

- [1] Auscher, P. Wavelet bases for $L^2(\mathbb{R})$ with rational dilation factor. In M. B. Ruskai, G. Beylkin, R. Coifman, I. Daubechies, S. Mallat, Y. Meyer, and L. Raphael, editor, *Wavelets and Their Applications*, pages 439–452. Jones and Bartlett Publishers, Boston, New York, USA, 1992.
- [2] Battle, G. Cardinal spline interpolation and the block spin construction of wavelets. In C.K. Chui, editor, *Wavelets: A tutorial in Theory and Applications*, pages 73–90. Academic Press, Inc., San Diego, California, USA, 1992.
- [3] Chui, C. K. *An Introduction to Wavelets*. Academic Press, Inc., San Diego, California, USA, 1992. 35
- [4] Chui, C.K. On cardinal spline-wavelets. In M. B. Ruskai, G. Beylkin, R. Coifman, I. Daubechies, S. Mallat, Y. Meyer, and L. Raphael, editor, *Wavelets and Their Applications*, pages 439–452. Jones and Bartlett Publishers, Boston, New York, USA, 1992. 35
- [5] Cohen, L. *Time-Frequency Analysis*. Prentice Hall PTR, Englewood Cliffs, New Jersey, USA, 1995. 1
- [6] Coifman, R., Y. Meyer, and M.V. Wickerhauser. Size properties of wavelet packets. In M. B. Ruskai, G. Beylkin, R. Coifman, I. Daubechies, S. Mallat, Y. Meyer, and L. Raphael, editor, *Wavelets and Their Applications*, pages 453–470. Jones and Bartlett Publishers, Boston, New York, USA, 1992.
- [7] Coifman, R., Y. Meyer, and M.V. Wickerhauser. Wavelet analysis and signal processing. In M. B. Ruskai, G. Beylkin, R. Coifman, I. Daubechies, S. Mallat, Y. Meyer, and L. Raphael, editor, *Wavelets and Their Applications*, pages 153–178. Jones and Bartlett Publishers, Boston, New York, USA, 1992.

- [8] Daubechies, I. *Ten Lectures on Wavelets*. SIAM, Philadelphia, USA, 1992. 42
- [9] Lee, Y.R. *Interaction Scales in a Wind, Wave, and Rain Coupling System*. Ph.D. Dissertation, University of Delaware, Newark, Delaware, Nov. 1999. 8
- [10] Lee, Y.R. Signal analysis from wave modulation perspective. Technical report, No.2001–09, Institute of Harbor and Marine Technology, Taichung, Taiwan, 2001. 2
- [11] Mallat, S., and S. Zhong. Wavelet transform maxima and multiscale edges. In M. B. Ruskai, G. Beylkin, R. Coifman, I. Daubechies, S. Mallat, Y. Meyer, and L. Raphael, editor, *Wavelets and Their Applications*, pages 67–104. Jones and Bartlett Publishers, Boston, New York, USA, 1992.
- [12] Massopust, P.R. *Fractal Runctions, Fractal Surfaces, and Wavelets*. Academic Press, Inc., San Diego, California, USA, 1994.
- [13] Meyer, Y. *Wavelets and operators*. Cambridge University Press, New York, USA, 1992.
- [14] Press, W. H., S. A. Teukolsky, W. T. Vetterling and B. P. Flennerly. *Numerical Recipes in Fortran*. Cambridge University Press, New York, USA, second edition, 1992.
- [15] Wickerhauser, M.V. Acoustic signal compression with wavelet packets. In C.K. Chui, editor, *Wavelets: A tutorial in Theory and Applications*, pages 679–700. Academic Press, Inc., San Diego, California, USA, 1992.
- [16] Wickerhauser, M.V. Comparison of picture compression methords: wavelet, wavelet packet, and local cosine. In C. K. Chui, editor, *Wavelets: Theory, Algorithms, and Applications*, pages 585–621. Academic Press, Inc., San Diego, California, USA, 1994.